



Resolving the Middle Jurassic dinoflagellate radiation: The palynology of the Bajocian of Swabia, southwest Germany



Nickolas J. Wiggan^{a,b,*}, James B. Riding^b, Matthias Franz^c

^a Department of Earth Sciences, University of Cambridge, Downing Street, Cambridge CB2 3EQ, United Kingdom

^b British Geological Survey, Environmental Science Centre, Nicker Hill, Keyworth, Nottingham NG12 5GG, United Kingdom

^c Regierungspräsidium Freiburg, Dept. 9, State Authority for Geology, Mineral Resources and Mining, Albertstraße 5, Freiburg D-79104, Germany

ARTICLE INFO

Article history:

Received 22 July 2016

Received in revised form 23 November 2016

Accepted 26 November 2016

Available online 9 December 2016

Keywords:

Dinoflagellate cysts

Radiation

Middle Jurassic (Bajocian)

Swabia

Germany

Biostratigraphy

ABSTRACT

Dinoflagellates underwent a major radiation during the Bajocian (Middle Jurassic, ~170–168 Ma). The group originated in the Middle Triassic and dinoflagellate cysts were relatively low in diversity until the Bajocian, when over 100 species appeared. The Gonyaulacaceae expanded during this interval to become the dominant family of cyst-forming dinoflagellates, and has remained the principal dinoflagellate family throughout the Mesozoic and Cenozoic. However, Bajocian dinoflagellate cysts have received relatively little study. In order to unravel the pattern of the Bajocian dinoflagellate radiation, we have generated a high resolution, quantitative, palynological record through an expanded Middle Jurassic succession in Swabia, southwest Germany. Previous research has indicated a rapid, stepwise order of first appearances through the Bajocian. By contrast, we clearly demonstrate that there was a more gradual, continuous increase in diversity from the Late Aalenian to the Early Bathonian, although the number of first appearances was highest during the latest Early Bajocian to Late Bajocian. Major experimentation in excystment mode in the gonyaulacaceans occurred during the Late Aalenian and Early Bajocian, when multi-plate precingular, single-plate precingular and epicystal archaeopyle types first appeared. Through the integration of our data with published information from northwest Europe, we demonstrate that the appearance of dinoflagellate cyst taxa through the Late Aalenian–Early Bathonian appears to have been controlled by a major second-order transgression. Although the cause of this radiation is yet to be constrained, given the contemporaneous diversifications of other plankton groups, as well as ammonites, bivalves and fishes, it is likely that it formed part of the wider Mesozoic Marine Revolution. There is a prominent acme of *Dissilodinium giganteum* in the Lower Bajocian which is a useful stratigraphical marker. *Acanthaulax crista* is confirmed as a key index species for the Bajocian. One new species, *Korystocysta aldrigei* sp. nov., is described.

© 2016 The Authors. Published by Elsevier B.V. This is an open access article under the CC BY license (<http://creativecommons.org/licenses/by/4.0/>).

1. Introduction

Dinoflagellates are a diverse group of flagellated freshwater and marine protists, the majority of which are photosynthetic or mixotrophic marine plankton. Together with the diatoms and coccolithophores, they form the majority of eukaryotic phytoplankton of the world's oceans and are important primary producers (Delwiche, 2007). Around 10–15% of modern dinoflagellates produce organic-walled resting cysts as part of their lifecycle (Head, 1996) and it is these cysts that form the basis of the dinoflagellate fossil record (along with the calcareous and siliceous cysts produced by certain forms). Despite its selective nature, the cyst fossil record allows dinoflagellate evolution to be tracked

through geological time (Fensome et al., 1996), whilst providing a powerful biostratigraphical tool.

The earliest fossil dinoflagellate cysts are known from the Ladinian of the Middle Triassic (Riding et al., 2010). Dinoflagellate cysts were low in diversity throughout the Middle Triassic to earliest Middle Jurassic, until a major radiation occurred during the Bajocian (170–168 Ma), when ~100 new species appeared (Fig. 1; Woollam and Riding, 1983; MacRae et al., 1996; Riding et al., 2010). The family Gonyaulacaceae expanded throughout the Bajocian and became the dominant group of cyst-forming dinoflagellates, which remains so to the Recent (Fig. 1; Fensome et al., 1996). Other groups of plankton also radiated at this time, including coccolithophores and planktonic foraminifera (Hart et al., 2003; Suchéras-Marx et al., 2015), implying major evolutionary innovations occurred within plankton during the Bajocian.

The principal objective of the current study is to unravel the pattern of the dinoflagellate cyst radiation stratigraphically. Bajocian dinoflagellate cysts have received relatively little study and there has been no

* Corresponding author at: Department of Earth Sciences, University of Cambridge, Downing Street, Cambridge CB2 3EQ, United Kingdom.
E-mail address: njw56@cam.ac.uk (N.J. Wiggan).

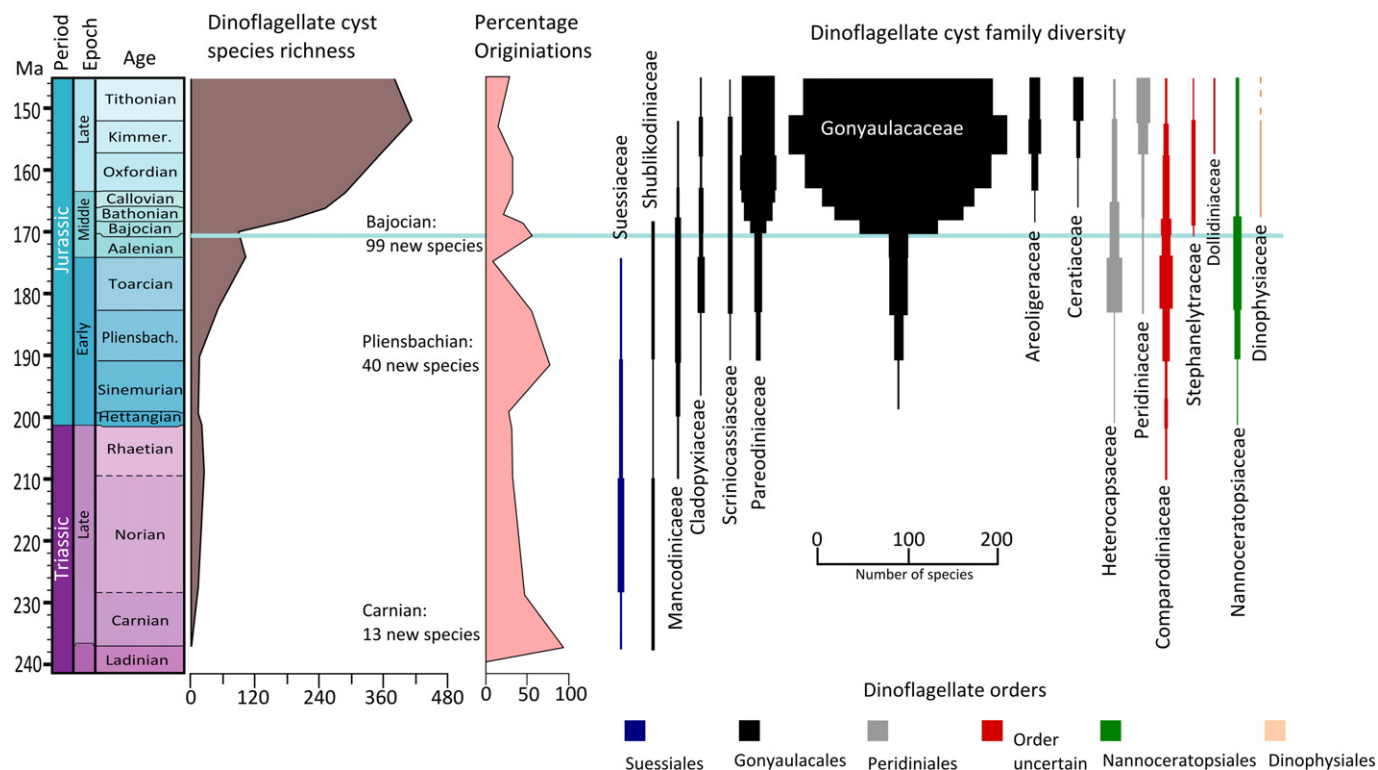


Fig. 1. Dinoflagellate cyst species richness and family diversity through the Triassic and Jurassic. Note the expansion of the Gonyaulacaceae during the Bajocian. Species richness curve redrawn from MacRae et al. (1996) raw data, percentage originations modified from MacRae et al. (1996). Family diversity modified from Fensome et al. (1996). Chronostratigraphy generated in Timescale Creator v6.4.

comprehensive examination of the Bajocian radiation. The only study focused on the Bajocian radiation was based on d'Orbigny's type section from northwest France, which highlighted a rapid, stepwise order of lowest occurrences through the Bajocian, with a sudden burst of lowest occurrence datums (LODs) around the Lower–Upper Bajocian transition (Feist-Burkhardt and Monteil, 1997). However, this succession is highly condensed (Riout et al., 1991).

Here we present the results of a high resolution, quantitative study of the dinoflagellate cyst record of an interval spanning the uppermost Aalenian, Bajocian and lowermost Bathonian Stages of Swabia, south-west Germany. In this region the Bajocian succession is expanded, virtually complete, and is correlated to the standard (sub-boreal) ammonite zonation (the term zone is used here to denote ammonite biozone). We integrated our results with published data to provide a comprehensive stratigraphical account of the Bajocian dinoflagellate cyst radiation. In order to set our results within a palaeoenvironmental context we have examined abundance changes within dinoflagellate cysts and other palynomorphs, using quantitative palynological analyses.

2. Previous research on Bajocian dinoflagellate cysts

Bajocian dinoflagellate cysts have been particularly understudied in comparison to other stages of the Jurassic (Riding, 2012, 2013, 2014). Many works have included the stage only as part of broader works on Jurassic dinoflagellate cysts, e.g. Fensome (1979), Prauss (1989) and Poulsen (1996).

Research which has focused on the Bajocian has largely been based on classic Jurassic localities such as Dorset and Yorkshire (England), the Isle of Skye (Scotland) and Normandy (France) (Fenton and Fisher, 1978; Davey, 1980; Fenton et al., 1980; Woollam, 1982; Bailey, 1987, 1990; Riding et al., 1991; Feist-Burkhardt and Monteil, 1997; Butler et al., 2005). In these regions Bajocian stratigraphy and ammonite

zonation is well known, providing independent age control for biostratigraphical calibration. However, the Bajocian in southern England and northwest France is highly condensed, and in northern England and Scotland the Upper Bajocian is largely missing due to a major unconformity, meaning a complete record of the dinoflagellate cyst radiation in these areas is missing. The most significant work on Bajocian dinoflagellate cysts is that of Feist-Burkhardt and Monteil (1997) who documented the dinoflagellate cyst record of d'Orbigny's Bajocian type section near Bayeux in Normandy, northwest France. These authors reported a two-step burst of lowest occurrences around the Lower–Upper Bajocian transition (*S. humphriesianum* and *S. niortense* zones), and in the Upper Bajocian (*P. parkinsoni* zone) respectively, and noted that the family Gonyaulacaceae radiated rapidly through this interval. However, the Bajocian succession around Bayeux is highly condensed (Riout et al., 1991). The *S. humphriesianum* and *S. niortense* zones are <10 cm thick and subject to considerable time averaging, meaning that some of the occurrence data are obscured, and this emphasises the rapid, stepwise pattern of lowest occurrences through the succession. Moreover, this study reported only absence/presence data, thereby making it impossible to detect any dinoflagellate cyst abundance changes through the Bajocian radiation and removing any palaeoecological data. Consequently, despite being the most complete work on dinoflagellate cysts of the Bajocian this work is limited by the nature of the succession examined and lack of quantitative data.

In other areas of Europe dinoflagellate cysts have been researched from Middle Jurassic successions that lack ammonites in order to date them. Many studies have examined dinoflagellate cysts from the Bajocian of Pieniny Klippen Belt of the Carpathian Mountains in southern Poland and northern Slovakia, but the data from these works lacks independent age control (Gedl, 2008, 2013; Barski et al., 2012; Gedl and Józsa, 2015; Segit et al., 2015).

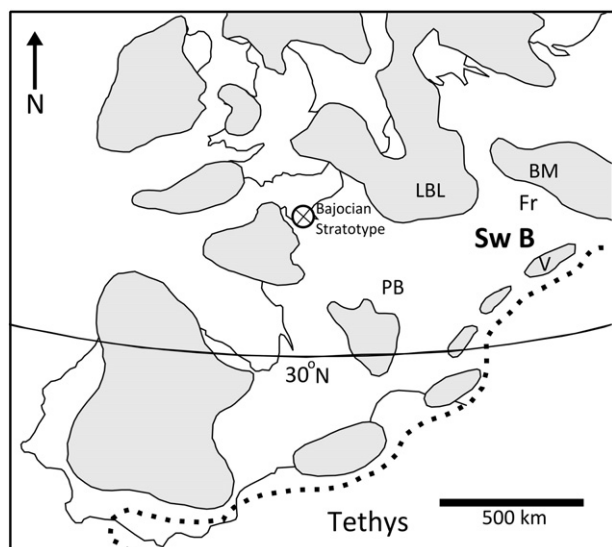


Fig. 2. Middle Jurassic palaeogeography for Europe. Emergent areas (grey): LBL = London Brabant Landmass, BM = Bohemia Massif, V = Vindeleian High. Submerged areas: PB = Paris Basin, Fr = Franconian platform, SwB = Swabian Basin. The location of the historical Bajocian stratotype is shown. Palaeogeography modified from Callomon (2003).

Outside of Europe, Bajocian dinoflagellate cysts have been examined from Qatar (Ibrahim et al., 2003), Iran (Skupien et al., 2015), Argentina (Stukins et al., 2013) and Australia (Mantle and Riding, 2012). The latter authors documented the Bajocian radiation from the North West shelf of Australia; however, all these studies lack independent age control, making correlation difficult. Summarily, there is no existing high resolution, quantitative study of Bajocian dinoflagellate cysts from an expanded succession with independent age control; this contribution aims to remedy this gap in the literature.

3. Geological background of the Swabian Alb, southwest Germany

The low-lying mountains of the Swabian Alb of southwest Germany are a classic locality of the European Jurassic, with a long history of

geological and palaeontological research (Pienkowski et al., 2008). Feist-Burkhardt and Wille (1992) provided a broad overview of the stratigraphic distributions of dinoflagellate cysts through the Jurassic of the Swabian Alb, and highlighted the large number of LODs from the Bajocian, particularly around the Lower/Upper Bajocian transition (*S. humphriesianum* and *S. niortense* zones). This, combined with the expanded nature of the Middle Jurassic in the Swabian Basin (over 280 m thick (Pienkowski et al., 2008)) and well known ammonite zonation, make Swabia an ideal locality for examining the Bajocian dinoflagellate cyst radiation.

During the Middle Jurassic the Swabian Basin was located on the border of the Boreal and Tethyan realms on the outer region of the European epicontinental seaway, at around 35° north (Fig. 2). This was situated between the Tethys to the south, the northwest German basin to the north, the eastern Paris Basin to the west and the Bohemian Massif to the east (Fig. 2; Callomon, 2003; Pienkowski et al., 2008). The southern German marginal sea during the Bajocian included the French-Swiss carbonate platform in the southwest, a mud dominated, moderately deep basin in the central area, and the Franconian iron-oolitic carbonate platform in the east (Ziegler, 1990).

The basis of the current study is a subsurface succession from borehole B404/2, located approximately 37 km southeast of Stuttgart, near the village of Gruibingen (Fig. 3, latitude and longitude: 48.59849°N, 9.61450°E), and is comprised of the uppermost Aalenian to Lower Bathonian (Fig. 4). This succession is located in the eastern part of the central Swabian basin, and was deposited on the outer shelf, around 25 km west of the border of the Franconian platform. The palaeocoastline was formed by the Vindelician High, located around 100 km to the south and the Bohemian Massif was approximately 200 km to the east (Fig. 2).

The (sub-boreal) ammonite zonal subdivision of the succession in borehole B404/2 is based on Dietl (1988, 2013) who described in detail the ammonite biostratigraphy of the Middle Jurassic from a road cutting (BAB A8), which is located 1 km from the site the borehole was drilled. As the borehole succession has a near-identical lithostratigraphy to the road cut section, the zonation of Dietl (1988, 2013) was applied to borehole B404/2. With the exception of the lowermost zone (*H. discites*), which is missing due to a hiatus, the entire Bajocian Stage is present (Fig. 4). There is some uncertainty in the recognition of the *S.*

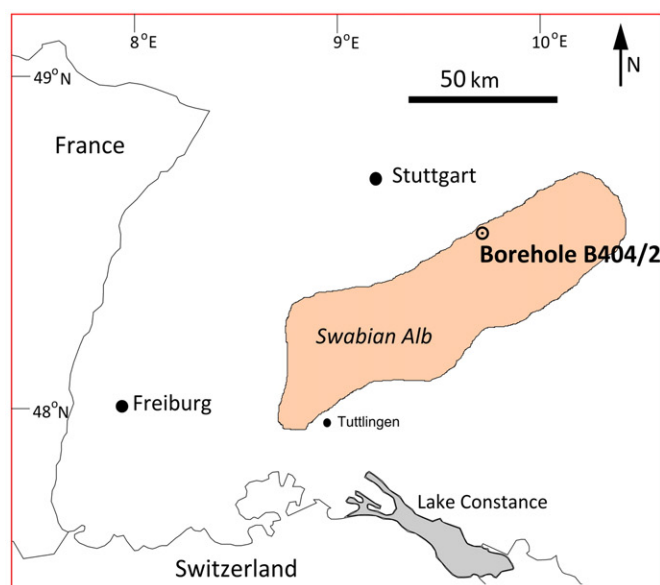


Fig. 3. Locality map for the area of study within Europe. Latitude and longitude for borehole B404/2: 48.59849°N, 9.61450°E.

propinquans zone of the Lower Bajocian which is hereby split into the *W. laeviuscula*/*S. propinquans* and *S. propinquans*/*S. humphriesianum* zones, all other zones are accurately correlated. In this locality the Bajocian is over 50 m thick (vs 11 m in Normandy), in particular, the *S. humphriesianum* and *S. niortense* zones (which represent the main radiation) are greatly expanded with respect to Normandy at 8 m thick each (Fig. 4).

The stratigraphical succession in B404/2 is represented by recurrent transgressive/regressive units. The fine-grained siliciclastics of the Wedelsandstein, Ostreenkalk, Hamitenton and Dentalienton Formations were deposited during highstands whilst the thin condensed carbonates of the Humphriesi, Subfurcaten and Parkinsoni Oolithe Members were deposited over regressive erosional surfaces during transgressive episodes (Feist-Burkhardt and Götz, 2002). There is an overall fining upward trend as the Lower Bajocian Wedelsandstein Formation contains abundant sandstone lenses and interbeds whilst the overlying units are finer grained. This trend reflects a major second-order transgression which occurred throughout Europe during the Late Aalenian to Early Bathonian (Hallam, 2001). In the Boreal Realm, this was a two-pulsed second order transgression. The first pulse was Late Aalenian to Early Bajocian (*G. concavum* to *S. humphriesianum* zones), and the second was Early Bajocian to earliest Bathonian (*S. humphriesianum* to *Z. zigzag* zones). A sequence boundary marks the base of the second pulse in the *S. humphriesianum* zone (Jacquin et al., 1998). In the B404/2 succession the sequence boundary at the base of the Humphriesi Oolithe Member (Fig. 4) marks the base of the second pulse of this transgression, and the nodule-rich part of Dentalienton Formation (*Z. zigzag* zone of the Lower Bathonian) represents the point of maximum transgression (Fig. 4).

4. Materials and methods

Ninety one samples from the 57 m thick section in borehole B404/2 were processed for palynomorphs, of these, seven were excluded from further study after processing due to the low abundance of palynomorphs and poor preservation (Table 1). All lithologies were sampled including phosphorite nodule bearing horizons as these often contain extremely well preserved palynomorphs (Barski, 2014). Sampling resolution was highest in the *S. humphriesianum* and *S. niortense* zones as these zones are poorly represented/absent in other areas of Europe, yet appear to represent the most critical interval in the Bajocian dinoflagellate cyst radiation (Feist-Burkhardt and Wille, 1992; Feist-Burkhardt and Monteil, 1997).

Approximately 20 g of rock was processed using standard palynological processing procedures (e.g. Wood et al., 1996) and all samples were spiked with *Lycopodium* spore tablets to allow absolute abundances to be calculated. Exceptions to standard procedures include the use of hot hydrochloric acid for the removal of carbonate, which prevents the precipitation of fluoride gels and increases processing speed. Sieving with a 10 µm screen was used during decantation to avoid the loss of *Lycopodium* spores (Mertens et al., 2009). Microscope slides were examined under transmitted light and around 300 palynomorphs were counted per sample. Dinoflagellate cysts were identified to species level, other microplankton were identified to species level where possible, and sporomorphs were counted in broad morphological groupings. An additional slide per sample was fully scanned to ensure that any rare palynomorphs were recorded. Absolute abundances were calculated according to the following equation (Lignum et al., 2008): $ppg = \left(\frac{PC}{LC}\right) * \left(\frac{L}{W}\right)$ where: ppg = palynomorphs per gram of dried sediment, pc = palynomorphs counted, lc = lycopodium counted, L = total lycopodium and w = dried weight of the sample in grams.

All slides are housed in the Department of Earth Sciences, University of Cambridge. The slides containing the holotype and paratype of *Korystocysta aldrigei* sp. nov. are stored in the Sedgwick Museum of Earth Sciences, which is part of the Department of Earth Sciences.

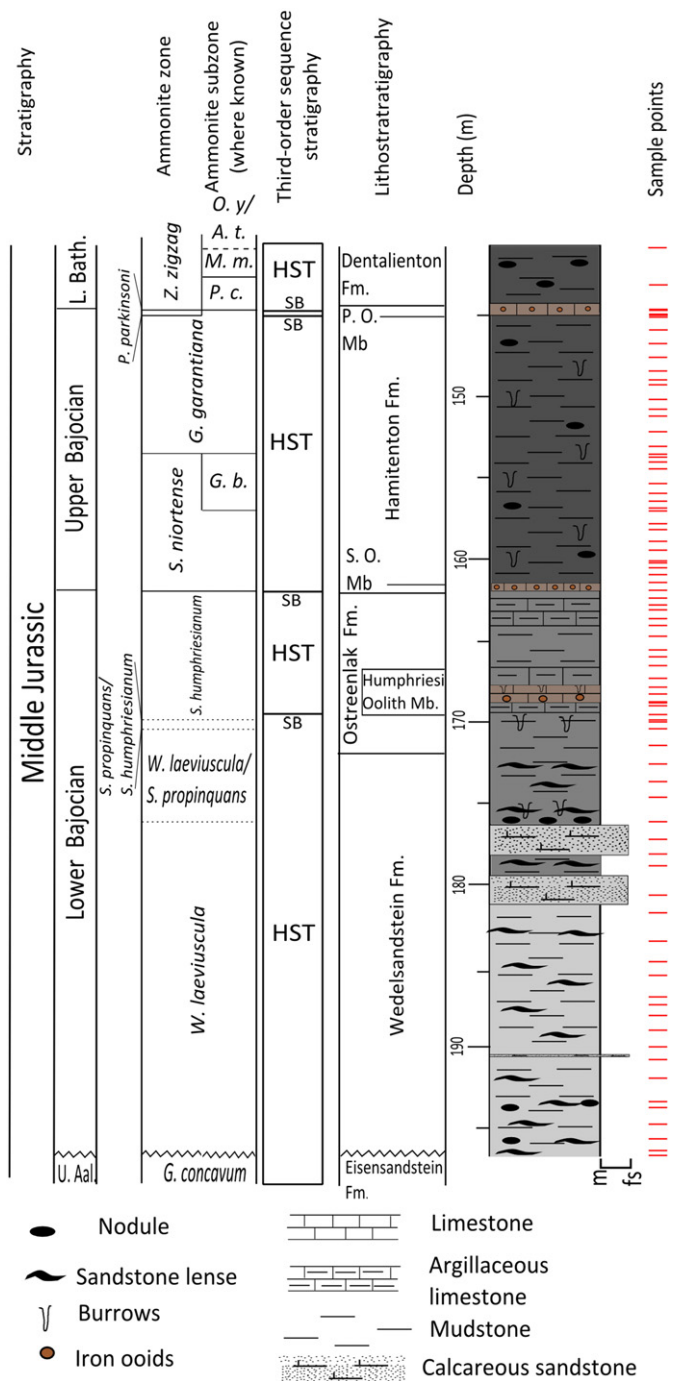


Fig. 4. Sedimentary log of borehole B404/2. The correlation of ammonite zones is based on Dietl (1988, 2013) and sequence stratigraphy is after Feist-Burkhardt and Götz (2002). Lithostratigraphy: P.O. = Parkinsoni Oolithe Member, S.O. = Subfurcaten Oolithe Mb. Subzones: G.b = *G. baculata*, P. c = *P. convergens*, M.m. = *M. macrascens*, O.y./A.t. = *O. yeovilensis*/*A. tenuiplicatus*. Sequence stratigraphy: HST = highstand systems tract, SB = sequence boundary.

5. The palynology and depositional environment of the borehole B404/2 succession

The majority of the samples examined produced abundant, well preserved palynomorphs. However the samples from the Humphriesi Oolithe Member and Ostreenkalk Formation are poorly preserved in places, and in the upper part of the Hamitenton Formation amorphous organic matter (AOM) is abundant and preservation is relatively poor.

The assemblages are dominated by marine palynomorphs which are, in turn, dominated by dinoflagellate cysts (Plates I–XII). Acritarchs (largely *Michrystidium* spp.) comprise the majority of the remaining marine component. Other palynomorph groups include foraminiferal test linings, prasinophytes and rare scolecodonts. The terrestrial palynofloras are dominated by trilete spores, with gymnosperm pollen comprising the remaining component. The relative and absolute abundances of palynomorphs is summarised in Fig. 5.

The marine:terrestrial ratio is variable in the Lower Bajocian, with significant terrestrial influxes in the lowermost and uppermost parts of the Wedelsandstein Formation (Fig. 5). The latter is associated with an increase in the relative abundance of acritarchs and prasinophytes. The high relative abundance of trilete spores in the Wedelsandstein Formation indicates that this unit was deposited in a relatively proximal palaeoenvironment, close to sources of terrigenous input. Due to the sandstone lenses and interbeds in this unit, it may represent a prodelta setting (Fig. 5). The presence of abundant and relatively diverse dinoflagellate cysts implies this was a relatively distal, offshore palaeoenvironment as dinoflagellate cysts indicative of reduced palaeosalinities such as *Nannoceratopsis* (see Riding, 1983) are low in abundance (Table 2a). By contrast, in the overlying Ostreenkalk Formation

and the succeeding units there is a trend of increasing (but fluctuating) marine influence (Fig. 5). However, the absolute abundance of terrestrial palynomorphs (including trilete spores) slightly increases through the Upper Bajocian, strongly suggesting proximity to a source of terrigenous material. The increase in marine:terrestrial ratio is driven by an enormous increase in the abundance of dinoflagellate cysts, but the increase in the absolute abundance in all palynomorphs groups suggests a decrease in sedimentation rate through the Upper Bajocian. Therefore the succession overlying the Wedelsandstein Formation may reflect a landward shift in shelf facies over prodelta sediments, with a reduced sedimentation rate and a pronounced increase in the abundance of dinoflagellate cysts associated with a more distal/offshore environment. The Lower Bathonian Dentalien Formation is marked by maximum marine:terrestrial ratio and a huge decrease in the absolute abundance of terrestrial palynomorphs.

The steadily increasing (but fluctuating) marine:terrestrial ratio through the Upper Bajocian and Lower Bathonian reflects the major episode of transgression which occurred through the Bajocian. The enormous increase in marine:terrestrial ratio and decrease in the abundance of terrestrially derived palynomorphs in the Lower Bathonian represents the point of maximum transgression in Europe.

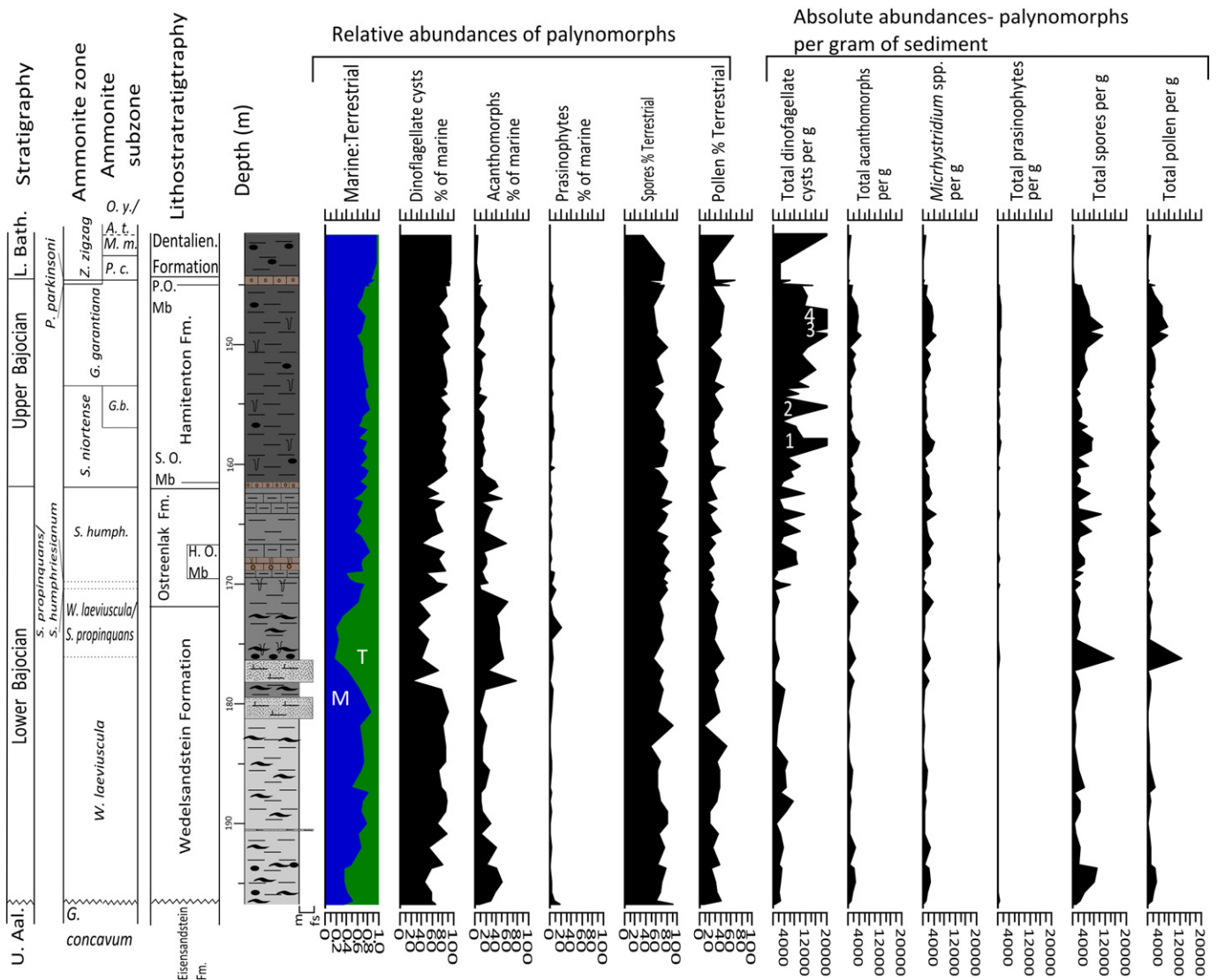


Fig. 5. Relative and absolute abundances of main marine and terrestrial palynomorph groups for borehole B404/2. It can clearly be seen that dinoflagellate cysts are the dominant marine palynomorph through the succession, with acanthomorphs (predominantly *Michrystidium* spp.) comprising the majority of the remaining marine component. There is a steady but fluctuating increase in the marine:terrestrial ratio from around 175 m depth, which reflects a major phase of transgression. Dinoflagellate cysts per gram — 4 values are off the scale of the graph. 1: 28,717.50, 2: 21,447.79, 3: 35,359.88, 4: 26,618.93.

Table 1

Thickesses of ammonite zones within borehole B404/2 and the number of samples per zone.

| Zone | Thickness (m) | Substage | Number of (palynologically productive) samples | Lithostratigraphical unit |
|--|---------------|-----------------|--|--|
| <i>G. concavum</i> (pars) | 0.2 | Upper Aalenian | 1 | Eisensandstein Formation |
| <i>W. laeviuscula</i> (pars) | 20.26 | Lower Bajocian | 20 | Wedelsandstein Formation |
| <i>W. laeviuscula</i> / <i>S. propinquans</i> | 5.76 | Lower Bajocian | 6 | Wedelsandstein Formation/Ostreenkalk Formation |
| <i>S. propinquans</i> / <i>S. humphriesianum</i> | 0.61 | Lower Bajocian | 2 | Ostreenkalk Formation |
| <i>S. humphriesianum</i> | 7.9 | Lower Bajocian | 17 | Ostreenkalk Formation (including Humphriesi Oolith Member) |
| <i>S. niortense</i> | 8.25 | Upper Bajocian | 18 | Hamitenton Formation (including Subfurcaten Oolith Member) |
| <i>G. garantiana</i> | 8.53 | Upper Bajocian | 13 | Hamitenton Formation |
| <i>P. parkinsoni</i> | 0.35 | Upper Bajocian | 4 | Parkinsoni Oolith Member |
| <i>Z. zigzag</i> (pars) | 4.56 | Lower Bathonian | 3 | Uppermost Parkinsoni Oolith Member/Dentalienton Formation |

6. Dinoflagellate cyst biostratigraphy of borehole B404/2

The pattern of lowest occurrences seen through the section (Tables 2a, 2b) is much more gradualistic than the pattern seen in northern France. The stratigraphic pattern seen through the section is described and discussed below, and has been subdivided into Upper Aalenian, Lower Bajocian, Lower–Upper Bajocian transition and Upper Bajocian–Lower Bathonian.

6.1. Upper Aalenian (*G. concavum* zone)

The single sample (S1) from the Upper Aalenian (*G. concavum* zone) Eisensandstein Formation yielded 7 dinoflagellate cyst taxa. These are *Batiacasphaera* spp., *Batiacasphaera*? spp., *Dissiliodinium giganteum*, *Dissiliodinium* spp., *Dissiliodinium*? spp., *Nannoceratopsis ambonis* and *Pareodinia halosa*. The assemblage is dominated by the genera *Batiacasphaera* and *Dissiliodinium*. The presence of *Dissiliodinium giganteum* is the oldest record to date, and this report extends downward the range of this species into the Upper Aalenian. Previously *Dissiliodinium giganteum* was thought to have had a LOD in the lowermost Bajocian *H. discites* zone (Feist-Burkhardt and Monteil, 2001). The range base of *Dissiliodinium* (as *D. lichenoides*) is in the *L. munchisonae* zone of the Aalenian (Feist-Burkhardt and Pross, 2010). *Batiacasphaera* spp. and *Pareodinia halosa* have LODs in the *H. variabilis* and *G. thouarsense* zones respectively of the Toarcian (Riding, 1984a; de Vains, 1988). The LOD of *N. ambonis* is in the Upper Pliensbachian *P. spinatum* zone (Riding, 1984b). Other marine palynomorphs include the acritarch *Michrystidium* spp. and the prasinophyte *Tasmanites* spp., which are moderately abundant, whilst the terrestrially derived palynomorphs are overwhelmingly dominated by trilete spores (Fig. 5).

6.2. Lower Bajocian: *W. laeviuscula* to *S. propinquans*/*S. humphriesianum* zones

A gradual increase in diversity occurs throughout this interval as 20 dinoflagellate cyst taxa have lowest occurrences, of which there are several LODs of important gonyaulacaceans. The occurrence of *Ctenidodinium* sp. 1 in the *W. laeviuscula* zone represents the lowest occurrence of this genus. This was previously reported at the Lower–Upper Bajocian transition as *Ctenidodinium continuum* in southern Germany (Feist-Burkhardt and Wille, 1992). The occurrence of *Chytroesphaeridia chytroides* represents the lowest recorded example of this species. The occurrence of *Dissiliodinium*? *hocneratum* lowers the LOD of this species which was previously in the *S. niortense* zone (Feist-Burkhardt and Wille, 1992). Likewise, the occurrence of *Orobodinium automobile* represents the earliest reported example of this somewhat enigmatic genus, the LOD of which has been previously placed in the Upper

Bajocian *P. parkinsoni* zone (Feist-Burkhardt and Wille, 1992). Other gonyaulacacean species to occur in this interval include *Durotrigia daveyi* and *Gongyloclonium erymnoteichon*, both of which have range bases in the *H. discites* zone in Europe (Riding and Thomas, 1992). The occurrence of these species in the *W. laeviuscula* zone in this study probably reflects the hiatus underlying this zone. *Kallosphaeridium*? *hypornatum* also has a lowest occurrence in the *W. laeviuscula* zone, which is consistent with Feist-Burkhardt and Monteil (1997). Several species of *Nannoceratopsis*, *N. gracilis*, *N. plegas* and *N. spiculata*, occur in the *W. laeviuscula* zone. These species are long-ranging, and have LODs in the Upper Pliensbachian *A. margaritatus* zone and the Upper Toarcian *H. bifrons* and *D. levesquei* zones (Prauss, 1989; Riding and Thomas, 1992). However, the range base of *N. spiculata* in Germany appears to be no lower than the *S. humphriesianum* zone (Prauss, 1989; Feist-Burkhardt and Wille, 1992) and thus this report lowers the local range base of this species to the *W. laeviuscula* zone. *Nannoceratopsis dictyambonis* occurs in the *S. propinquans*/*S. humphriesianum* zone (sample S44), and also occurs in sample S46 in the lowermost *S. humphriesianum* zone (Table 2a). The LOD of this species is in the *D. levesquei* zone of the Upper Toarcian (Riding, 1984b). However, the highest occurrence datum (HOD) of *N. dictyambonis* has been reported from the *W. laeviuscula* zone (Riding and Thomas, 1992; Feist-Burkhardt and Wille, 1992). Thus, this report extends the range of this species into the *S. humphriesianum* zone. However, as this species only occurs as two isolated specimens it is possible that these have been reworked. *Valvaeodinium* spp. occurs in the *S. propinquans*/*S. humphriesianum* zone, this group has been recorded from the *W. laeviuscula* zone to the *P. parkinsoni* zone of northwest France by Feist-Burkhardt and Monteil (1997) but the genus *Valvaeodinium* has a LOD in the Upper Pliensbachian (*A. margaritatus* zone) as *V. armatum* (Morgenroth, 1970; Riding and Thomas, 1992). Other long-ranging species include the gonyaulacacean *Kallosphaeridium* spp. which has a LOD in the *L. opalinum* zone of the Lower Aalenian (Feist-Burkhardt and Wille, 1992). The non-gonyaulacaceans *Mancodinium semitabulatum*, *Moesiodinium railanui* and *Pareodinia ceratophora* have LODs in the Pliensbachian–lowermost Aalenian (Prauss, 1989; Riding and Thomas, 1992).

The Late Aalenian to Early Bajocian was an interval of significant archaeopyle experimentation within gonyaulacacean dinoflagellates, during which a number of new archaeopyle types appeared (Mantle and Riding, 2012). The appearance of the multi-plate precingular archaeopyle in *Dissiliodinium* and *Durotrigia*, in which two to five precingular plates are lost independently, is highly significant as this was the dominant excystment mode within gonyaulacaceans at this time. Furthermore, the appearance of *Chytroesphaeridia chytroides* represents the first appearance of the single-plate precingular archaeopyle (along with that of *Leptodinium* sp. cf. *L. subtile* in the *W. laeviuscula* zone in Scotland (Riding et al., 1991)). This became one of

Quantitative dinoflagellate cyst range chart for borehole B404/2 showing lowest occurrences from the Upper Aalenian to Lower Bajocian. P = present outside of count, ? = questionable occurrence. Taxa belonging to the family Gonyaulacaceae are highlighted in grey. Substages: U.A. — Upper Aalenian, L.B. — Lower Bathonian. Ammonite biozones: G. c — *G. concavum*, W./I. S.p — *W. laeviscula*/S. *propinquans*, S. p/S.h — *S. propinquans*/S. *humphriesianum*. Lithostratigraphical units: E. Fm. — Eisensandstein Formation, H. O. Mb — Humphriesi Oolith Member, S. Mb — Subfurcatus Oolith Member, P. Mb — Parkinsoni Oolith Member. Dent. Fm. — Dentalienum Formation.

[illegible]

Quantitative dinoflagellate cyst range chart for corehole B404/2 showing lowest occurrences for the Upper Bajocian to Lower Bathonian. P = present outside of count, ? = questionable occurrence. Taxa belonging to the family Gonyaulacaceae are highlighted in grey. Substages: L.B. – Lower Bathonian. Lithostratigraphical units: S. Mb – Subfucaten Oolith Member, P. Mb – Parkinsoni Oolith Member, Dent. Fm – Dentalient Formation.

[illegible]

Dinoflagellate cyst diversity increases through *S. humphriesianum* and *S. niortense* zones, and a number of important gonyaulacacean taxa have lowest occurrences through this interval, with a steady increase in diversity. In the *S. humphriesianum* zone, 15 dinoflagellate cyst species occur, 13 of these belong to the family Gonyaulacaceae, and many mark the LOD of each genus and/or species. *Acanthaulax crista*, *Ellipsoidictyum/Valensiella* complex, *Meiourogonyaulax valensii*, *Meiourogonyaulax* spp., *Rhynchodiniopsis? regalis* and *Valensiella ovulum* are known to have LODs in the *S. humphriesianum* zone, and these

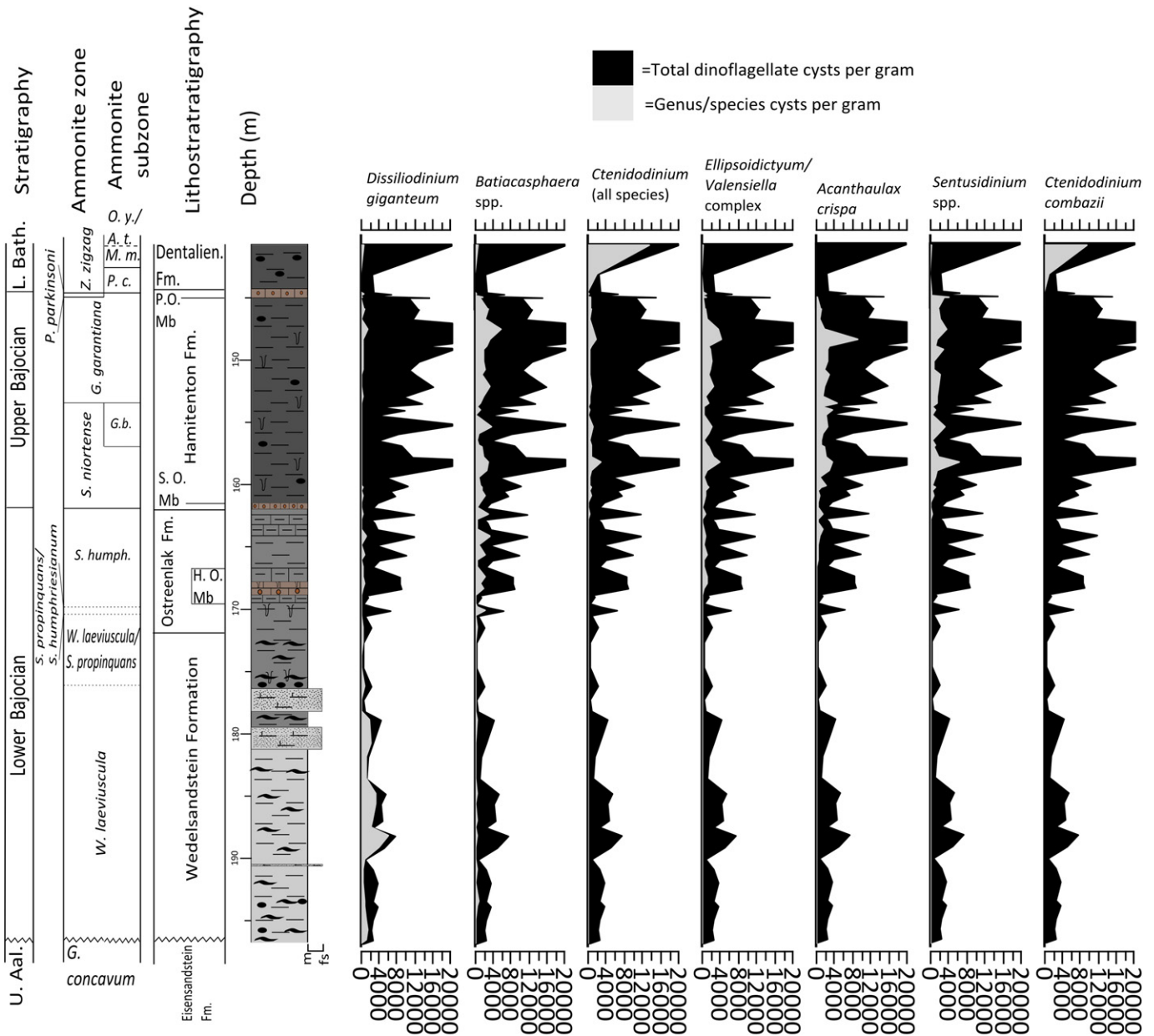


Fig. 6. Absolute abundances of dominant groups of dinoflagellate cysts for borehole B404/2. Note the abundance of *D. giganteum* in the Lower Bajocian. This species declines in abundance through the *S. humphriesianum* zone as several other groups increase in abundance.

represent the lowest occurrences of these genera (Feist-Burkhardt and Wille, 1992; Riding and Thomas, 1992; Feist-Burkhardt and Monteil, 1997). Similarly, *Korystocysta* is known to have a LOD in the *S. humphriesianum* zone as *K. gochti* (Feist-Burkhardt and Wille, 1992) and the occurrence of *Korystocysta* sp. 1 in lower part of this zone (sample S49) is coeval with this. The occurrence of *Ctenidodinium sellwoodii* in the uppermost part of the *S. humphriesianum* zone places the LOD of this species close to the Lower/Upper Bajocian transition, which has previously been reported as Upper Bajocian *G. garantiana* zone (Feist-Burkhardt and Wille, 1992; Riding and Thomas, 1992). The presence of *Jansonias psilata* is the first record of this species from Europe, and marks the LOD of this small distinctive genus, which has previously been placed in the Lower Bathonian as *Jansonias* sp. (Riding and Thomas, 1992).

Several morphotypes appear through the *S. humphriesianum* zone which may be early representatives of gonyaulacacean genera which became prominent components of Middle–Late Jurassic dinoflagellate cyst floras. *Rhynchodiniopsis*? spp., is a group of

enigmatic gonyaulacacean morphotypes, which may represent early representatives of the *Gonyaulacysta* complex and has a lowest occurrence in this zone. Likewise, *Endoscrinium*? spp. comprises a group with poorly developed cavation, which may be precursors of true species of this genus, although the LOD of this genus is in the *W. laeviuscula* zone as *Endoscrinium* sp. (Feist-Burkhardt and Wille, 1992). The occurrence of *Endoscrinium* represents the first cavate gonyaulacacean dinoflagellate cyst, and thus the separation of wall layers appears to have been developed in gonyaulacaceans during the Early Bajocian.

In the *S. niortense* zone, 10 dinoflagellate cyst taxa, 8 of which are gonyaulacaceans, have lowest occurrences (Table 2b). The occurrence of *Ctenidodinium cornigerum* in this zone represents the LOD of this species, which was previously recorded from the *P. parkinsoni* zone of the Upper Bajocian (Feist-Burkhardt and Monteil, 1997; Poulsen, 1998). *Ctenidodinium continuum* also occurs in this zone although the LOD of this species is in the *S. humphriesianum* zone in southern Germany (Feist-Burkhardt and Wille, 1992). Similarly, *Gonyaulacysta pectinigera* also has a LOD in the *S. humphriesianum* zone of southern Germany

(Feist-Burkhardt and Wille, 1992). The occurrence of *Korystocysta pachyderma* in the uppermost part of the zone (sample S82) represents the LOD of this species which has previously been recorded from the *P. parkinsoni* zone (Prauss, 1989).

Endoscrinium sp. cf. *E. luridum* has been reported from the Upper Bajocian–Lower Bathonian of Australia by Mantle and Riding (2012), the LOD of this morphotype herein is in the lower *S. niortense* zone. The occurrence of *Eodinia?* spp. may be an early representative (precursor) of this genus, as *Eodinia* sp. appears in the uppermost Bajocian (Feist-Burkhardt and Monteil, 1997).

Non-gonyaulaccean taxa which occur in the *S. niortense* zone include *Valvaeodinium vermicylindratum*, which has a LOD in the *S. niortense* zone of northwest France (Feist-Burkhardt and Monteil, 1997). However, *Carphodinium predae* has a LOD in the lowermost Bajocian *H. discites* zone of northern Germany (Prauss, 1989).

Our data show (Fig. 6) that the decline in the absolute abundance of *Dissilodinium giganteum* occurs concomitantly with the increase in the abundances of other gonyaulacceans. *Dissilodinium giganteum* and other species of this genus form a comparatively minor component of the dinoflagellate cyst flora through this interval compared to the Lower Bajocian. By comparison, the gonyaulacceans *Acanthaulax crisa*, *Batiacosphera* spp., *Ellipsoidictyum/Valensiella* complex, *Ctenidodinium* and *Sentusidinium* spp., increase in abundance. The absolute abundance of dinoflagellate cysts markedly increases through the *S. humphriesianum* and *S. niortense* zones.

Michrystidium spp. comprises 20–50% of the aquatic palynoflora through the *S. humphriesianum* zone although this decreases through the *S. niortense* zone to <20%. This is caused by the increase in the absolute abundance of dinoflagellate cysts as the absolute abundance of *Michrystidium* spp. remains relatively constant. The terrestrial palynoflora continues to be dominated by trilete spores.

6.4. Upper Bajocian to Lower Bathonian: *G. garantiana*, *P. parkinsoni* and *Z. zigzag* zones

Diversity increases continuously through the Upper Bajocian and lowermost Bathonian, with numerous LODs. In the *G. garantiana* zone, there are lowest occurrences of 7 taxa, 6 of which are gonyaulacceans. *Endoscrinium asymmetricum* and *Wanaea acollaris* occur in the uppermost part of the *G. garantiana* zone. The LODs of these species are in the *S. niortense* and *S. humphriesianum* zones in southern Germany respectively (Feist-Burkhardt and Wille, 1992). *Mendicodinium* sp. is the first recorded example of this genus from the Bajocian of Germany, although it is long-ranging, with a LOD in the Pliensbachian of Germany as *M. reticulum* (Morgenroth, 1970). *Korystocysta aldrigei* sp. nov. questionably occurs in one sample (S89). The occurrence of the pareodiniacean *Protobatioladinium mercieri* lowers the LOD of this species which was recorded from the *P. parkinsoni* zone of northern France (Feist-Burkhardt and Pross, 1999).

In the *P. parkinsoni* zone 13 taxa, 11 of which are gonyaulacceans have lowest occurrences. The occurrence of *Ctenidodinium combazii* in the *P. parkinsoni* zone represents the LOD of this species (Feist-Burkhardt and Wille, 1992), which is a reliable marker for the Bajocian/Bathonian transition. *Aldorfia aldrifensis* has a range base in the *P. parkinsoni* zone, though the LOD of this species is in the *S. humphriesianum* zone (Feist-Burkhardt and Wille, 1992). *Leptodinium* sp. represents the lowest occurrence of this genus from the Bajocian of Germany; although the LOD has been reported from the lowermost Bajocian *W. laeviuscula* zone of the Inner Hebrides by Riding et al. (1991) as *Leptodinium* sp. cf. *L. subtile*. The occurrence of *Tubotuberella* sp. is the lowest reported example of this genus in the Jurassic of Germany, previously recorded from the Lower Bathonian *Z. zigzag* zone as *Tubotuberella dangeardii* (Feist-Burkhardt and Wille, 1992). However, the genus has been reported from Upper Bajocian (*G. garantiana* zone) of England by Woollam and Riding (1983) as

Tubotuberella spp. Other gonyaulacceans to occur include *Korystocysta* sp. 2. and *Wanaea* sp. 1 and sp. 2. These genera are known to have range bases in the *S. humphriesianum* zone (Feist-Burkhardt and Wille, 1992). *Bradleyella* sp. was reported from sample S105. However, the LOD of this genus, as *B. adela*, is in the lowermost Bajocian (*H. discites* zone) (Riding and Thomas, 1992). *Valensiella ampulla* also occurs in the *P. parkinsoni* zone, but has a LOD in the *G. garantiana* zone of northern Germany (Prauss, 1989).

Seven species occur in the *Z. zigzag* zone of the Lower Bathonian. Gonyaulaccean species include *Atopodinium polygonale*, *Ctenidodinium ornatum*, *Gonyaulacysta jurassica* subsp. *adecta*, *Korystocysta gochtii* and *Meiourogonyaulax* sp. cf. *M. caytonensis*. However, this zone has been incompletely sampled and thus is not fully represented. The lowest occurrence of *Gonyaulacysta jurassica* subsp. *adecta* is coeval in southern England (Fenton et al., 1980). *Orobodinium* sp. A of Wille & Gocht (1990) is the only non-gonyaulaccean to have a lowest occurrence in this zone, whilst the higher taxonomic classification of *Impletosphaeridium* is uncertain, but may be gonyaulaccean.

The appearance of species of *Ctenidodinium*, *Korystocysta*, *Mendicodinium* and *Wanaea* demonstrates that taxa with epicystal archaeopyles became prominent during the Late Bajocian and Early Bathonian. Whilst the occurrence of *Aldorfia aldrifensis*, *Atopodinium polygonale* and *Gonyaulacysta jurassica* subsp. *adecta* demonstrate that the 1P archaeopyle was becoming increasingly common within gonyaulacceans at this time. This is further demonstrated by the high abundance of *Acanthaulax crisa* through the Upper Bajocian.

The abundance data (Fig. 6) show a similar pattern through the *G. garantiana* and *P. parkinsoni* zones to that of the underlying *S. humphriesianum* and *S. niortense* Zones, with the dominance of *Acanthaulax crisa*, *Batiacosphera* spp., *Ctenidodinium*, *Ellipsoidictyum/Valensiella* complex and *Sentusidinium* spp. However, a sudden change occurs in the *Z. zigzag* zone, where *Ctenidodinium* becomes superabundant, comprising 60–70% of the dinoflagellate cyst flora. This is due to an enormous increase in the abundance of *Ctenidodinium combazii* which is present in one sample from the *P. parkinsoni* zone (S103) as a single specimen, yet comprises 45% of the dinoflagellate cyst flora in the two uppermost samples from the *Z. zigzag* zone (Fig. 6). The relative and absolute abundance of acritarchs, largely *Michrystidium* spp., remains relatively constant through the *G. garantiana* and *P. parkinsoni* zones before declining significantly in the *Z. zigzag* zone. Within the terrestrial palynoflora, the *G. garantiana* and *P. parkinsoni* zones continue to be dominated by trilete spores. However in the *Z. zigzag* zone trilete spores decline enormously in abundance and pollen becomes the dominant terrestrial palynomorphs group. Although the absolute abundance of terrestrial palynomorphs declines in the *Z. zigzag* zone, pollen dominates over spores as there is a huge decrease in the absolute abundance of trilete spores.

7. The overall stratigraphical pattern of the Bajocian dinoflagellate cyst radiation

The integration of our stratigraphical data with published data on European Bajocian dinoflagellate cysts (Tables 3a, 3b) supports this more gradualistic and continuous pattern for this evolutionary radiation than the more stepwise configuration observed by Feist-Burkhardt and Monteil (1997). These authors reported a distinctly stepped pattern of inceptions, with the first burst of LODs at the Lower–Upper Bajocian transition (*S. humphriesianum* and *S. niortense* zones), and the second in the uppermost Bajocian (*P. parkinsoni* zone). There is a steady increase in LODs through the Lower Bajocian, prior to the *S. humphriesianum* zone, with the lowest occurrences of gonyaulaccean genera such as *Dissilodinium*, *Durotrigia*, *Chytroesphaeridia*, *Ctenidodinium* and *Gongylodinium* in the Upper Aalenian and Lower Bajocian. From the *S. humphriesianum* zone to the *Z. zigzag* zone, there is a rapid and continuous increase in diversity as nearly 100 species have lowest

Table 3a

Summary range chart for the Late Aalenian to Early Bathonian of western Europe, showing lowest occurrences from the *G. concavum* zone to the *S. humphriesianum* zone. Ranges are based on data from this study, Prauss (1989), Riding et al. (1991), Feist-Burkhardt and Wille (1992), Riding and Thomas (1992), Feist-Burkhardt and Monteil (1997), Feist-Burkhardt and Monteil (2001) and Feist-Burkhardt and Pross (2010). Taxa belonging to the family Gonyaulacaceae are highlighted in grey. X = present, X range altered from data from this study or new species range, ^ = ranges up, v = ranges down, T = range top, ? = questionable occurrence. Ammonite zones: *G. c* – *G. concavum*, *H. d* – *H. discites*, *W. l* – *W. laeviuscula*, *S. p* – *S. propinquans*, *S. h* – *S. humphriesianum*, *S. n* – *S. niortense*, *G. g* – *G. garantiana*, *P. p* – *P. parkinsoni*, *Z. z* – *Z. zigzag*.

| Substage/subage | Ammonite biozone | E/L. Bath. | Z. z. | P. p. | G. g. | S. n. | S. h. | S. p. | W. l. | H. d. | L/U. Aal. | G. c. |
|-----------------|---|------------|-------|-------|-------|-------|-------|-------|-------|-------|-----------|-------|
| | <i>Scrioceras weberi</i> | | x | | | | x | | | | T | v |
| | <i>Namoceras opambonis</i> | | | x | | | | | | | v | v |
| | <i>Valvaedonium spongiosum</i> | | | | | | | | | | v | v |
| | <i>Pareodinia ceratophora</i> | | | | | | | | | | v | v |
| | <i>Eschaspheeridia rudis</i> | | | | | | | | | | v | v |
| | <i>Valvaedonium punctatum</i> | | | | | | | | | | v | v |
| | <i>Susadnium delmense</i> | | | | | | | | | | v | v |
| | <i>Kalliosphaeridium prausi</i> | | | | | | | | | | v | v |
| | <i>Kalliosphaeridium capulatum</i> | | | | | | | | | | v | v |
| | <i>Namocerasopsis plegas</i> | | | | | | | | | | v | v |
| | <i>Namocerasopsis eve</i> | | | | | | | | | | v | v |
| | <i>Valvaedonium armatum</i> | | | | | | | | | | v | v |
| | <i>Beriacasphaera spp.</i> | | | | | | | | | | v | v |
| | <i>Valvaedonium brevipellitum</i> | | | | | | | | | | v | v |
| | <i>Namocerasopsis ditymbonis</i> | | | | | | | | | | v | v |
| | <i>Namocerasopsis spiculata</i> | | | | | | | | | | v | v |
| | <i>Moesiodinium ralleonii</i> | | | | | | | | | | v | v |
| | <i>Namocerasopsis gracilis</i> | | | | | | | | | | v | v |
| | <i>Namocerasopsis tricaros</i> | | | | | | | | | | v | v |
| | <i>Susadnium scrofoloides</i> | | | | | | | | | | v | v |
| | <i>Valvaedonium cavum</i> | | | | | | | | | | v | v |
| | <i>Maracodinium semibulatum</i> | | | | | | | | | | v | v |
| | <i>Phidolopsis elongata</i> | | | | | | | | | | v | v |
| | <i>Maracodinium coitum</i> | | | | | | | | | | v | v |
| | <i>Kalliosphaeridium spp.</i> | | | | | | | | | | v | v |
| | <i>Pareodinia ceratophora</i> | | | | | | | | | | v | v |
| | <i>Evansia spongogramulata</i> | | | | | | | | | | v | v |
| | <i>Evansia eschschensis</i> | | | | | | | | | | v | v |
| | <i>Preboldinium arcticum</i> | | | | | | | | | | v | v |
| | <i>Wellodinium cylindricum</i> | | | | | | | | | | v | v |
| | <i>Scrioceras priscus</i> | | | | | | | | | | v | v |
| | <i>Pareodinia labosa</i> | | | | | | | | | | v | v |
| | <i>Disisodinium giganteum</i> | | | | | | | | | | v | v |
| | <i>Disisodinium lichenoides</i> | | | | | | | | | | v | v |
| | <i>Disisodinium spp.</i> | | | | | | | | | | v | v |
| | <i>Disisodinium psilatum</i> | | | | | | | | | | v | v |
| | <i>Sentusidinium sp. cf. S. asymmetricum of Prauss (1989)</i> | | | | | | | | | | v | v |
| | <i>Valvaedonium euraeum</i> | | | | | | | | | | v | v |
| | <i>?Batiacaspheera sp. of Prauss (1989)</i> | | | | | | | | | | v | v |
| | <i>Hysterochidium sp. of Prauss (1989)</i> | | | | | | | | | | v | v |
| | <i>Durargia daveyi</i> | | | | | | | | | | v | v |
| | <i>Carpathodinium praecox</i> | | | | | | | | | | v | v |
| | <i>Bradleyella adida</i> | | | | | | | | | | v | v |
| | <i>Gongylodinium erymnoetichon</i> | | | | | | | | | | v | v |
| | <i>Durargia sp. cf. D. daveyi</i> 1 of F-B & M (1997) | | | | | | | | | | v | v |
| | <i>Durargia sp. 1 (this study)</i> | | | | | | | | | | v | v |
| | <i>Ctenodinium sp. 1 (this study)</i> | | | | | | | | | | v | v |
| | <i>Chyroesphaeridia dyrooides</i> | | | | | | | | | | v | v |
| | <i>Valvaedonium vermipellitum</i> | | | | | | | | | | v | v |
| | <i>Kalliosphaeridium? hypomatum</i> | | | | | | | | | | v | v |
| | <i>Leptodinium sp. cf. L. subtile of Riding et al. (1991)</i> | | | | | | | | | | v | v |
| | <i>Reutlingia gochti</i> s. l | | | | | | | | | | v | v |
| | <i>Namocerasopsis spp.</i> | | | | | | | | | | v | v |
| | <i>Disisodinium? boeatum</i> | | | | | | | | | | v | v |
| | <i>Valvaedonium spp.</i> | | | | | | | | | | v | v |
| | <i>Kalyptra stegata</i> | | | | | | | | | | v | v |
| | <i>Orobodinium automobile</i> | | | | | | | | | | v | v |
| | <i>Meiouragonyaulax caytonensis</i> | | | | | | | | | | v | v |
| | <i>Sentusidinium spp.</i> | | | | | | | | | | v | v |
| | <i>Ellipsodictyum/Walsella complex</i> | | | | | | | | | | v | v |
| | <i>Jansonia psila</i> | | | | | | | | | | v | v |
| | <i>Ctenodinium sp. 2 (this study)</i> | | | | | | | | | | v | v |
| | <i>Endoscrinium ? spp. (this study)</i> | | | | | | | | | | v | v |
| | <i>Meiouragonyaulax spp.</i> | | | | | | | | | | v | v |
| | <i>Valensella ovulum</i> | | | | | | | | | | v | v |
| | <i>Endoscrinium spp.</i> | | | | | | | | | | v | v |
| | <i>Dinaurella sp. 1 of F-B & M (1997)</i> | | | | | | | | | | v | v |
| | <i>Valvaedonium sp. cf. V. sphaerecthinum of F-B & M (1997)</i> | | | | | | | | | | v | v |
| | <i>Batiacaspheera laevigata</i> | | | | | | | | | | v | v |
| | <i>Durargia flupicata</i> s. l | | | | | | | | | | v | v |
| | <i>Wanaea acollaris</i> | | | | | | | | | | v | v |
| | <i>Dinaurella pygma</i> | | | | | | | | | | v | v |
| | <i>Acanthaulax crispata</i> | | | | | | | | | | v | v |

occurrences. However, it is notable that the number of LODs is highest in the *S. humphriesianum* and *P. parkinsoni* zones. Around half the LODs in the *P. parkinsoni* zone in our literature compilation are only recorded in northern France. There were fewer occurrences

in Swabia through this interval. This may reflect the condensed nature of the *P. parkinsoni* zone in this region, whereas in northern France it is greatly expanded, and provides a more complete record.

Table 3b

Summary range chart for the Late Aalenian to Early Bathonian of western Europe, showing lowest occurrences from the *S. niortense* zone to the *Z. zigzag* zone. Ranges are based on data from this study, Prauss (1989), Riding et al. (1991), Feist-Burkhardt and Wille (1992), Riding and Thomas (1992), Feist-Burkhardt and Monteil (1997), Feist-Burkhardt and Monteil (2001) and Feist-Burkhardt and Pross (2010). Taxa belonging to the family Gonyaulacaceae are highlighted in grey. X = present, X range altered from data from this study or new species range, ^ = ranges up, v = ranges down, T = range top, ? = questionable occurrence. Ammonite zones: *G. c* – *G. concavum*, *H. d* – *H. discites*, *W. l* – *W. laeviuscula*, *S. p* – *S. propinquans*, *S. h* – *S. humphriesianum*, *S. n* – *S. niortense*, *G. g* – *G. garantiana*, *P. p* – *P. parkinsoni*, *Z. z* – *Z. zigzag*.

| Substage/subage | | Ammonite biozone | E/L Bath. | Z. z. | P. p. | G. g. | S. n. | S. h. | S. p. | W. l. | H. d. | L/U Aal. | G. c. |
|--|------------------|---|-----------|-------|-------|-------|-------|-------|-------|-------|-------|----------|-------|
| Late/Upper Bajocian | Ammonite biozone | <i>Meiouragonyaulax valensii</i> s. l | x | ^ | x | x | x | x | x | x | x | | |
| | | <i>Rhychnodiniopsis?</i> <i>regalis</i> | ^ | | x | x | x | x | x | x | x | x | |
| | | <i>Aldorfia alderjensis</i> | ^ | | x | x | x | x | x | x | x | x | |
| | | <i>Valvaedonium spinosum</i> | ^ | | x | x | x | x | x | x | x | x | |
| | | <i>Gonyaulacysta pectinifera</i> | ^ | | x | x | x | x | x | x | x | x | |
| | | <i>Korysocyssa gochti</i> | ^ | | x | x | x | x | x | x | x | x | |
| | | <i>Rossvangia simplex</i> | ^ | | x | x | x | x | x | x | x | x | |
| | | <i>Ctenododium continuum</i> | ^ | | x | x | x | x | x | x | x | x | |
| | | <i>Altopodium polygonale</i> | ^ | | x | x | x | x | x | x | x | x | |
| | | <i>Valvaedonium vermicyclindratum</i> | ^ | | x | x | x | x | x | x | x | x | |
| | | <i>Endoscrinium luridum</i> s. l | ^ | | x | x | x | x | x | x | x | x | |
| | | <i>Lithodina jurassica</i> s. l | ^ | | x | x | x | x | x | x | x | x | |
| | | <i>Rhychnodiniopsis?</i> spp. (this study) | ^ | x | | x | x | x | x | x | x | x | |
| | | <i>Durongia</i> ? sp. 2 (this study) | ^ | x | | x | x | x | x | x | x | x | |
| | | <i>Eodina</i> ? spp. (this study) | ^ | x | | x | x | x | x | x | x | x | |
| | | <i>Meiouragonyaulax?</i> spp. (this study) | ^ | x | | x | x | x | x | x | x | x | |
| | | <i>Ctenododium corrugum</i> | ^ | x | | x | x | x | x | x | x | x | |
| | | <i>Endoscrinium</i> sp. cf. <i>E. luridum</i> (this study) | ^ | x | | x | x | x | x | x | x | x | |
| | | <i>Korysocyssa pachyderma</i> | ^ | x | | x | x | x | x | x | x | x | |
| | | <i>Wanaea indolenta</i> | ^ | x | | x | x | x | x | x | x | x | |
| | | <i>Comedodium</i> sp. 1 of F-B & M (1997) | ^ | x | | x | x | x | x | x | x | x | |
| | | <i>Valvaedonium</i> sp. 1 of F-B & M (1997) | ^ | x | | x | x | x | x | x | x | x | |
| | | <i>Endoscrinium asymmetricum</i> | ^ | x | | x | x | x | x | x | x | x | |
| | | <i>Ctenododium ornatum</i> | ^ | x | | x | x | x | x | x | x | x | |
| | | <i>Rhychnodiniopsis</i> sp. cf. <i>R? regalis</i> (this study) | ^ | x | | x | x | x | x | x | x | x | |
| | | <i>Mendicodinium</i> sp. (this study) | ^ | x | | x | x | x | x | x | x | x | |
| | | <i>Eodina?</i> sp. (this study) | ^ | x | | x | x | x | x | x | x | x | |
| | | <i>Sentusidinium</i> sp. cf. <i>S. baculatum</i> | ^ | x | | x | x | x | x | x | x | x | |
| | | <i>Chlamydophorella</i> sp. cf. <i>C. nyei</i> of Prauss (1989) | ^ | x | | x | x | x | x | x | x | x | |
| | | <i>Ctenodinium</i> spp. (this study) | ^ | x | | x | x | x | x | x | x | x | |
| | | <i>Rhychnodiniopsis?</i> spp. (this study) | ^ | x | | x | x | x | x | x | x | x | |
| | | <i>Valensella ampulla</i> | ^ | x | | x | x | x | x | x | x | x | |
| | | <i>Ctenodinium tenellum</i> | ^ | x | | x | x | x | x | x | x | x | |
| | | <i>Ambonesphaera hemicavata</i> | ^ | x | | x | x | x | x | x | x | x | |
| | | <i>Probolodinium mercuri</i> | ^ | x | | x | x | x | x | x | x | x | |
| | | <i>Bradleyella</i> sp. (this study) | ^ | x | | x | x | x | x | x | x | x | |
| <i>Leptodinium</i> sp. (this study) | ^ | x | | x | x | x | x | x | x | x | | | |
| <i>Tuboubarella</i> sp. (this study) | ^ | x | | x | x | x | x | x | x | x | | | |
| <i>Wanaea</i> sp. 1 (this study) | ^ | x | | x | x | x | x | x | x | x | | | |
| <i>Wanaea</i> sp. 2 (this study) | ^ | x | | x | x | x | x | x | x | x | | | |
| <i>Korysocyssa aldrigeli</i> sp. nov. | ^ | x | | x | x | x | x | x | x | x | | | |
| <i>Orobodinium</i> sp. A of Gocht & Wille (1990) | ^ | x | | x | x | x | x | x | x | x | | | |
| <i>Orobodinium</i> sp. B of Gocht & Wille (1990) | ^ | x | | x | x | x | x | x | x | x | | | |
| <i>Epilophosphaera gochti</i> | ^ | x | | x | x | x | x | x | x | x | | | |
| <i>Orobodinium</i> sp. C of Gocht & Wille (1990) | ^ | x | | x | x | x | x | x | x | x | | | |
| <i>Orobodinium rete</i> | ^ | x | | x | x | x | x | x | x | x | | | |
| <i>Durongia omenifera</i> | ^ | x | | x | x | x | x | x | x | x | | | |
| <i>Willeidinium baocassum</i> | ^ | x | | x | x | x | x | x | x | x | | | |
| <i>Disisodinium minimum</i> | ^ | x | | x | x | x | x | x | x | x | | | |
| <i>Disisodinium?</i> sp. 1 of F-B & M (1997) | ^ | x | | x | x | x | x | x | x | x | | | |
| <i>Valvaedonium</i> sp. 2 of F-B & M (1997) | ^ | x | | x | x | x | x | x | x | x | | | |
| <i>Pareodinia</i> sp. 1 of F-B & M (1997) | ^ | x | | x | x | x | x | x | x | x | | | |
| <i>Orobodinium</i> sp. 1 of F-B & M (1997) | ^ | x | | x | x | x | x | x | x | x | | | |
| <i>Cleisrosphaeridium</i> sp. of F-B & M (1997) | ^ | x | | x | x | x | x | x | x | x | | | |
| <i>Sirindiniopsis orbis</i> | ^ | x | | x | x | x | x | x | x | x | | | |
| <i>Meiouragonyaulax borealis</i> | ^ | x | | x | x | x | x | x | x | x | | | |
| <i>Pareodinia prolongata</i> | ^ | x | | x | x | x | x | x | x | x | | | |
| <i>Meiouragonyaulax</i> sp. cf. <i>M. callomani</i> of Prauss (1989) | ^ | x | | x | x | x | x | x | x | x | | | |
| <i>Gonyaulacysta esenackii</i> | ^ | x | | x | x | x | x | x | x | x | | | |
| <i>Sirindiniopsis</i> sp. of Prauss (1989) | ^ | x | | x | x | x | x | x | x | x | | | |
| <i>Ctenodinium combazii</i> | ^ | x | | x | x | x | x | x | x | x | | | |
| <i>Mosacodinium</i> sp. cf. <i>M. mosaicum</i> of F-B & M (1997) | ^ | x | | x | x | x | x | x | x | x | | | |
| <i>Ellipsodictyum cinctum</i> | ^ | x | | x | x | x | x | x | x | x | | | |
| <i>Sentusidinium asymmetricum</i> | ^ | x | | x | x | x | x | x | x | x | | | |
| <i>Gen. and sp. indet. 1 of F-B & M (1997)</i> | ^ | x | | x | x | x | x | x | x | x | | | |
| <i>Meiouragonyaulax</i> sp. cf. <i>M. caytonensis</i> (this study) | ^ | x | | x | x | x | x | x | x | x | | | |
| <i>Impleosphaeridium</i> sp. 1 (this study) | ^ | x | | x | x | x | x | x | x | x | | | |
| <i>Wanaea</i> sp. 1 of F-B & M (1997) | ^ | x | | x | x | x | x | x | x | x | | | |
| <i>Epilophosphaera</i> spp. | ^ | x | | x | x | x | x | x | x | x | | | |
| <i>Eodina</i> sp. of F-B & M (1997) | ^ | x | | x | x | x | x | x | x | x | | | |
| <i>Tuboubarella dangardi</i> | ^ | x | | x | x | x | x | x | x | x | | | |
| <i>Gonyaulacysta jurassica</i> subsp. <i>adacta</i> | ^ | x | | x | x | x | x | x | x | x | | | |
| <i>Impleosphaeridium</i> sp. 2 (this study) | ^ | x | | x | x | x | x | x | x | x | | | |

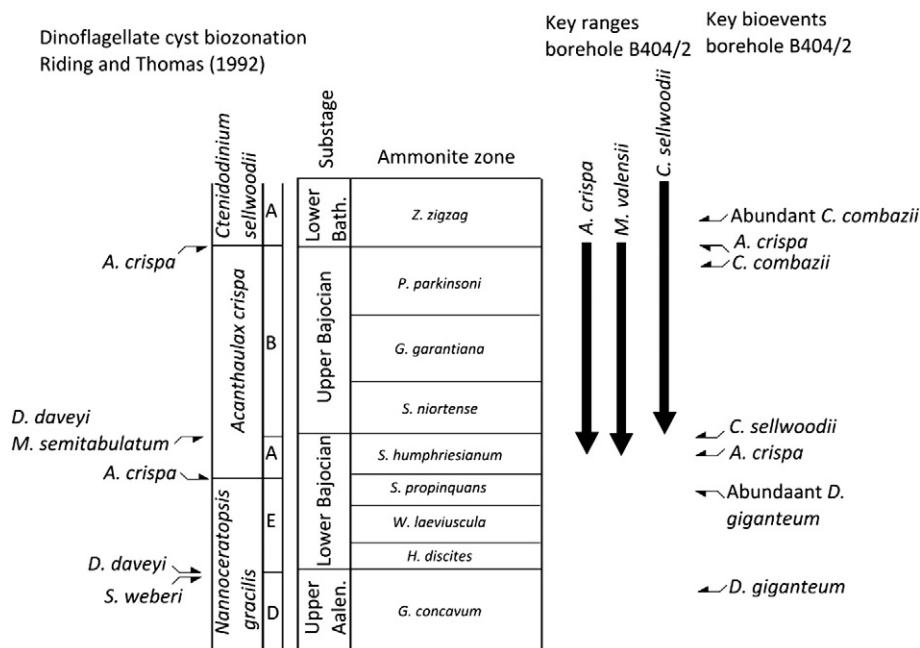


Fig. 7. Biostratigraphic summary of the dinoflagellate cyst zonation of Europe (after Riding and Thomas (1992)), with comparison to key ranges and bioevents within borehole B404/2. Chronostratigraphy generated in Timescale Creator v. 6.4.

Relative sea level appears to have played an important role in controlling the stratigraphical appearance of dinoflagellate cysts as a major marine transgression occurred during the Bajocian (Hallam, 2001). In the Boreal Realm, this was a two-pulsed second-order transgression (Jacquin et al., 1998). The steady increase in LODs throughout the Upper Aalenian and Lower Bajocian may reflect the first pulse of this transgression, while the large number of LODs from the *S. humphriesianum* to *Z. zigzag* zones may reflect the second pulse of the transgression throughout Europe at this time. The high number of LODs in the *S. humphriesianum* zone reflects this rapid initial phase of this transgression. In borehole B404/2, the sequence boundary which marks the base of the second transgressive pulse is at the base of the Humphresi Oolite Member (Fig. 4) and many LODs occur above this point.

8. Biostratigraphical and palaeoenvironmental implications

8.1. Dinoflagellate cyst markers in the Bajocian of Swabia

The Lower Bajocian *W. laeviuscula* and *W. laeviuscula/S. propinquans* zones are defined by an acme of *Dissiliodinium giganteum*, which typically comprises 30–85% of dinoflagellate cysts through this interval. Gedl (2008) and Gedl and Józsa (2015) reported abundant *D. giganteum* in Lower Bajocian deep marine flysch and hemipelagic deposits of the Pieniny Klippen Basin of southern Poland and northern Slovakia (although the presence of *D. giganteum* has been used in this region to recognise the Lower Bajocian). In contrast, this species occurs rarely in the Lower Bajocian carbonate facies of Dorset and Normandy (unpublished data; Feist-Burkhardt and Monteil, 1997). This implies there may be some facies control on the distribution of this species. We interpret *D. giganteum* as a species which thrived in environments with elevated nutrient levels as it occurs abundantly in facies which contain large amounts of terrigenous material (this study; Gedl, 2008; Gedl and Józsa, 2015). Nutrient levels would have been elevated due to terrestrial run-off. In contrast it occurs rarely in areas which received little terrestrial input during the Middle Jurassic such as the carbonate ramps of Dorset and Normandy. The large size of this species further suggests it inhabited high nutrient environments as large phytoplankton cells require higher nutrient levels (Marañón, 2015). The abundance of *D. giganteum* in successions with abundant terrestrial material also

suggests it could inhabit environments with reduced salinities. The acme of *D. giganteum* in the Lower Bajocian is therefore a useful biostratigraphical marker in the Swabian Basin, southern Poland and northern Slovakia. This work extends the total range of *D. giganteum* significantly; the LOD is lowered to (at least) the *G. concavum* zone of the Upper Aalenian and the HOD is extended from the *S. humphriesianum* zone to (at least) the *Z. zigzag* zone of the Lower Bathonian. Therefore the range of *D. giganteum* is not stratigraphically useful in the subdivision of the Bajocian, at least within Swabia.

The *W. laeviuscula/S. propinquans* and lower part of the *S. humphriesianum* zones is the interval between the acme of the *Dissiliodinium giganteum* (top of abundant *D. giganteum*) and the LOD of *Acanthaulax crisa* (Fig. 7). The middle of the *S. humphriesianum* zone to the lowermost part of the *Z. zigzag* zone (*P. convergens* subzone) is defined by the total range of *Acanthaulax crisa*, an excellent stratigraphical marker as it occurs consistently and in moderate to high abundance. *Meiourogoniaulax valensii* has a range identical to that of *Acanthaulax crisa* herein and also occurs in moderate abundance, making it a useful marker species. *Acanthaulax crisa* was widely distributed during the Bajocian, and has been reported from marginal-marine to offshore facies from the Upper Bajocian throughout Europe as well the Upper Bajocian of offshore Western Australia (Mantle and Riding, 2012). This implies it was a cosmopolitan species and was euryhaline/eurythermal.

The LOD of *Ctenidodinium sellwoodii* is an excellent stratigraphical marker in the B404/2 borehole for the Lower/Upper Bajocian transition and the overlap range of this species with *Acanthaulax crisa* is a good marker for the Upper Bajocian (*S. niortense*, *G. garantiana* and *P. parkinsoni* zones). *Acanthaulax crisa* and *Meiourogoniaulax valensii* have HODs in the *P. convergens* subzone of the *Z. zigzag* zone and are good markers for the Bajocian/Bathonian boundary. The lowermost Bathonian — *Z. zigzag* zone, *M. macrescens* and *O. yeovilensis/A. tenuiplicatus* subzones, are characterised by the acme of *Ctenidodinium*, particularly *Ctenidodinium combazii*, which comprises around 45% of dinoflagellate cysts (Fig. 6). This acme of *Ctenidodinium combazii* in the Lower Bathonian has been reported throughout much of northwest Europe, including southern Germany, northern France and southern England (Riding et al., 1985; Feist-Burkhardt and Monteil, 1997); however, it was absent in paralic/deltaic environments of central/northern

England, the North Sea and the Isle of Skye, Scotland (Riding et al., 1985; Riding et al., 1991). In these regions, *Ctenidodinium sellwoodii* and *Korystocysta* spp. were dominant; Riding et al. (1985) interpreted *C. combazii* as a species which occupied open marine environments and could not tolerate reduced salinities, and *C. sellwoodii* and *Korystocysta* spp. as euryhaline. The B404/2 data support this interpretation as the enormous increase in the abundance of *C. combazii* occurs within the *M. macrescens* subzone, which corresponds to the maximum transgression in Europe (Jacquin et al., 1998). This deepening environment brought *C. combazii* into the Swabian Basin. Moreover, the sedimentology of the succession indicates that this point corresponds to a maximum flooding surface as there are abundant nodules which often form during intervals of sediment starvation and condensation associated with transgression in distal areas. However, Gedl (2012) and Gedl et al. (2012) reported peaks in the abundance of *C. combazii* associated with terrestrial influx and higher sedimentation rates in the Middle Bathonian of central Poland. Consequently, these authors interpreted *C. combazii* as having thrived in conditions of lowered salinity and elevated nutrient levels. In contrast, the absence/low abundance of this species from the marginal-marine facies of central/northern England and Scotland strongly suggests it could not tolerate extremely reduced salinities. Therefore it is possible this species inhabited a wide range of marine environments but was unable to inhabit nearshore areas with very low salinities. Consequently, the acme of *Ctenidodinium combazii* is an excellent stratigraphical marker for the Lower Bathonian *Z. zigzag* zone (*M. macrescens* and *O. yeovilensis/A. tenuiplicatus* subzones) in southern Germany, northern France and southern England, but may be diachronous outside of these areas.

8.2. Implications for the dinoflagellate cyst zonation of northwest Europe

The Jurassic dinoflagellate cyst biozonation of Europe was proposed by Woollam and Riding (1983) based predominantly on the dinoflagellate cyst biostratigraphy of Britain, and was later modified by Riding and Thomas (1992). The zonation of Poulsen and Riding (2003) combined data from northwest Europe to create a dinoflagellate cyst biozonation for sub-boreal Europe, which largely mirrors that of Riding and Thomas (1992). This zonation is summarised in Fig. 7.

The Bajocian is subdivided by the *Nannoceratopsis gracilis* interval biozone, sub-biozone E, which is defined as the interval between the LODs of *Durotrigia daveyi* and *Acanthaulax crispa* and corresponds to the Lower Bajocian, *H. discites* to *S. propinqua* zones. The *Acanthaulax crispa* total range biozone corresponds to the *S. humphriesianum* to *P. parkinsoni* zones. The crucial datum in these biozonations is the LOD of *Acanthaulax crispa*, which marks the top of the *Nannoceratopsis gracilis* biozone (and sub-biozone E) and the base of the *Acanthaulax crispa* biozone. As this work has examined the *S. humphriesianum* zone in unprecedented detail, we show that the LOD of *A. crispa* is in the middle of the zone, we also raise the HOD from the *P. parkinsoni* zone to the lowermost Bathonian, *Z. zigzag* zone, *P. convergens* subzone. Consequently, the top of the *Nannoceratopsis gracilis* and the base of the *Acanthaulax crispa* biozones are raised to the middle of the *S. humphriesianum* zone. As the HOD of *A. crispa* occurs in the lowest subzone of the lowest zone of the Bathonian, the top of the *A. crispa* biozone is effectively well calibrated with the Bajocian/Bathonian boundary (*P. parkinsoni* zone/*Z. zigzag* zone).

8.3. The application of existing dinoflagellate cyst biozonations in Swabia

The acme of *Dissiliodinium giganteum* and the interval between the abundant occurrence of *Dissiliodinium giganteum* and the LOD of *Acanthaulax crispa* is broadly comparable with *Nannoceratopsis gracilis* biozone, subbiozone E, and corresponds to the *W. laeviuscula* to *S. humphriesianum* zones. Unfortunately, as the *H. discites* zone is missing in borehole B404/2 due to a hiatus, it is not possible to locate the base of the abundance of *Dissiliodinium giganteum*, but in the sample from the

G. concavum zone, *Dissiliodinium giganteum* is only present in relatively low abundance, implying that the base of abundant *Dissiliodinium giganteum* is located between the *G. concavum* zone and the *W. laeviuscula* zone.

The *Acanthaulax crispa* total range biozone (Fig. 7) can be recognised in Swabia, and in this region the range of *Meiourogonia valensii* is also a good marker for this biozone as the range is identical to that of *Acanthaulax crispa*. Riding and Thomas (1992) and Poulsen and Riding (2003) subdivided this biozone into two subbiozones (Fig. 7). Subbiozone A corresponds to the *S. humphriesianum* zone, and is the interval between the LOD of *Acanthaulax crispa* and the HODs of *Durotrigia daveyi* and *Mancodinium semitabulatum*. Subbiozone B represents the *S. niortense* to *P. parkinsoni* zones, and is defined as the interval between the HODs of *Durotrigia daveyi*/*Mancodinium semitabulatum* and the HOD of *Acanthaulax crispa*. In the B404/2 section the HODs of *Durotrigia daveyi* and *Mancodinium semitabulatum* occur before the LOD of *Acanthaulax crispa*, although the former has been reported as ranging into the *G. garantiana* zone in southern Germany by Feist-Burkhardt and Wille (1992). Consequently, in Swabia the *Acanthaulax crispa* biozone is more usefully subdivided by the LOD of *Ctenidodinium sellwoodii*, which occurs in the uppermost sample of the *S. humphriesianum* zone (S62). The interval between the LODs of *Acanthaulax crispa* and *Ctenidodinium sellwoodii* corresponds to subbiozone A, whilst the interval between the LOD of *Ctenidodinium sellwoodii* and the HOD of *Acanthaulax crispa* corresponds to subbiozone B.

9. Conclusions

Cyst-forming dinoflagellates underwent a major radiation during the Late Aalenian to Early Bathonian, during which the gonyaulacaceans expanded to become the dominant family. Previous work has highlighted the importance of the Early–Late Bajocian transition as the critical step in this diversification. However, our work has revealed that this evolutionary burst was substantially more gradualistic, with a continuous increase in diversity throughout the Late Aalenian to Early Bathonian. However, the number of first appearances was highest during the Late Bajocian to Early Bathonian. The stratigraphical pattern of dinoflagellate cysts through this interval appears to have been controlled by relative sea level changes, as there was a major second order transgression during the Late Aalenian–Early Bathonian, which was particularly pronounced during the Late Bajocian. Biostratigraphically, we have confirmed the use of *Acanthaulax crispa* as a key index for the Upper/Late Bajocian, and have shown that the acme of *Dissiliodinium giganteum* is a useful stratigraphical marker for the Lower/Early Bajocian. The cause of the Bajocian dinoflagellate radiation remains to be resolved. However, in addition to plankton, ammonites, fishes and bivalves also diversified at this time (Hallam, 1976; O'Dogherty et al., 2006; Guinot and Cavin, 2015), implying that there were major evolutionary and ecological innovations in pelagic ecosystems as a whole, which may form part of the wider Mesozoic Marine Revolution.

Acknowledgements

This work has arisen from the PhD project of Nickolas J. Wiggan which is supported by NERC BGS DTG award reference BUFI S246, entitled *The mid Jurassic plankton explosion*. James B. Riding publishes with the approval of the Executive Director, British Geological Survey (NERC). Nick Butterfield is thanked for comments on earlier drafts of this manuscript. Michael Prauss is gratefully acknowledged for providing holotype photos of *Dissiliodinium psilatatum* which assisted with this study. We also thank Jennie Bull for the databasing of literature range chart data. Marcin Barski and an anonymous

reviewer are thanked for providing critical comments which improved this manuscript.

Appendix A. Systematic palaeontology

The taxonomic classification follows that of Fensome et al. (1993), except where emendations have been made. Minimum, mean and maximum dimensions are given as: minimum (mean) maximum.

Division DINOFLAGELLATA Fensome et al. 1993

Subdivision DINOPHYCAEA Fensome et al. 1993

Class DINOPHYCEAE Pascher 1914

Subclass PERIDINIPHYCIDAE Fensome et al. 1993

Order GONYAULACAEAE Taylor 1980

Suborder CLADOPYXIINEAE Fensome et al. 1993

Family CLADOPYXIACEAE Stein 1883

Jansonina Pocock 1972 emend. Riding & Walton in Riding et al. 1991

Jansonina psilata Martinez et al. 1999 (Plate X, 2)

Remarks: *Jansonina psilata* was recorded sporadically, and in low numbers from the *S. humphriesianum* zone to the *G. garantiana* zone, and is distinguished by its clearly defined tabulation (as low sutural crests), and psilate autophragm. This is the first record of this species from Europe.

Family PAREODINIACEAE Gocht 1957

Subfamily PAREODINIOIDEAE (Autonym)

Pareodinia Deflandre 1947 emend. Below 1990

Pareodinia ceratophora Deflandre 1947 emend. Gocht 1970 (Plate VIII, 1–2)

Remarks: *Pareodinia ceratophora* was encountered sporadically and in low to moderate abundances from the *W. laeviuscula* to the *Z. zigzag* zones and is variable in its morphology but is distinguished by its apical horn and elongate body; some specimens bear a kalyptra.

Dimensions: mean width: 54 µm; mean length including apical horn: 79 µm; 5 specimens measured.

Pareodinia halosa (Filatoff 1975) Prauss 1989 emend. Prauss 1989 (Plate VIII, 3–4)

Remarks: *Pareodinia halosa* was encountered consistently, in varying abundance, through *G. concavum* to *Z. zigzag* zones. This distinctive species is characterised by its subcircular shape and prominent kalyptra which is often highly variable in shape and size (which may be the result of differing preservation), a few specimens exhibit 'sculpting' of the kalyptra (Plate VIII, 4).

Dimensions: mean width of cyst with kalyptra: 50 µm; mean width of cyst body without kalyptra: 35 µm; length of cyst body with kalyptra: 59 µm; length of cyst body without kalyptra: 41 µm; 30 specimens measured.

Protobatioladinium Nøhr-Hansen 1986

Protobatioladinium mercieri Feist-Burkhardt & Pross 1999 (Plate VIII, 5–6)

Remarks: *Protobatioladinium mercieri* was recorded in three samples, one from the lowest part of the *G. garantiana* zone (S84) and two from the *Z. zigzag* zone. It is distinguished from *Pareodinia* by its archaeopyle which is formed from a combination of the anterior intercalary plates and apical homologues.

Subfamily BROOMEIOIDEAE (Eisenack 1969) Fensome et al. 1993

Carpathodinium Drugg 1978 emend. Below 1990

Carpathodinium predae (Beju 1971) Drugg 1978 emend. Below 1990 (Plate VI, 6)

Remarks: *Carpathodinium predae* was encountered sporadically and in low abundance from the *S. niortense* to *Z. zigzag* zones.

Kalyptea Cookson & Eisenack 1960 emend. Wiggins 1975

Kalyptea stegasta (Sarjeant 1961) Wiggins 1975

Remarks: *Kalyptea stegasta* was recorded outside of the count from one sample from the *P. parkinsoni* zone (S105) as a single specimen, its apical and antapical horns and kalyptra make this a highly distinctive species.

Family MANCODINIACEAE Fensome et al. 1993

Subfamily MANCODINIOIDEAE (Autonym)

Mancodinium Morgenroth 1970 emend. Below 1987

Mancodinium semitabulatum Morgenroth 1970 emend. Below 1987

Remarks: This species was recorded from three samples of the *W. laeviuscula* zone as a single specimen in each. The sulcal tab of the anterior sulcal plate and disintegration archaeopyle make it very distinctive.

Suborder GONYAULACINEAE (autonym)

Family GONYAULACEAE Lindemann 1928 emend. Feist-Burkhardt 1995

Subfamily GONYAULACOIDEAE (autonym)

Tubotuberella Vozzhennikova 1967 emend. Dodekova 1990

Tubotuberella sp.

Remarks: A single specimen with prominent apical and antapical cavation was recorded from sample S104 in the *P. parkinsoni* zone. The poor preservation prevented identification to species level.

Subfamily LEPTODINIOIDEAE Fensome et al. 1993

Acanthaulax Sarjeant 1968 emend. Sarjeant 1982

Acanthaulax crispa (Wetzel 1967) Woollam and Riding 1983 (Plate I, 1–6).

Remarks: *Acanthaulax crispa* was encountered consistently, in moderate to high abundance from the *S. humphriesianum* zone to the lowermost *Z. zigzag* zone. This species displays considerable morphological variation. Some forms (Plate I, 1) were very close to the morphology of the holotype in possessing a differentiated autophragm, intratabular crests, sutural crests with small capitate and/or baculate processes and an apical horn. However, many specimens are enigmatic and difficult to interpret, but have a thick, spongy differentiated autophragm, which is covered in dense rugulate ornamentation. Tabulation is variably expressed, usually indistinctly by low sutural ridges, sometimes formed from the merging of rugulate ornament. The development of sutural crests is highly variable. Some of these forms resemble *Aldorfia aldorfensis* (e.g. Plate I, 6), suggesting that *A. crispa* and *A. aldorfensis* are closely related. However these forms fall on a continuous morphological spectrum and have thus been included within *A. crispa*. A type 1P archaeopyle was commonly observed, formed by the loss of the 3" plate and in some specimens the archaeopyle is markedly elongate. The restricted range of *Acanthaulax crispa* makes it an excellent stratigraphical marker.

Dimensions: width: 43 (68) 83 µm; length: 54 (77) 103 µm; 50 specimens measured.

Aldorfia Stover & Evitt 1978

Remarks: Stover and Evitt (1978) erected *Aldorfia* to include species of the *Gonyaulacysta* complex which have two wall layers connected by dense fibrous ornament, with *Aldorfia aldorfensis* as the type species. However, *Aldorfia* is now monotypic and there is uncertainty regarding the precise nature of the wall layers. Fensome et al. (1993) assigned

Plate I. Selected dinoflagellate cysts from the B404/2 borehole. Scale bar represents 10 µm. The slide number and England Finder co-ordinates (EF co.) of figured specimens are noted.

1–6: *Acanthaulax crispa* (Wetzel 1967) Woollam and Riding 1983.

1: Dorsal view low focus, slide S63-1, EF co. S71, 2: dorsal view median focus, slide S71-B, EF co. Q51/3, 3: lateral view median focus, slide S74-B, EF co. T45/3, 4: dorso-lateral median focus, slide S91-C, EF co. V52/1, 5: dorso-lateral view median focus, slide S71-B, EF co. M35, 6: dorsal view median focus, slide S71-B, EF co. Q43/3.

7–12: *Aldorfia aldorfensis* (Gocht 1970) Stover & Evitt 1978.

7–9: Same specimen, dorso-ventral view 7: high focus 8: median focus 9: low focus, slide S105-A, EF co. F36.

10–12: Same specimen, dorso-ventral view 10: high focus 11: median focus 12: low focus, slide S105-A, EF co. K68/1.

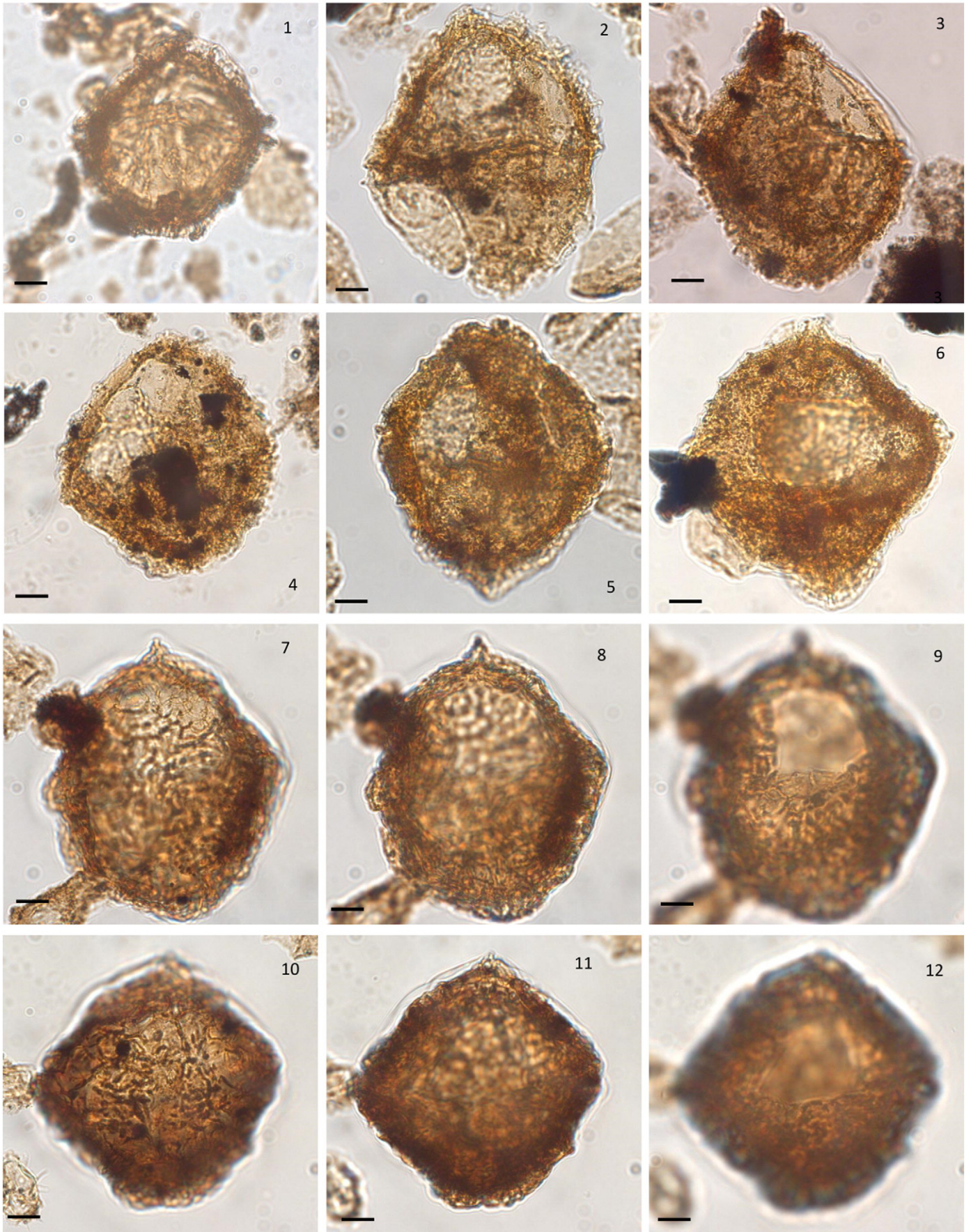


Plate I.

Aldorfia to the Cribroperidinoideae, however we place it in the Leptodinioidae as *Aldorfia aldoorfensis* clearly exhibits neutral torsion.

Aldorfia aldoorfensis (Gocht 1970) Stover & Evitt 1978 (Plate I, 7–12)

Remarks: *Aldorfia aldoorfensis* was encountered in the *P. parkinsoni* and *Z. zigzag* zones. This species is distinguished by its highly distinctive wall structure, composed of two layers, a dense, spongy differentiated autophragm and reticulate ectophragm which are connected by fibrous ornamentation. The outline is subovoidal with an apical horn; the ornamentation tends to be longer in the apical and antapical regions. The archaeopyle is type 1P, formed from the loss of the 3" plate.

Dimensions: mean width: 77 µm; mean length: 81 µm; 10 specimens measured.

Bradleyella Woollam 1983

Bradleyella sp. (Plate XI, 7)

Remarks: two specimens were recorded from sample S105 in the *P. parkinsoni* zone. It is distinguished from *B. adela* as it has a thicker autophragm and more prominently defined tabulation.

Ctenidodinium Deflandre 1939 emend. Benson 1985

Ctenidodinium combazii Dupin 1968 (Plate II, 1–3)

Remarks: *Ctenidodinium combazii* was recorded in high abundances from the *Z. zigzag* zone with a LOD in the *P. parkinsoni* zone. It is typified by its large size, prominent sutural crests which bear processes and a relatively small 1" plate. The autophragm is scabrate and relatively thick, and the sutural crests are highly variable in height between specimens (ranging from 2–13 µm) but are typically around 5 µm. Processes can be conical, bifurcate, trifurcate or multifurcate, often within a single specimen. The processes are frequently longest around the cingulum and the 1" plate. Disarticulated epicysts and hypocysts are common. Some specimens show intratabular growth bands on the hypocyst.

Dimensions: width with processes: 86 (108) 135 µm; width without processes: 54 (80) 95 µm; 30 specimens measured.

Ctenidodinium continuum Gocht 1970 (Plate II, 6)

Remarks: This species is typified by distinctive sawtooth-like denticular sutural crests; it was recorded consistently in low abundances from the lower part of the *S. niortense* zone to the *Z. zigzag* zone.

Ctenidodinium cornigerum Valensi 1953 emend. Jan du Chêne et al. 1985 (Plate II, 5)

Remarks: This species is similar in morphology to *C. sellwoodii*, but is distinguished by its longer processes. *Ctenidodinium cornigerum* can be distinguished from *C. combazii* by its less well-developed and lower su-

tural crests. Processes are often simple but can bifurcate, trifurcate multifurcate. It was recorded sporadically and in low numbers from the *S. niortense* to the *Z. zigzag* zones

Dimensions: width with processes: 65 (77) 108 µm; width without processes: 50 (63) 83 µm. 15 specimens measured.

Ctenidodinium ornatum (Eisenack 1935) Deflandre 1939 (Plate II, 4)

Remarks: a single specimen of *C. ornatum* was recorded from the uppermost sample (S109) of the *Z. zigzag* zone.

Ctenidodinium sellwoodii (Sarjeant 1975) Stover & Evitt 1978 (Plate III, 1–3)

Remarks: *Ctenidodinium sellwoodii* was recorded consistently from the uppermost sample of the *S. humphriesianum* zone to the *Z. zigzag* zone, generally occurring in low abundances through the Upper Bajocian. It occurs abundantly in the *Z. zigzag* zone of the Lower Bathonian. The consistent occurrence of this species makes its range base an excellent stratigraphical marker for the Lower–Upper Bajocian transition. This species is highly variable and is characterised by low sutural ridges or low crests which bear short processes, typically <7 µm in length. These are predominantly distally simple, but occasional bifurcate processes are rarely present. The number of processes is highly variable with some specimens having very few processes.

Dimensions: width: 54 (68) 94 µm; 30 specimens measured.

Ctenidodinium sp. 1 (Plate III, 4)

Diagnosis: proximate, acavate dinoflagellate cyst, autophragm only. The autophragm is <1 µm thick, scabrate in texture and dark in colour. Tabulation is indicated by low sutural ridges and crests which are surmounted by very fine (<0.5 µm in width) processes which are no longer than 2 µm in length. Operculum remains attached in nearly all specimens.

Remarks: *Ctenidodinium* sp. 1 was recorded sporadically, and in low abundances from the *S. laeviuscula* to the *S. humphriesianum* zones. This morphotype is defined by its small size, thick, scabrate autophragm, low sutural crests and ridges which may bear short (<2 µm) spines. The cingulum is prominent. Superficially, it strongly resembles *Durotrigia daveyi* and they can be difficult to distinguish when the archaeopyle is not easily observable. With its simple morphology, and strong resemblance to *Durotrigia daveyi*, *Ctenidodinium* sp. 1 may be an early representative of the genus. This form is similar to *C. sellwoodii*, but differs by its thicker, more robust autophragm and slender spines which are more densely inserted.

Plate II. Selected dinoflagellate cysts from the B404/2 borehole. Scale bar represents 10 µm. The slide number and England Finder co-ordinates (EF co.) of figured specimens are noted.

- 1–3: *Ctenidodinium combazii* Dupin 1968. 1: Antapical view, median focus, slide S108-A, EF co. S48, 2: dorsal-antapical view, median focus, S108-A, EF co. U73/2, 3: dorso-ventral view, median focus, slide S108-A, EF co. U47/2.
- 4: *Ctenidodinium ornatum* (Eisenack 1935) Deflandre 1939. Dorso-ventral view, median focus, slide S108-A, EF co. V67-1.
- 5: *Ctenidodinium cornigerum* Valensi 1953 emend. Jan du Chêne et al. 1985. Dorsal view, low focus, slide S108-A, EF co. V67/1.
- 6: *Ctenidodinium continuum* Gocht 1970. Ventral view, median focus, slide S97-A, EF co. J50.
- 7: *Korystocysta gochti* (Sarjeant 1976) Woollam 1983. Apical view, low focus, slide S108-A, EF co. Q60/4.
- 8: *Korystocysta pachyderma* (Deflandre 1938) Woollam 1983. Lateral view, median focus, slide S81-A, EF co. T43.
- 9: *Korystocysta* sp. 2. Dorso-ventral view, median focus, slide S104-A, EF co. N60/1.
- 10: *Korystocysta* sp. 1. Dorso-ventral view, median focus, slide S49-B, EF co. N57.
- 11: *Wanaea acollaris* Dodekova 1975 emend. Riding & Helby 2001. Dorso-ventral view/apical view, median focus, slide S108-A, EF co. R47/4.
- 12: *Mendicodinium* sp. Dorso-ventral view, median focus, slide S97-C, P53.

Plate III. Selected dinoflagellate cysts from the B404/2 borehole. Scale bar represents 10 µm. The slide number and England Finder co-ordinates (EF co.) of figured specimens are noted. (see on page 72)

- 1–3: *Ctenidodinium sellwoodii* (Sarjeant 1975) Stover & Evitt 1978. 1: Dorsal view, median focus, slide S108-A, EF co. V55/3, 2: antapical view, low focus, slide S108-B, EF co. N62/1, 3: dorsal view, high focus, slide S108-B, EF co. M35/1.
- 4: *Ctenidodinium* sp. 1. Ventro-lateral view, median focus, slide S24-1, EF co. CONTROL box
- 5: *Ctenidodinium* sp. 2. Antapical view, median focus, slide S71-B, EF co. L62.
- 6–9: *Eodinia?* spp. 6: Ventral view, high focus, slide S101-B, EF co. J65/1, 7: dorsal view, median focus, slide S74-B, EF co. P49, 8: dorso-ventral view, high focus, slide S74-B, EF co. T65/3, 9: dorso-ventral view, low focus, slide S71-B, EF co. E48/3.
- 10: *Rhynchodiniopsis? regalis* (Gocht 1970) Jan du Chêne et al. 1985. Dorso-ventral view, high focus, slide S99-A, EF co. F37/3.
- 11: *Rhynchodiniopsis* sp. cf. *R? regalis* (Gocht 1970) Jan du Chêne et al. 1985. Dorso-ventral view/lateral view, low focus, slide S95-A, EF co. W44.
- 12: *Leptodinium* sp. Dorso-ventral view, median focus, slide S105-A, EF co. O66/2.

Dimensions: mean width: 59 μm ; mean length: 49 μm ; 5 specimens measured.

Ctenodinium sp. 2 (Plate III, 5)

Remarks: This form resembles *C. sellwoodii*, but is distinguished by the processes around the cingulum which bear very slender, short, bifurcate to multifurcate processes. Some specimens exhibit

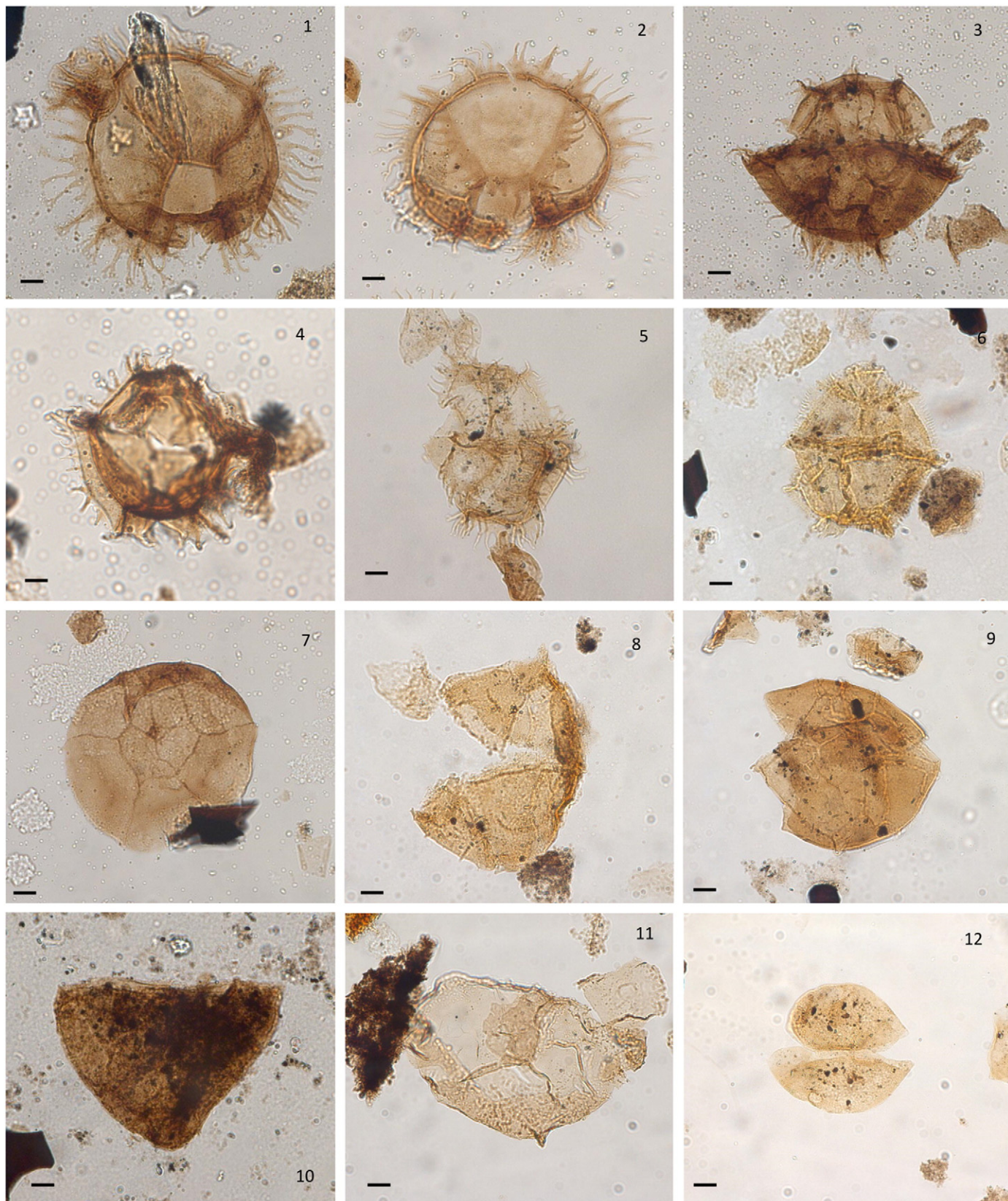


Plate II.

anastomosing processes. Specimens of *Ctenidodinium* sp. 2 were almost always encountered as disarticulated hypocysts or epicysts. This form was recorded consistently, in low numbers from the uppermost *S. humphriesianum* zone to the *Z. zigzag* zone.

Dimensions: mean width: 60 μm ; 5 specimens measured.
Ctenidodinium spp.

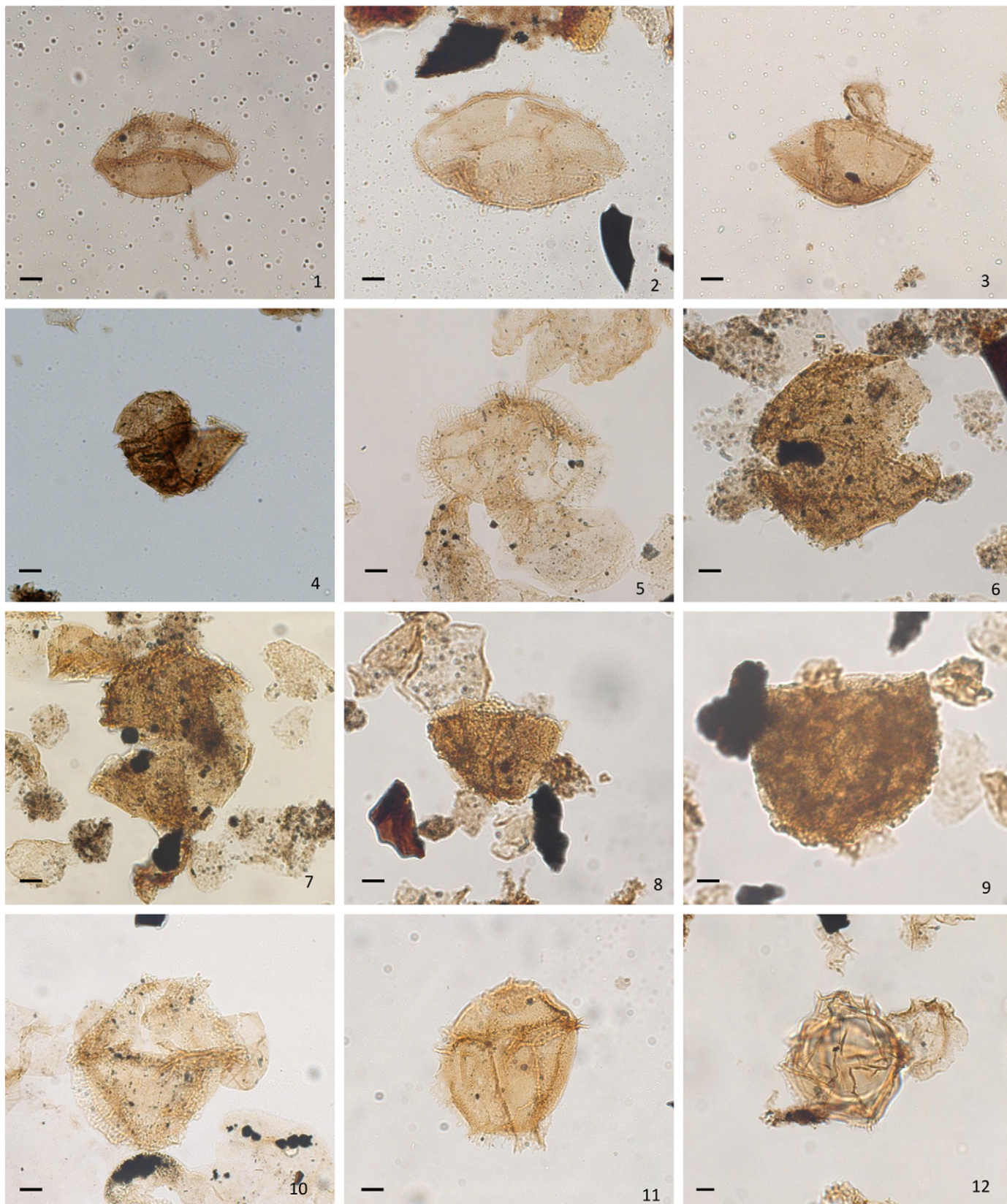


Plate III (caption on page 70).

Remarks: morphotypes of *Ctenidodinium* that could not be placed within any existing species were encountered from the upper part of the *G. garantiana* zone to the *Z. zigzag* zone.

Dissiliodinium Drugg 1978 emend. Feist-Burkhardt & Monteil 2001
Dissiliodinium giganteum Feist-Burkhardt 1990 (Plate IV, 1–6; Plate V, 1)

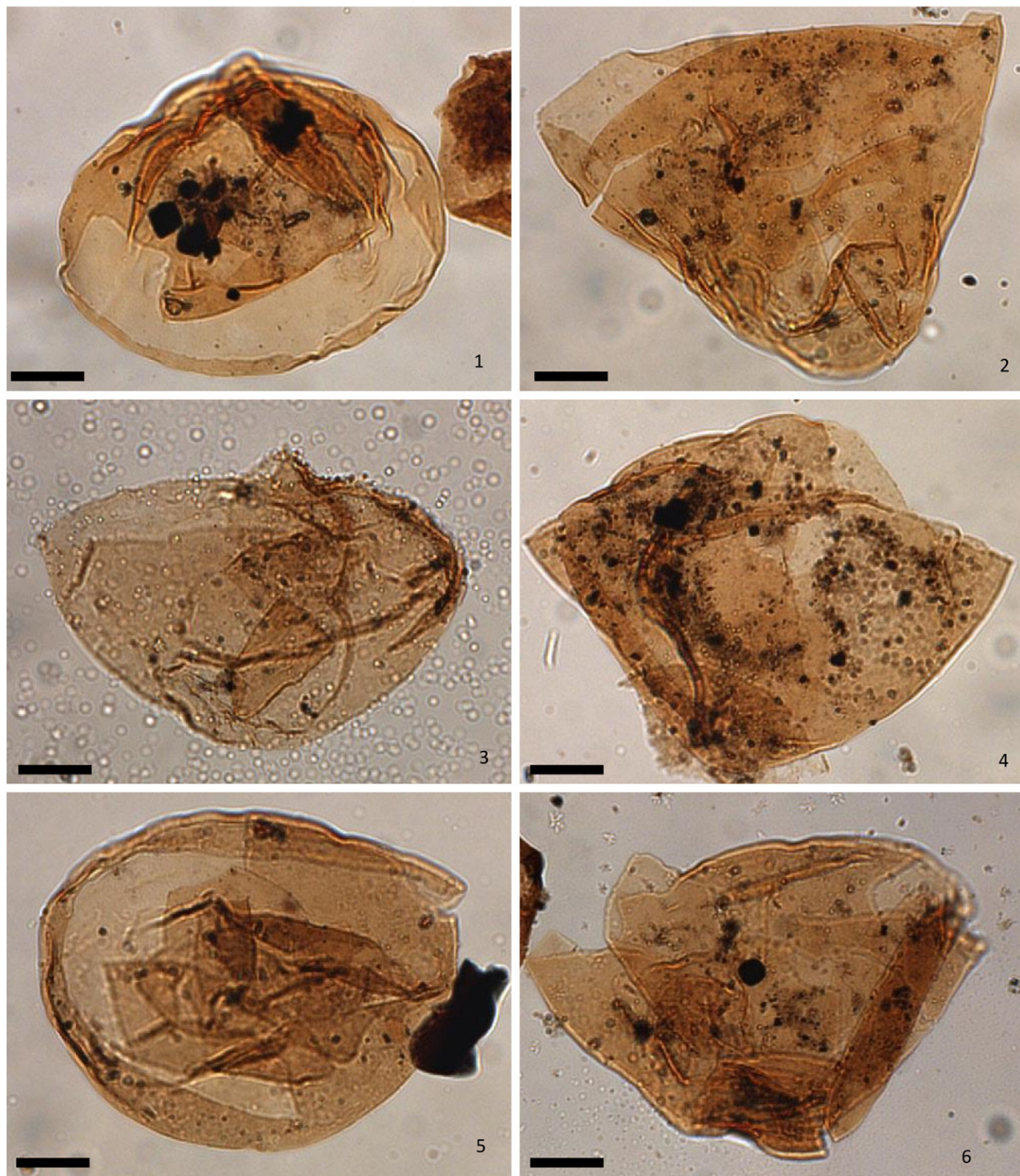


Plate IV. Selected dinoflagellate cysts from the B404/2 borehole. Scale bar represents 15 μ m. The slide number and England Finder co-ordinates (EF co.) of figured specimens are noted.

1–6: *Dissiliodinium giganteum* Feist-Burkhardt 1990. 1: Apical view, high focus, slide S2-C, EF co. R54/1, 2: dorso-ventral view, low focus, slide S2-C, EF co. V43/3, 3: dorso-ventral view, median focus, slide S17-B, EF co. E45/2, 4: dorso-ventral view, low focus, slide S17-B, EF co. L42/3 5: high focus, slide S18-B, EF co. C60, 6: dorso-ventral view, high focus, slide S17-B, EF co. U65/2.

Remarks: *Dissiliodinium giganteum* has a thin ($<0.5\ \mu\text{m}$) autophragm and is psilate, and occasionally scabrate. Due to the thin wall, specimens are often folded or wrinkled and mechanically damaged. In some specimens the apical, anterior sulcal and, 1" and 6" plates

are folded back into the cyst. The opercular plates are also frequently found within the cyst body.

Dimensions: Width: 66 (92.5) 138 μm ; 100 specimens measured.
Dissiliodinium? hocneratum (Fenton et al. 1980) Lentin & Williams 1993 (Plate V, 8)

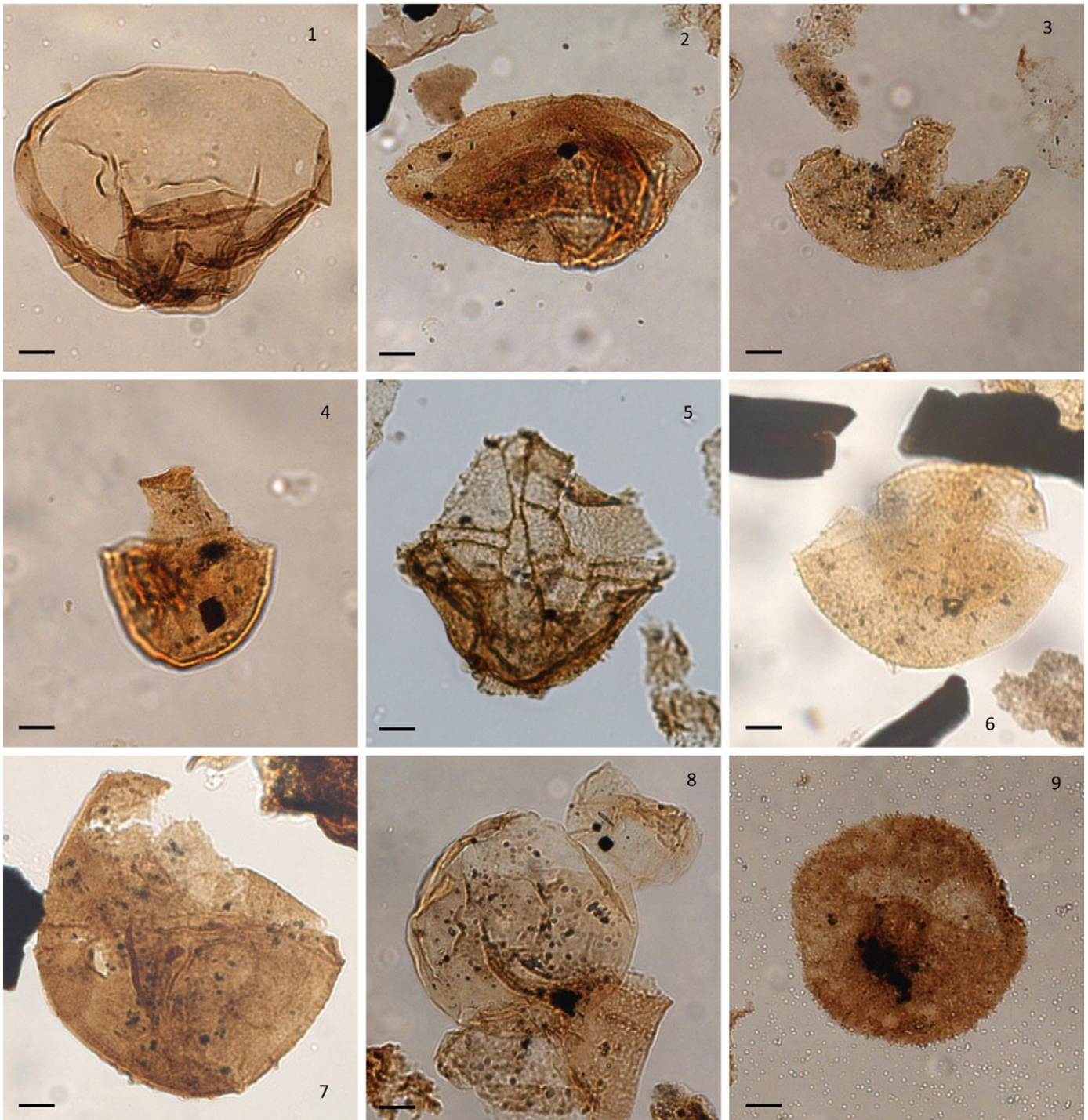


Plate V. Selected dinoflagellate cysts from the B404/2 borehole. Scale bar represents 10 μm . The slide number and England Finder co-ordinates (EF co.) of figured specimens are noted.

- 1: *Dissiliodinium giganteum* Feist-Burkhardt 1990. Apical view, low focus, slide S18-B, EF co. W56/1.
- 2–4: *Dissiliodinium* spp. 2: Ventro-apical view, high focus, slide S48–5, EF co. P47/3, 3: ventral view, slide S74–B, EF co. V48/2–4, high focus 4: dorsal view, median focus, side S92–3, EF co. K55.
- 5: *Durotrigia daveyi* Bailey 1987. Ventral view, high focus, slide S28–C, EF co. R59/2.
- 6: *Durotrigia* sp. 1. Dorso-ventral view, high focus, slide S8–B, EF co. J/K62.
- 7: *Durotrigia* sp. 2. Lateral view, median focus, slide S50–A, EF co. G48/1–3.
- 8: *Dissiliodinium? hocneratum* (Fenton et al. 1980) Lentin & Williams 1993. Dorsal view, high focus, slide S71–B, EF co. V48/2–4.
- 9: *Gongylodinium erymnoteichon* Fenton et al. 1980 emend. Feist-Burkhardt & Monteil 1997. Dorso-ventral view, low focus, slide S109–A, EF co. T50/2.

Remarks: *Dissiliodinium? hocneratum* is characterised by its type 2P archaeopyle formed by the loss of the 3" and 4" plates, and hence is questionably assigned to *Dissiliodinium*. The autophragm is thin (<0.5 μm) and psilate to scabrate. In a few specimens the opercular

plates were located inside the cyst. *Dissiliodinium? hocneratum* was encountered in low numbers, in two samples from the *W. laeviuscula* zone, one sample from the *S. humphreisianum* zone and sporadically throughout the Upper Bajocian–lowermost Bathonian.

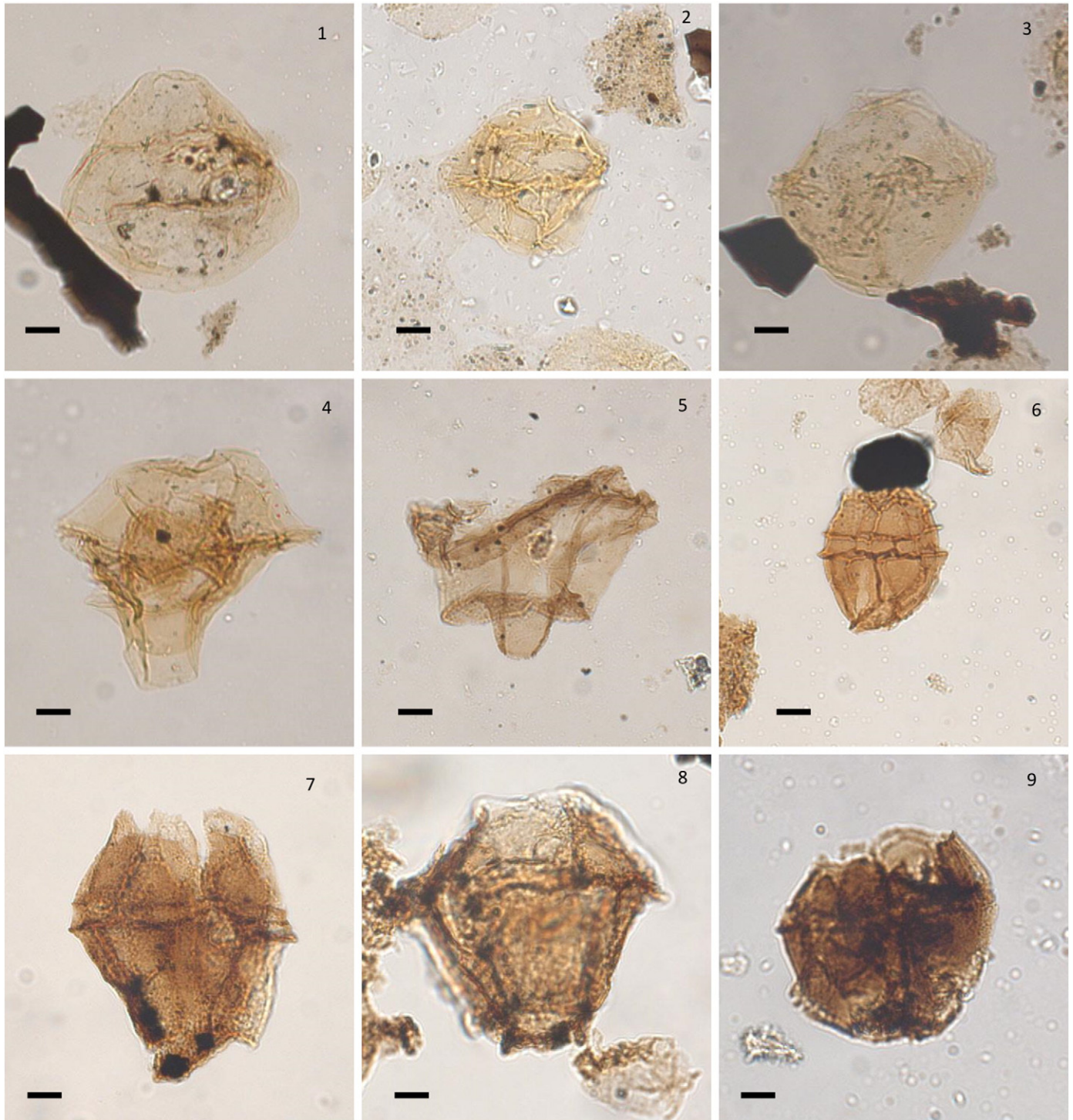


Plate VI. Selected dinoflagellate cysts from the B404/2 borehole. Scale bar represents 10 μm . The slide number and England Finder co-ordinates (EF co.) of figured specimens are noted.

- 1: *Endoscrinium?* spp. Dorsal view, high focus, slide S78-2, EF co. K47/3.
 2–3: *Endoscrinium* sp. cf. *E. luridum* (Deflandre 1938) Gocht 1970. 2: Dorso-ventral view, low focus, slide S69-2, EF co. U44, 3: lateral view, median focus, slide S68-B, EF co. J37.
 4: *Endoscrinium asymmetricum* Riding 1987. Dorso-ventral view, median focus, slide S95-A, EF co. R36.
 5: *Atopodinium polygonale* (Beju 1983) Masure 1991 emend. Masure 1991. Dorso-ventral view, high focus, slide S106-B, EF co. L53/1.
 6: *Carpathodinium predae* (Beju 1971) Drugg 1978 emend. Below 1990. Dorso-ventral view, median focus, slide S108-A, EF co. L60.
 7–8: *Meiourogonyaulax valensii* Sarjeant 1966. 7: Dorso-ventral view, median focus, slide S102-1, EF co. V49/3, 8: dorso-ventral view, high focus, slide S105-A, EF co. U62/1.
 9: *Meiourogonyaulax* sp. cf. *M. caytonensis*. Dorso-lateral view, low focus, slide S106-B, EF co. M52/2.

Dimensions: mean width: 66 µm; mean length: 67 µm; 5 specimens measured.

Dissiliodinium spp. (Plate V, 2–4)

Remarks: *Dissiliodinium* spp. includes all morphotypes that could not be attributed to established species. The morphology is highly variable; some forms have a thick (1–2 µm) autophragm which is commonly granulate, rugulate or scabrate, and rarely perforate. *Dissiliodinium* spp. was encountered consistently, in low to moderate abundances from the *G. concavum* to *Z. zigzag* zones.

Dimensions: width: 45 (68) 90 µm; 25 specimens measured.

Dissiliodinium? spp.

Remarks: These are morphotypes which are crushed, wrinkled, and otherwise poorly preserved cysts which lack tabulation and are medium to large in size. These could not be confidently placed within *Dissiliodinium*, but probably belong to this genus due to their style of preservation. Thus *Dissiliodinium?* spp. does not represent a true morphological grouping as specimens of this group are most likely taphomorphs of *Dissiliodinium* spp.

Durotrigia Bailey 1987.

Remarks: *Durotrigia* is similar in morphology to *Dissiliodinium* due to its 2P–5P archaeopyle. However, it is distinguished by its tabulation of positive-relief structures such as ridges and crests, whereas *Dissiliodinium* usually lacks tabulation, and if present, it is marked by negative-relief structures such as grooves (Feist-Burkhardt and Monteil, 2001).

Durotrigia daveyi Bailey 1987 (Plate V, 5)

Remarks: *Durotrigia daveyi* was recorded infrequently and in low abundance from the *W. laeviuscula* and *W. laeviuscula/S. propinqua* zones of the Lower Bajocian. The tabulation is demarcated by low sutural crests which bear short (2–3 µm) processes, and the autophragm is scabrate to rugulate.

Dimensions: mean width: 63 µm; mean length: 71 µm; 6 specimens measured.

Durotrigia sp. cf. *D. daveyi* Bailey 1987

Remarks: Several specimens comparable to *D. daveyi* were encountered in the *W. laeviuscula* and *S. propinqua/W. laeviuscula* zones. These morphotypes have low sutural crests and ridges which lack processes which differentiate them from *D. daveyi*.

Durotrigia sp. 1 (Plate V, 6)

Remarks: The tabulation is poorly expressed in most specimens except for the cingulum, which is marked by low ridges surmounted by short (<2 µm) spines. The archaeopyle is formed by the loss of 75 precingular plates. The autophragm is scabrate to rugulate, and some specimens exhibit creases and folds. This species is placed within *Durotrigia* rather than *Dissiliodinium* as the tabulation is expressed by positive-relief structures in the form of low ridges. *Durotrigia* sp. was encountered rarely from the *W. laeviuscula* to *S. niortense* zones of the Bajocian.

Dimensions: mean width: 83 µm; 5 specimens measured.

Durotrigia sp. 2 (Plate V, 7)

Remarks: Two specimens were encountered in sample S50 from the *S. humphriesianum* zone. It has a thick scabrate autophragm, clear cingulum and faint tabulation indicated by low, discontinuous ridges.

Plate VII. *Korystocysta aldridgei* sp. nov. Scale bar represents 10 µm. The slide number and England Finder co-ordinates (EF co.) of figured specimens are noted. 1–6 *Korystocysta aldridgei* sp. nov.

- 1–3: Holotype, right lateral view, 1: high focus, 2: low focus 3: high, median and low foci stacked, slide S105-A, EF co. L48/2.
4: Paratype, right lateral view, median focus, slide S105-B, EF co. G36, 5: ventro-lateral view, low focus, slide S105-A, EF co. U43/1, 6: lateral view, median focus, slide S105-B, EF co. K58/1.

Plate VIII. Selected dinoflagellate cysts from the B404/2 borehole. Scale bar represents 10 µm. The slide number and England Finder co-ordinates (EF co.) of figured specimens are noted. (see on page 78)

- 1–2: *Pareodinia ceratophora* Deflandre 1947 emend. Gocht 1970. 1: Dorso-ventral view, normal focus, slide S105-A, EF co. H40/3, 2: dorsal-ventral view, normal focus, slide S109-B, EF co. H54.
3–4: *Pareodinia halosa* (Filatoff 1975) Prauss 1989 emend. Prauss 1989. 3: Dorso-ventral view, normal focus, slide S109-A, EF co. P36, 4: specimen with irregular, 'sculpted' kalyptra, dorso-ventral view normal focus, slide S105-A, EF co. M57/1.
5–6: *Protobatioladinium mercieri* Feist-Burkhardt and Pross 1999. 5: Lateral view, normal focus, slide S109-B, EF co. M40/1, 6: dorso-ventral view, normal focus, slide S109-B, EF co. Q34.
7: *Nannoceratopsis gracilis* Alberti 1961 emend. van Helden 1977 Right lateral view, median focus, slide S36-B, EF co. N40/2.
8: *Nannoceratopsis spiculata* Stover 1966. Lateral view, low focus, slide S105-B, EF co. V39.
9: *Nannoceratopsis plegas* Drugg 1978. Left-lateral view, high focus, slide S24-1, EF co. S62/2.

Plate IX. Selected dinoflagellate cysts from the B404/2 borehole. Scale bar represents 10 µm. The slide number and England Finder co-ordinates (EF co.) of figured specimens are noted. (see on page 79)

- 1–4: *Sentusidinium* spp. 1: Dorso-ventral view, median focus, slide S71-B, EF co. M68, 2: dorso-ventral view, high focus, slide S69-2, EF co. O69, 3: dorso-ventral view, median focus, slide S71-B, EF co. H47/3, 4: dorso-ventral view, low focus, slide S71-B, EF co. M57.
5–9: *Batiacasphaera* spp. 5: Dorso-ventral view, low focus, slide S108-B, EF co. Q55/1-2, 6: dorso-ventral view, median focus, slide S71-B, EF co. J72/1, 7: dorso-ventral view, median focus, S71-A, EF co. V45, 8: dorso-ventral view, high focus, slide S71-A, EF co. W71/1, 9: dorso-ventral view, median focus, slide S71-B, EF co. W54.
10: *Kallosphaeridium hypornatum* Prauss 1989 emend Wood et al. 2016 dorso-ventral view, high focus, slide S66-A, EF co. V62.
11: *Kallosphaeridium* spp. Dorso-ventral view, median focus, slide S7-B, EF co. C55/3.
12: *Lithodinia jurassica* Eisenack 1935 emend. Gocht 1975. Dorso-ventral view, low focus, slide S102-1, EF co. T54/3-4.

Plate X. Selected dinoflagellate cysts from the B404/2 borehole. Scale bar represents 10 µm except in 1 where it represents 15 µm, 2 where it represents 7 µm and in 9–12 where it represents 5 µm. The slide number and England Finder co-ordinates (EF co.) of figured specimens are noted. (see on page 80)

- 1: *Chytroisphaeria chytroides* (Sarjeant, 1962) Downie & Sarjeant 1965 emend. Davey 1979. Right lateral view, high focus, slide S109-B, EF co. M62/2-4.
2: *Jansoniasia psilata* Martinez et al. 1999. Dorso-ventral view, median focus, slide S66-A, EF co. H72/1-3.
3: *Impletosphaeridium* sp. 1. Apical view, median focus, slide S102-1, EF co. J71/4.
4: *Impletosphaeridium* sp. 2. Dorso-ventral view, median focus, slide S108-B, EF co. J45/3.
5: *Valvaedinium spinosum?* (Fenton et al. 1980) Below 1987. Dorso-ventral view, median focus, slide S48-2, EF co. N67-2.
6: *Valvaedinium vermicylindratum* Below 1987. Dorso-ventral view, median focus, slide S66-A, EF co. G45/3.
7–8: *Valvaedinium* spp. 7: Lateral view, median focus, slide S102-1, EF co. U68, 8: lateral view, low focus, slide S69-2, EF co. U40/1-3.
9–10: *Orobodinium automobile* Gocht & Wille 1990. 9: dorso-ventral view, high focus, slide S109-B, EF co. G65/2, 10: dorso-ventral view, median focus, note the operculum which has fallen back inside the cyst body, slide S36-A, EF co. H52/3.
11–12: *Orobodinium* sp. A of Wille & Gocht 1990. Same specimen apical view, 11: median focus, 12: low focus, slide S109-A, EF co. O63/1.

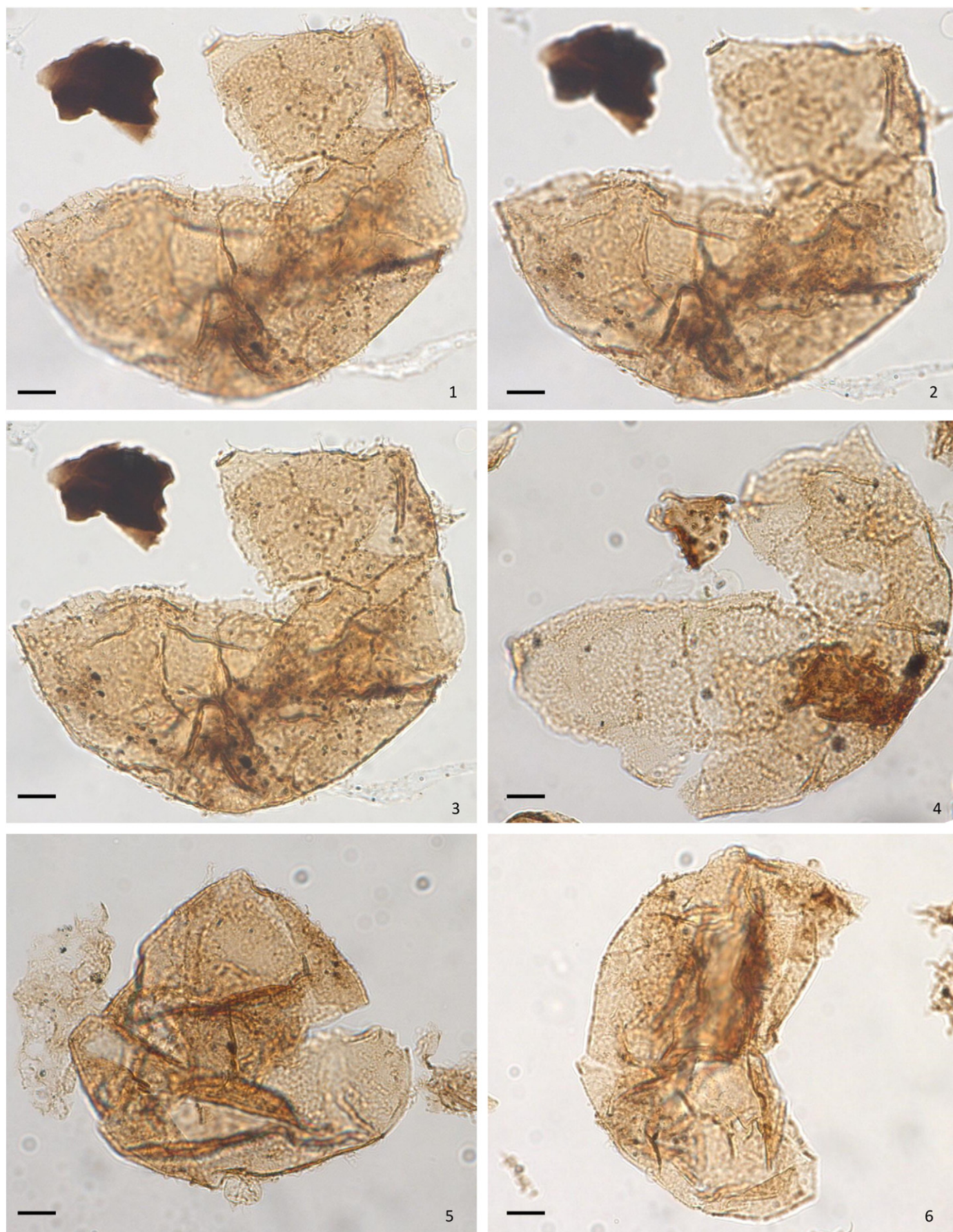


Plate VII.

Endoscrinium (Klement 1960) Vozzhennikova 1967 emend. Riding & Fensome 2002

Endoscrinium asymmetricum Riding 1987 (Plate VI, 4)

Remarks: This extremely distinctive species was recorded from samples S95 and S99 in the *G. garantiana* zone. It is defined by the asymmetrical hypocystal lobes, the left lobe is wing-like whilst the two layers

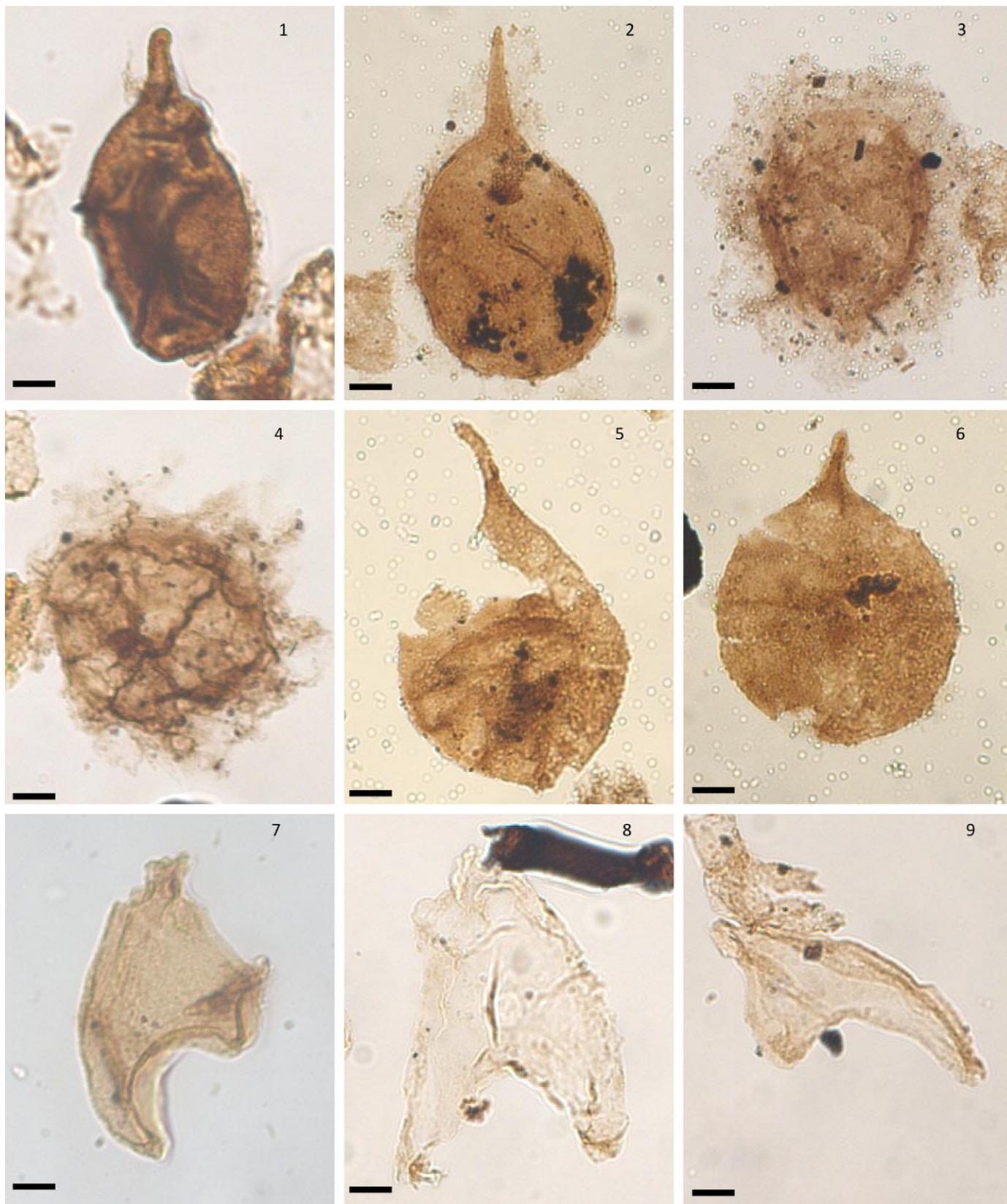


Plate VIII (caption on page 76).

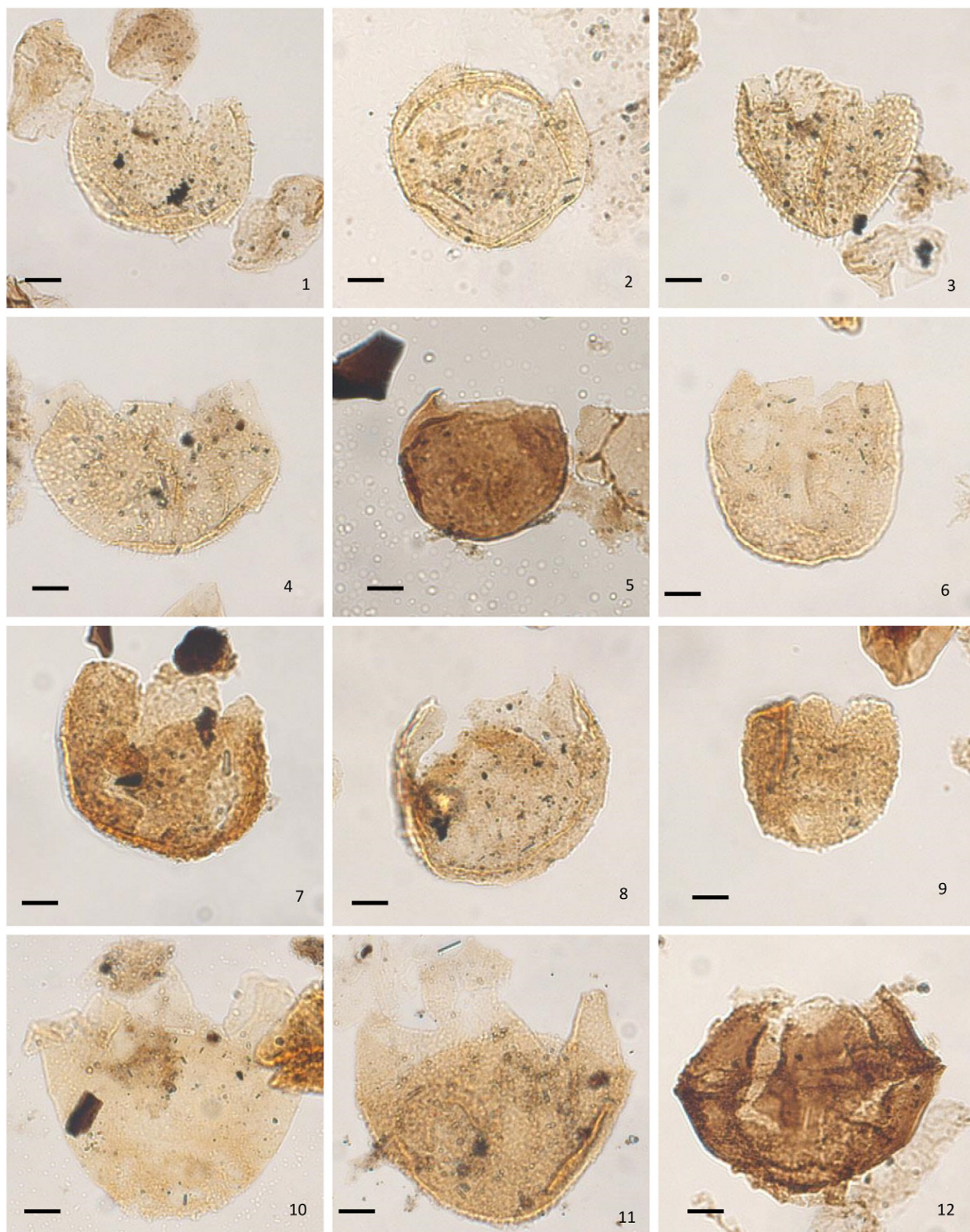


Plate IX (caption on page 76).

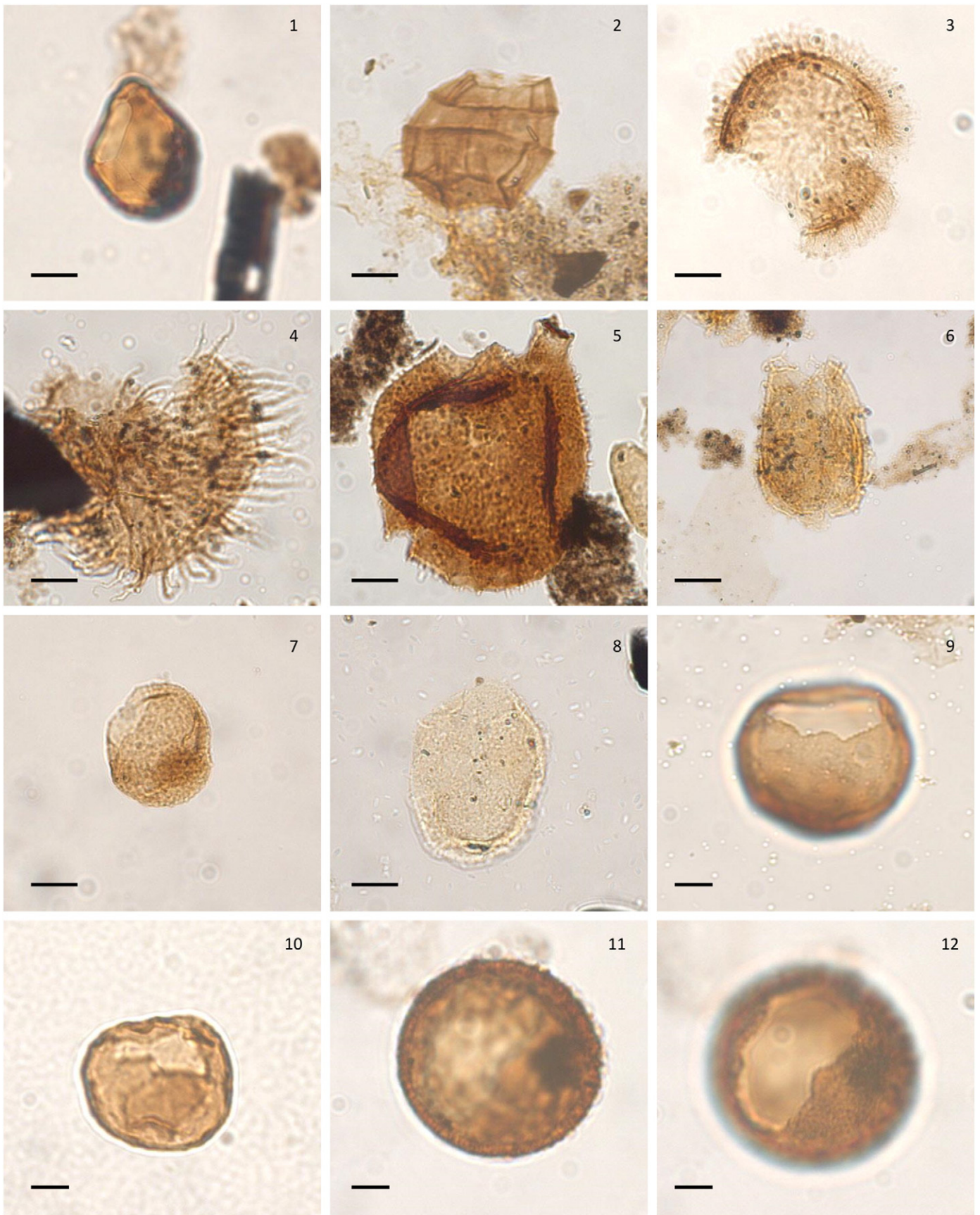


Plate X (caption on page 76).

on the right side of the hypocyst are more closely appressed, imparting an asymmetrical outline.

Dimensions: width: 77 μm ; length: 68 μm ; one specimen measured.

Endoscrinium sp. cf. *E. luridum* (Deflandre 1938) Gocht 1970 (Plate VI, 2–3)

Remarks: This form is subspherical to elongate subovoidal in outline, the pericoel is much narrower than *E. luridum*. Some specimens were more elongate with more pronounced antapical cavation, however these forms apically acavate. *Endoscrinium* sp. cf. *E. luridum* was encountered moderately consistently from the *S. niortense* to the *P. parkinsoni*

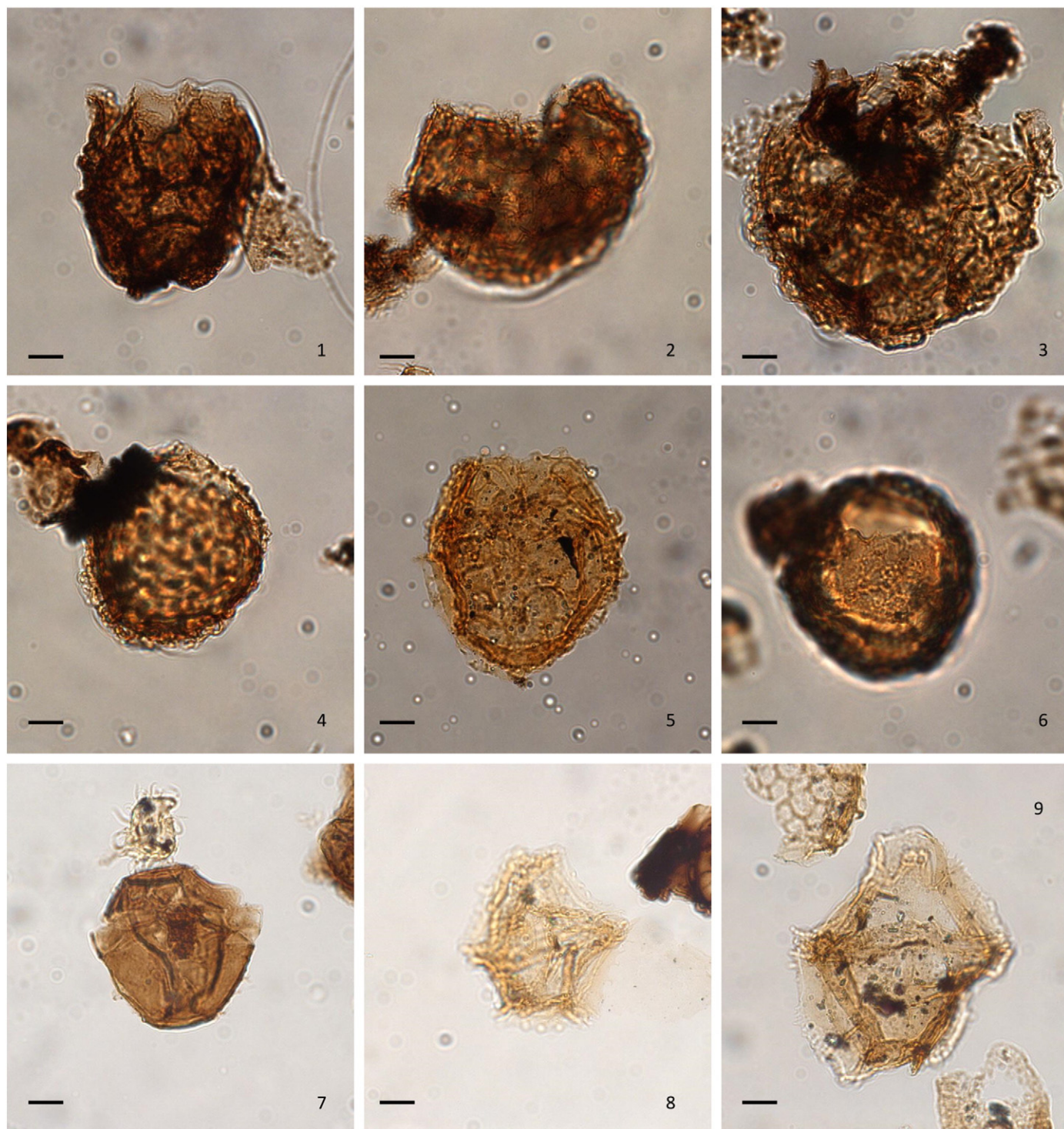


Plate XI. Selected dinoflagellate cysts from the B404/2 borehole. Scale bar represents 10 μm . The slide number and England Finder co-ordinates (EF co.) of figured specimens are noted.

- 1–3: *Ellipsoidictyum-Valensiella* complex. 1: Median focus, slide S105-A, EF co. G49/4, 2: high focus, slide S105-A, EF co. H49, 3: low focus, slide S105-A, EF co. M69/2.
 4–5: *Valensiella ovulum* (Deflandre 1947) Eisenack 1963 emend. Courtinat 1989. 4: Median focus, slide S105-A, EF co. J46/1, 5: median focus, slide S66-B, EF co. S71.
 6: *Valensiella ampulla* Gocht 1970. Low focus, slide S105-A, EF co. U43/4.
 7: *Bradleyella* sp. Ventral view, median focus, slide S105-A, EF co. S59/1.
 8: *Rhynchodiniopsis?* spp. Dorso-ventral view, high focus, slide S95-A, EF co. T59.
 9: *Gonyaulacysta pectinifera* (Gocht 1970) Fensome, 1979. Dorso-ventral view, median focus, slide S71-B, EF co. W55/2.

zones, with one questionable occurrence in the *Z. zigzag* zone. This morphotype has been reported from the Upper Bajocian–Lower Bathonian of offshore Western Australia by Mantle and Riding (2012).

Dimensions: mean width: 62 µm; mean length: 66 µm; 5 specimens measured.

Endoscrinium? spp. (Plate VI, 1)

Remarks: These are morphotypes with poorly developed cavation and were encountered from the *S. humphriesianum* to *P. parkinsoni* zones. These forms are commonly hypocavate, and in some the presence of cavation is difficult to determine as the endophragm and periphragm are closely appressed. One specimen clearly shows a 1P type archaeopyle (Plate VI, 1).

Dimensions: mean width: 61 µm; mean length: 65 µm; 5 specimens measured.

Eodinia Eisenack 1936 emend. Berger 1986

Eodinia? spp. (Plate III, 6–9)

Remarks: Specimens of *Eodinia?* spp. are distinguished by their epicystal archaeopyle and thick, spongy autophragm. The differentiation of the autophragm varies between specimens and across individual cysts, but the outer layer is commonly rugulate. Some specimens show the development of sutural crests, commonly around the antapex, which are capped with capitate processes which often merge into ridges. Specimens were commonly encountered as disarticulated epicysts or hypocysts. One specimen displayed an apical horn, and another exhibits faint intratabular ridges. The shape of some hypocysts suggests a flat epicyst (cf. *Wanaea*) (e.g. Plate III, 9), although none of these were directly observed. An attached operculum was found in some specimens, and the principal archaeopyle suture appears to be located along the anterior margin of the cingulum, with the operculum attached ventrally. These morphotypes are questionably assigned to *Eodinia* as the autophragm only shows partial differentiation rather than the development of a true second wall layer. Intriguingly some of these forms resemble *Acanthaulax crista*.

Dimensions: mean width: 82 µm; 10 specimens measured.

Eodinia? sp.

Remarks: Two specimens were encountered in samples S95 and S97 from the *G. garantiana* zone. The cyst body is ovoidal in outline and longer than broad. The autophragm is scabrate to microgranulate in places is differentiated and has a partially developed fine reticulum. The archaeopyle is not clear but one specimen shows a small schism above the cingulum. The partial development of a differentiated autophragm means this morphotype has been questionably placed in *Eodinia*, and is distinguished from *Eodinia?* spp. by its morphology and small size.

Dimensions: width: 47 and 52 µm; length: 54 and 57 µm; two specimens measured.

Gonyaulacysta Deflandre 1964 emend. Helenes & Lucas-Clark 1997

Gonyaulacysta jurassica (Deflandre 1938) Norris & Sarjeant 1965 subsp. *adecta* Sarjeant 1982

Remarks: One specimen was recorded from the uppermost sample of the *Z. zigzag* zone (S109).

Gonyaulacysta pectinigera (Gocht 1970) Fensome 1979 (Plate XI, 9)

Remarks: *Gonyaulacysta pectinigera* was recorded from sample S71 in the *S. niortense* zone. This specimen has prominent sutural crests capped by small denticles which are particularly well developed on one side of the hypocyst and has a distinct apical protuberance. As *G. pectinigera* is cornucavate it may belong within *Rhynchodiniopsis*, although a study of the type material is needed.

Korystocysta Woollam 1983 emend. Benson 1985

Remarks: *Korystocysta* was assigned to the subfamily Cribroperidinoideae by Fensome et al. (1993, p. 89). However it clearly exhibits neutral torsion (Sarjeant, 1976, Fig. 2), hence is herein transferred to the Leptodinioidae

Korystocysta gochtii (Sarjeant 1976) Woollam 1983 (Plate II, 7)

Remarks: One specimen of this, the type species, was encountered in the *Z. zigzag* zone (sample S108) as a disarticulated epicyst.

Korystocysta pachyderma (Deflandre 1938) Woollam 1983 (Plates 2, 8).

Remarks: A single specimen of was recorded outside of the count of sample S81 from the uppermost *S. niortense* zone.

Korystocysta aldridgeii sp. nov. (Plate VII, 1–6).

Diagnosis: A species of *Korystocysta* with faint to discontinuous sutural ridges which may be capped by short spines, a small, broad apical protuberance, and scabrate to slightly granulate or rugulate autophragm; it is consistently broader than long.

Description: A species of *Korystocysta* which is primarily dorsoventrally flattened, and with a subovoidal dorsoventral outline. It is large in size. *Korystocysta aldridgeii* sp. nov. is consistently slightly broader than it is long, and has a short, rounded apical protuberance. The species is acavate, and the autophragm is of moderate thickness and is scabrate to slightly granulate or rugulate. The gonyaulacacean tabulation is indicated by low, and dominantly discontinuous sutural ridges which often bear denticles or small (<5 µm) spines. The cingulum however, is fully indicated by continuous ridges irregularly capped by denticles or small spines. The epicystal archaeopyle is normally clearly expressed.

Dimensions: width: 80 (99) 119 µm, 30 specimens measured.

Holotype: width: 114 µm, length: 103 µm.

Paratype: width: 118 µm, length: 104 µm.

Derivation of name: *Korystocysta aldridgeii* sp. nov. is named in memory of the late Richard J. Aldridge (1945–2014), who was F.W. Bennett Professor of Geology at the University of Leicester, UK.

Remarks: *Korystocysta aldridgeii* sp. nov. is a highly distinctive representative of this genus because its width is consistently slightly greater than its length. The size, general morphology, stratigraphical extent and overall similarity to *Korystocysta gochtii* and *Korystocysta pachyderma* of this species clearly indicates that it belongs within the genus *Korystocysta*. Further to its distinctive relatively squat/stout overall shape, it is also characterised by a short, distally-rounded apical protuberance, moderately thick, scabrate to slightly granulate autophragm and discontinuous, sutural ridges which are irregularly ornamented with denticles and small spines. The sutures, despite being markedly discontinuous, clearly indicate a gonyaulacacean tabulation. The autophragm is relatively thin, and specimens are therefore susceptible to mechanical damage, particularly the epicyst which is frequently broken, and rarely encountered intact.

Comparison: *Korystocysta aldridgeii* sp. nov. is shorter, more squat, and generally larger than the other two valid species of this genus, *Korystocysta gochtii* and *Korystocysta pachyderma*. Both the latter are longer than they are broad (Woollam, 1983). *Korystocysta gochtii*, the type, has a much more pronounced apical horn and whilst *Korystocysta pachyderma* also bears prominent intratabular ridges and is thick walled (Woollam, 1983, pl. 1, 9).

Stratigraphical range: *Korystocysta aldridgeii* sp. nov. ranges from the *P. parkinsoni* to *Z. zigzag* zones, where it occurs abundantly and is a good marker for the Bajocian–Bathonian transition. There a questionable occurrence in the *G. garantiana* zone (sample S89) and the lowermost sample (S102) of the *P. parkinsoni* zone.

Plate XII. Selected dinoflagellate cysts from the B404/2 borehole. Scale bar represents 10 µm. The slide number and England Finder co-ordinates (EF co.) of figured specimens are noted.

- 1: *Meiourugonyaulax?* spp. Dorso-ventral view, high focus, slide S93-1, EF co. P45.
- 2–3: *Meiourugonyaulax* spp. 2: Dorso-ventral view, high focus, slide S57-A, EF co. U58/2, 3: dorso-ventral view, low focus, slide S52-B, EF co. P63.
- 4: *Nannoceratopsis ambonis* Drugg 1978 emend. Riding 1984. Left-lateral view, median focus, slide S18-A, EF co. P57/3.
- 5–6: *Nannoceratopsis* spp. 5: Left-lateral view, normal focus, slide S24-1, EF co. P67/3, 6: right lateral view, low focus, slide S28-D, EF co. S42/2.

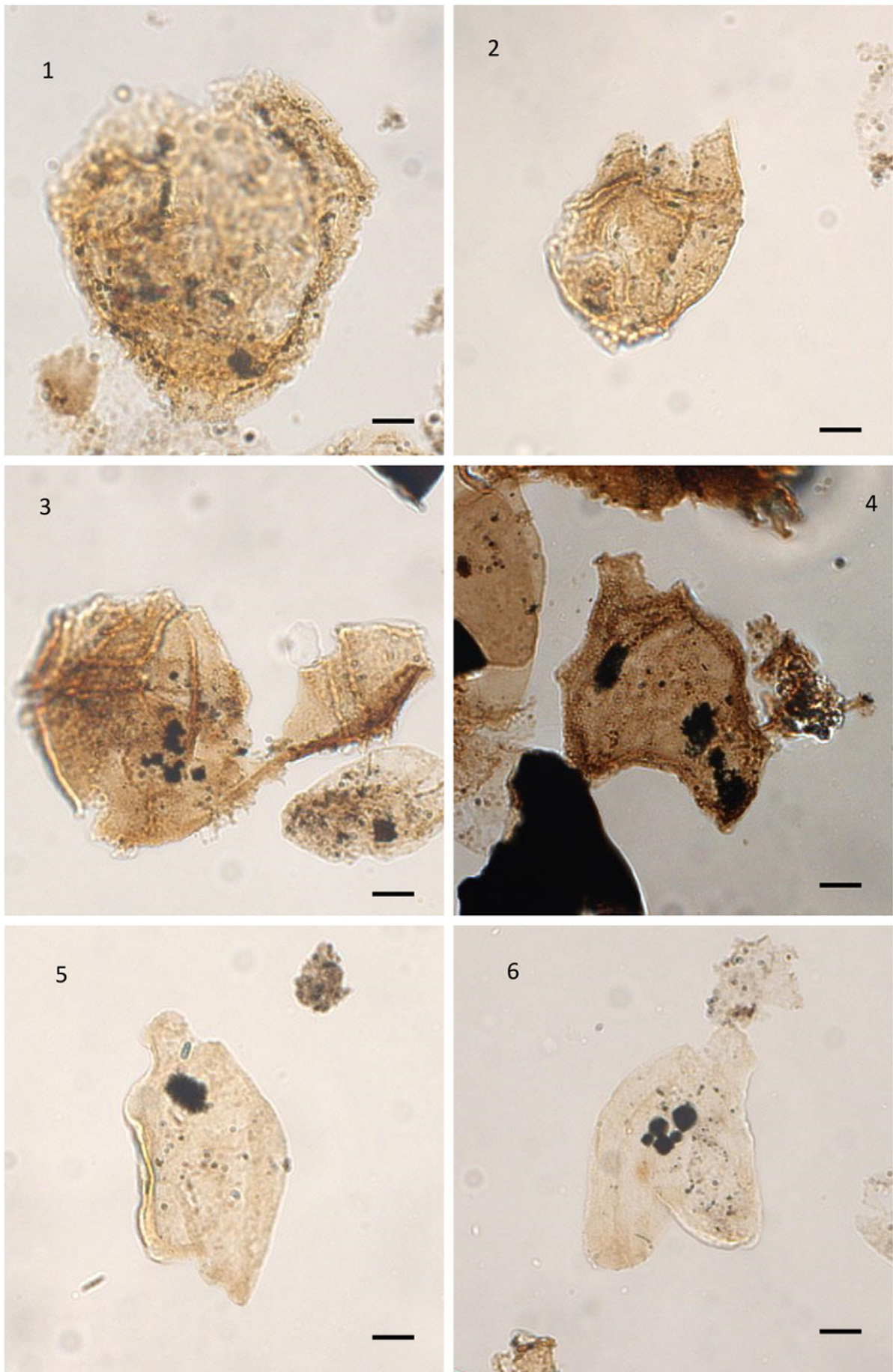


Plate XII.

Repository: The type material is curated in the collections of the Sedgwick Museum, Department of Earth Sciences, University of Cambridge, Downing Street, Cambridge, UK. Holotype: slide S105-A, England finder co-ordinates: L48/2, museum accession number CAMSM X.50257.1. Paratype: slide S105-B, G36, museum accession number CAMSM X.50257.2.

Korystocysta sp. 1 (Plate II, 10).

Remarks: A single specimen was encountered in the lowermost *S. humphriesianum* zone (sample S46) and is an isolated hypocyst which is triangular in shape and slightly pointed at the antapex. It has a granular to rugulate autophragm with indistinct tabulation; the cingulum is marked by low ridges.

Dimensions: width: 63 µm; length: 47 µm.

Korystocysta sp. 2 (Plate II, 9).

Remarks: One specimen was encountered in sample S104 from the *P. parkinsoni* zone. It is distinguished by its thick (ca. 1 µm) autophragm which is scabrate, the tabulation is defined by low sutural ridges, and the 1P plate is markedly elongate.

Dimensions: width: 85 µm; length: 79 µm.

Kallosphaeridium de Coninck 1969 emend. Wood et al. 2016.

Remarks: *Kallosphaeridium* is similar to *Batiacasphaera* and *Sentusidinium*, but differs as the operculum is attached and has 5 plates.

Kallosphaeridium? *hypornatum* Prauss 1989 emend. Wood et al. 2016 (Plate IX, 10).

Remarks: A distinctive species characterised by granular ornamentation around the antapex, the rest of the cyst is psilate to scabrate. It was recorded confidently from the *S. propinquans*/*S. humphriesianum* zone to the *P. parkinsoni* zone of the Bajocian. A single questionable specimen was recorded from the *W. laeviuscula* zone, although the preservation was too poor to confidently assign it to *K?* *hypornatum*. This species was questionably assigned to *Kallosphaeridium* by Wood et al. (2016) as the presence of a mid-dorsal (1a/3') plate on the operculum is yet to be confirmed.

Dimensions: mean width: 62 µm; mean length: 55 µm; 5 specimens measured.

Kallosphaeridium spp. (Plate IX, 11).

Remarks: Specimens of *Kallosphaeridium* with variable morphologies were encountered rarely, and in low numbers from the *W. laeviuscula* to *Z. zigzag* zones. They have been grouped together as *Kallosphaeridium* spp. and are scabrate to rugulate; one specimen has small spines on the antapex.

Dimensions: mean width: 62 µm; mean length: 68 µm; 4 specimens measured.

Leptodinium Klement 1960 emend. Sarjeant 1982.

Leptodinium sp. (Plate III, 12).

Remarks: Single specimens were recovered from two samples in the *P. parkinsoni* zone (S102 and S105). It has a subhexagonal/subspherical outline, is small, smooth walled and has distinct tabulation indicated by low denticular sutural ridges and a 1P archaeopyle, formed by the loss of the 3" plate.

Dimensions: width: 54 µm; length: 61 µm; one specimen measured.

Lithodinia Eisenack 1935 emend. Williams et al. 1993.

Lithodinia jurassica Eisenack 1935 emend. Gocht 1975 (Plate IX, 12).

Remarks: One specimen was encountered in sample S102 of the *P. parkinsoni* zone.

Dimensions: width: 78 µm; length: 59 µm.

Meiourogonayaulax Sarjeant 1966.

Meiourogonayaulax valensii Sarjeant 1966 (Plate VI, 7–8).

Remarks: This is distinguished by its prominent sutural crests which commonly increase in height towards the antapex. The autophragm is scabrate, rugulate or finely reticulate, the crests also display this variation. *Meiourogonayaulax valensii* was encountered consistently, in varying abundances, from the middle of the *S. humphriesianum* to the *Z. zigzag* zone.

Dimensions: mean width with crests: 61 µm; mean width without crests: 56 µm; mean length with crests: 71 µm; mean length without crests: 62 µm; 10 specimens measured.

Meiourogonayaulax sp. cf. *M. caytonensis* (Sarjeant 1959) Sarjeant 1969 (Plate VI, 9)

Remarks: Three specimens were encountered in the lowermost sample of the *Z. zigzag* zone (S106). This form is broader than long, and bears low sutural crests which are surmounted by small spines. This form is similar in morphology to *M. caytonensis* but lacks punctate/perforate sutural crests.

Meiourogonayaulax spp. (Plate XII, 2–3).

Remarks: Various morphotypes were recorded consistently, in low numbers, from the *S. humphriesianum* to the *Z. zigzag* zones. Their morphology is highly variable and they have been grouped together. The autophragm is variable in thickness but can be up to 3 µm and is commonly scabrate to rugulate or very finely reticulate. Some bear small processes near the antapex. The length and width are typically subequal.

Dimensions: mean width: 56 µm; mean length: 59 µm; 10 specimens measured.

Meiourogonayaulax? spp. (Plate XII, 1).

Remarks: These are defined by the thick, spongy structure of the differentiated autophragm. The tabulation is indistinct but some forms show low sutural ridges. The spongy ornament varies from rugulate to reticulate. They are questionably placed in *Meiourogonayaulax* due to the spongy differentiated autophragm which resembles that of *Acanthaulax crista*. *Meiourogonayaulax*? sp. was encountered sporadically and in low numbers from the *S. niortense* to the *P. parkinsoni* zones.

Dimensions: mean width: 79 µm; mean length: 77 µm; 6 specimens measured.

Rhynchodiniopsis Deflandre, 1935 emend. Jan du Chêne et al., 1985.

Rhynchodiniopsis? *regalis* (Gocht 1970) Jan du Chêne et al., 1985 (Plate III, 10).

Remarks: This species was encountered sporadically, and in low numbers, from the *S. humphriesianum* to the *P. parkinsoni* zones and is distinguished by its prominent denticular crests with a transverse midbar.

Dimensions: mean width: 64 µm; mean length: 67 µm; 5 specimens measured.

Rhynchodiniopsis sp. cf. *R?* *regalis* (Gocht 1970) Jan du Chêne et al. 1985 (Plate III, 11).

Remarks: Two specimens of this form were encountered in the *S. niortense* zone (sample S65) and the *G. garantiana* zone (sample S95). *Rhynchodiniopsis* sp. is distinguished from *R?* *regalis* by its sutural crests which are proximally finely fenestrate and distally denticular.

Rhynchodiniopsis? spp. (Plate XI, 8).

Remarks: Morphotypes placed in *Rhynchodiniopsis?* spp. are small, subspherical to subovoidal somewhat enigmatic forms with denticular sutural crests, distinct tabulation and an L-type sulcus. All specimens lack an apical horn, the autophragm is psilate. *Rhynchodiniopsis?* spp. was encountered sporadically and in low abundance from the *S. humphriesianum* to the *Z. zigzag* zones.

Wanaea Cookson & Eisenack 1958 emend. Riding & Helby 2001.

Wanaea acollaris Dodekova 1975 emend. Riding & Helby 2001 (Plate II, 11).

Remarks: *Wanaea acollaris* was recorded in low abundances from the *G. garantiana*, *P. parkinsoni* and *Z. zigzag* zones. These specimens have a squat antapical horn and autophragm which is granular to rugulate.

Wanaea sp. 1.

Remarks: One specimen of *Wanaea* sp. 1 was recorded from sample S104 in the *P. parkinsoni* zone, and is distinguished by its rugulate to microreticulate autophragm.

Wanaea sp. 2.

Remarks: This is distinguished by its psilate wall which is folded and crinkled, and its prominent antapical horn; it was recorded outside of the count from sample S105 from the uppermost *P. parkinsoni* zone.

Subfamily UNCERTAIN.

Atopodinium Drugg 1978 emend. Masure 1991.

Atopodinium polygonale (Beju 1983) Masure 1991 emend. Masure 1991 (Plate VI, 5).

Remarks: a single specimen of this highly distinctive species was encountered in sample S106 from the *P. parkinsoni* zone, and was recorded outside of the count.

Batiacasphaera Drugg 1970 emend. Wood et al. 2016.

Batiacasphaera spp. (Plate IX, 5–9).

Diagnosis: Acavate, proximate dinoflagellate cysts, subspherical to ovoidal in outline. Tabulation shown only by the apical (tA) archaeopyle. Faint cingulum sometimes present. Autophragm psilate, scabrate, rugulate and granular. Small to intermediate in size.

Remarks: *Batiacasphaera* spp. was recorded consistently, in varying abundances from the *G. concavum* to *Z. zigzag* zones. The simple, highly variable morphology makes species level identification difficult, hence representatives were not speciated. Forms vary from smooth to granular, the thickness of the autophragm is highly variable, and in some specimens is relatively thick (1–2 µm).

Dimensions: width: 36 (48) 59 µm; length: 36 (47) 67 µm; 50 specimens measured.

Batiacasphaera? spp.

Remarks: Small, spherical to subspherical/ovoidal/pentagonal acavate cysts which commonly have creases and folds and are frequently slightly wider than long. Tabulation is absent and the autophragm is scabrate, granulate or rugulate. Small size and poor preservation make these forms difficult to interpret and hence were questionably assigned to *Batiacasphaera*. These were encountered consistently and in varying abundances through the succession examined.

Dimensions: mean width: 39 µm; mean length: 37 µm; 20 specimens measured.

Chytroisphaeridia (Sarjeant, 1962) Downie & Sarjeant 1965 emend. Davey 1979.

Chytroisphaeridia chytroides (Sarjeant, 1962) Downie & Sarjeant 1965 emend. Davey 1979 (Plate X, 1).

Remarks: A small, smooth-walled species with a 1P type archaeopyle. *Chytroisphaeridia chytroides* was encountered as single specimens in samples from the *W. laeviuscula*, *P. parkinsoni* and *Z. zigzag* zones. Four questionable occurrences, due to poor preservation, were also recorded from the *S. propinquans*/*W. laeviuscula*, *S. niortense* and *Z. zigzag* zones.

Gongylodinium Fenton et al. 1980 emend. Feist-Burkhardt & Monteil 1997.

Gongylodinium erymnoteichon Fenton et al. 1980 emend. Feist-Burkhardt & Monteil 1997 (Plate V, 9).

Remarks: This species was recorded relatively consistently in low numbers from the *W. laeviuscula* to the *Z. zigzag* zones. With its 2P type archaeopyle, it is similar to *Dissiliodinium? hocneratum* but differs in that the autophragm is thicker and covered in very short (<1 µm) spines.

Dimensions: mean width: 57 µm; mean length: 52 µm; 5 specimens measured.

Mendicodinium Morgenroth 1970 emend. Bucefalo Palliani et al. 1997.

Mendicodinium sp. (Plate II, 12).

Remarks: *Mendicodinium* sp. was recorded from sample S97 in the *G. garantiana* zone, and has a hypocyst which is slightly larger than the epicyst and a scabrate autophragm.

Mosaicodinium Dodekova 1990.

Mosaicodinium sp. cf. *M. mosaicum* (Dodekova 1975) Dodekova 1990.

Remarks: This morphotype was recorded as a single specimen from sample S105 in the *P. parkinsoni* zone; it is distinguished by its highly distinctive mosaic-like ornamentation.

Sentusidinium Sarjeant & Stover 1978 emend. Wood et al. 2016

Sentusidinium spp. (Plate IX, 1–4).

Diagnosis: Acavate, proximate to proximochorate dinoflagellate cysts. Autophragm covered in short simple non-tabular spines which are conical and either pointed or blunt distally. Tabulation indicated only by the apical archaeopyle. Ovoidal to subspherical in outline, commonly wider than long, small to intermediate in size.

Remarks: The simple but variable morphology of this group makes consistent speciation difficult and hence are grouped together as *Sentusidinium* spp. The process length and distribution density is highly variable. Most specimens are proximate as the processes are usually <10% of the width of the cyst body, but occasional proximochorate forms were observed. The intra-process areas are smooth. Specimens of *Sentusidinium* spp. were encountered consistently in moderate to high abundances from the uppermost *S. humphriesianum* (sample 62) to the *Z. zigzag* zones.

Dimensions: width: 34 (47) 63 µm; length: 27 (42) 56 µm; 50 specimens measured.

Valensiella Eisenack 1963 emend. Courtinat 1989.

Valensiella ampulla Gocht 1970 (Plate XI, 6).

Remarks: *Valensiella ampulla* is distinguished by its finely reticulate ornamentation which is comprised of discontinuous elements. It was recorded in two samples from the *P. parkinsoni* zone (S102 and S105).

Valensiella ovulum (Deflandre 1947) Eisenack 1963 emend. Courtinat 1989 (Plate XI 4–5).

Remarks: *Valensiella ovulum* was encountered sporadically and in low abundances from the uppermost part of the *S. humphriesianum* to the *Z. zigzag* zones.

Dimensions: mean width: 57 µm; mean length: 60 µm; 5 specimens measured.

Ellipsoidictyum/Valensiella complex (Plate XI, 1–3).

Remarks: Numerous specimens with reticulate ornamentation and an apical archaeopyle were encountered through from the *S. humphriesianum* to the *Z. zigzag* zones. The genera *Valensiella* and *Ellipsoidictyum* are differentiated on the basis that the former possess an ectophragm whilst the latter has an autophragm only and a cingulum. However, many specimens were encountered with a partially developed ectophragm. Some specimens had no ectophragm and others a fully developed ectophragm. These lie on a continuous morphological spectrum. Moreover, mechanical damage and degradation can result in the loss of the ectophragm. Therefore morphotypes with a reticulate ornamentation and an apical archaeopyle that could not be accommodated within existing species of *Ellipsoidictyum* or *Valensiella* were grouped together as the *Ellipsoidictyum/Valensiella* complex. The density of the reticulation is highly variable, the muri in some specimens are closely packed whilst others are widely spaced with large lumina. The lumina are microscabrate to psilate. This group was recorded from the Bajocian of northern France by Feist-Burkhardt and Monteil (1997).

Dimensions: width: 31 (54) 81 µm; length: 36 (54) 78 µm; 30 specimens measured.

Order UNCERTAIN**Suborder UNCERTAIN.****Family COMPARODINIACEAE Vozzhennikova 1979.**

Valvaeodinium Morgenroth 1970 emend. Below 1987.

Valvaeodinium spinosum? (Fenton et al. 1980) Below 1987 (Plate X, 5).

Remarks: A single specimen was encountered in sample S48 of the *S. humphriesianum* zone, and sporadically in low abundance through the *G. garantiana*, *P. parkinsoni* and *Z. zigzag* zones. These are squat and ovoidal in outline and have small simple spines. This form is questionably assigned to due to the outline; *V. spinosum* is elongate (Fenton et al. 1980, pl. 14, Fig. 13).

Valvaeodinium vermicylindratum Below 1987 (Plate X, 6).

Remarks: The distinctive vermiculate ornamentation of this species distinguishes it from *V. spinosum*. This was recorded from two samples (S66 and S71) in the *S. niortense* zone.

Valvaeodinium spp. (Plates 10, 7–8).

Remarks: Elongate to subovoidal in shape, scabrate to granulate autophragm, sometimes with longitudinal folds, autophragm typically <1 µm thick. Specimens of *Valvaodinium* spp. were encountered sporadically and in low numbers from the *S. propinquans*/*S. humphriesianum* zone to the *Z. zigzag* zone.

Dimensions: mean width: 36 µm; mean length: 44 µm; 8 specimens measured.

Order GONYAULACALES Taylor 1980

Suborder UNCERTAIN

Family UNCERTAIN

Impletosphaeridium Morgenroth 1966 emend. Islam 1993.

Impletosphaeridium sp. 1 (Plate X, 3).

Remarks: Two specimens of this small simple chorate species with dense, extremely fine (0.5 µm wide) bifurcating processes were recorded from the *P. parkinsoni* and *Z. zigzag* zones. The archaeopyle is apical and both specimens are damaged.

Dimensions: width excluding processes: 35 µm.

Impletosphaeridium sp. 2 (Plate X, 4).

Remarks: A single specimen was recorded from sample S108 from the *Z. zigzag* zone. This form is larger than *Impletosphaeridium* sp. 1 and has fewer processes which are conical and distally simple.

Dimensions: width excluding processes: 50 µm.

Subclass DINOPHYSPHYCIDAE Möhn 1984 ex Fensome et al. 1993

Order NANNOCERATOPSIALES Piel & Evitt 1980

Family NANNOCERATOPSACEAE Gocht 1970

Nannoceratopsis Deflandre 1939 emend. Riding and Helby 2001.

Nannoceratopsis ambonis Drugg 1978 emend. Riding 1984 (Plate XII, 4).

Remarks: *Nannoceratopsis ambonis* was encountered sporadically from the *G. concavum* to the lowest part of the *S. humphriesianum* zone; it is similar to *N. gracilis* but is distinguished by its thickened, solid, sagittal band.

Nannoceratopsis dictyambonis Riding 1984.

Remarks: *Nannoceratopsis dictyambonis* is distinguished by its reticulate sagittal band.

Nannoceratopsis gracilis Alberti 1961 emend. van Helden 1977 (Plate VIII, 7).

Remarks: *Nannoceratopsis gracilis* has two antapical horns of unequal length and a psilate to microreticulate autophragm. The morphology is variable, particularly the development of the ventral antapical horn. In some specimens this is a distinct, pointed horn, whilst in others it is a slightly-rounded protrusion. This variability seems to reflect a continuous morphological spectrum. It was encountered consistently, in varying abundances, from the *G. concavum* to the lower part of the *S. humphriesianum* zone, and sporadically from the *S. niortense*, *G. garantiana* and *Z. zigzag* zones.

Dimensions: mean dorso-ventral width: 44 µm; mean length 73 µm; 15 specimens measured.

Nannoceratopsis plegas Drugg 1978 (Plate VIII, 9).

Remarks: This species has a sickle-like outline due to the prominent dorsal antapical horn. It was recorded sporadically and in low numbers from the *W. laeviuscula* and *S. humphriesianum* zones and in two samples from the *G. garantiana* zone.

Nannoceratopsis spiculata Stover 1966 (Plate VIII, 8).

Remarks: Defined by its two prominent antapical horns of approximately equal length, with apparent cavation at the tips, *Nannoceratopsis spiculata* was found sporadically and in low abundances from the *W. laeviuscula* to *Z. zigzag* zones.

Nannoceratopsis spp. (Plate XII, 5–6).

Remarks: Morphotypes of *Nannoceratopsis* are often highly variable yet simple in morphology. Consequently forms were recorded which could not be assigned to an existing species but not enough to allow the erection of new species. These are grouped together as *Nannoceratopsis* spp. and vary from triangular to sub-ovoidal with a scabrate to microreticulate autophragm. The antapical horns are pointed to bulbous/globulose. They were

encountered sporadically and in low numbers from the *W. laeviuscula* to the *Z. zigzag* zones.

Dimensions: Mean dorso-ventral width: 64 µm; mean length: 40 µm; 5 specimens measured.

Subclass PERIDINIPHYCIDAE Fensome et al. 1993

Order PERIDINIALES Haeckel 1894

Suborder HETEROCAPSINEAE Fensome et al. 1993

Family HETEROCAPSACEAE Fensome et al. 1993

Moesiodinium Antonescu 1974 emend. Below 1987.

Moesiodinium raileanui Antonescu 1974.

Remarks: This distinctive, small, circumcavate species was recorded from two samples (S36 and S40) from the *W. laeviuscula*/*S. propinquans* zone of the Lower Bajocian.

Order UNCERTAIN

Suborder UNCERTAIN

Family UNCERTAIN

Orobodinium Gocht & Wille 1990.

Orobodinium automobile Gocht & Wille 1990 (Plate X, 9–10).

Remarks: This species has a fairly thick (1 µm) autophragm which is psilate to scabrate, and was encountered rarely and in low numbers from the *W. laeviuscula*/*S. propinquans* zone to the *Z. zigzag* zone.

Dimensions: mean width: 20 µm; mean length: 20 µm; 5 specimens measured.

Orobodinium sp. A of Wille & Gocht 1990 (Plate X, 10–11).

Remarks: A single specimen was encountered outside of the count from the uppermost sample (S109) of the *Z. zigzag* zone. It is distinguished from *O. automobile* by its differentiated autophragm, the outer layer of which is covered in vermiculate ornamentation, and is larger with a width of 25 µm and a length of 27 µm.

Appendix B. Supplementary data

Supplementary data to this article can be found online at <http://dx.doi.org/10.1016/j.revpalbo.2016.11.010>.

References

- Bailey, D.A., 1987. *Durotrigia daveyi* gen. et sp. nov., an Early Bajocian dinocyst with a variable precingular archaeopyle. *J. Micropaleontol.* 6, 89–96.
- Bailey, D.A., 1990. Some dinoflagellate cysts from latest Bajocian and Bathonian sediments in southern England. *Palynology* 14, 135–144.
- Barski, M., 2014. Shapes of organic walled dinoflagellate cysts in early diagenetic concretions—markers for mechanical compaction. *Rev. Palaeobot. Palynol.* 208, 50–54.
- Barski, M., Matyja, B.A., Segit, T., Wierzbowski, A., 2012. Early to Late Bajocian age of the “black flysch” (Szlachtowa Fm.) deposits: implications for the history and geological structure of the Pieniny Klippen Belt, Carpathians. *Geol. Quart.* 56, 391–410.
- Butler, N., Charnock, M.A., Hager, K.O., Watkins, C.A., 2005. The Ravenscar Group: a coeval analogue for the Middle Jurassic reservoirs of the North Sea and offshore Mid-Norway. In: Powell, A.J., Riding, J.B. (Eds.), *Recent Developments in Applied Biostratigraphy/Micropaleontological Society Special Publications*. Geological Society of London, London, pp. 43–53.
- Callomon, J.H., 2003. The Middle Jurassic of western and northern Europe: its subdivisions, geochronology and correlations. *Geol. Surv. Denmark Greenl. Bull.* 1, 61–73.
- Davey, R.J., 1980. Palynology. In: Penn, I.E., Dingwall, R.G., Knox, R.W.O.’B. (Eds.), *The Inferior Oolite (Bajocian) Sequence from a Borehole in Lyme Bay 79/3*. Institute of Geological Sciences Report, Dorset, pp. 6–11.
- de Vains, G., 1988. Etude palynologique préliminaire de l’Hettangien à l’Aalénien du Quercy (France). *Bull. Centres Rech. Explor. Prod. Elf-Aquitaine* 12, 451–469.
- Delwiche, C.F., 2007. The origin and evolution of dinoflagellates. In: Falkowski, P.G., Knoll, A.H. (Eds.), *Evolution of Primary Producers in the Sea*. Academic Press, Burlington, pp. 191–205.
- Dietl, G., 1988. Der Hamitenton (Ober-Bajocium, Mittl. Jura) in Bauaufschlüssen der neuen Bundesautobahn A8, Streckenabschnitt Aichelberg-Gruibingen. *Jahr. Ges. Naturk. Württemberg* 143, 59–77.
- Dietl, G., 2013. Der Braunjura am Fuß der Schwäbischen Alb. Fossilien. Special ed. Quelle & Meyer, Wiebelsheim, pp. 1–62.
- Feist-Burkhardt, S., 1990. Dinoflagellate cyst assemblages of the Hausen coreholes (Aalenian to early Bajocian), southwest Germany. *Bull. Centres Rech. Explor. Prod. Elf-Aquitaine* 14, 611–632.
- Feist-Burkhardt, S., Götz, A.E., 2002. *Palynofazies und Sequenzstratigraphie (K1)*. *Sediment* 29, 57–72.
- Feist-Burkhardt, S., Monteil, E., 1997. Dinoflagellate cysts from the Bajocian stratotype (Calvados, Normandy, western France). *Bull. Centres Rech. Explor. Prod. Elf-Aquitaine* 21, 31–105.

- Feist-Burkhardt, S., Monteil, E., 2001. Gonyaulacacean dinoflagellate cysts with multi-plate precingular archaeopyle. *N. Jb. Geol. Palaont. Abh.* 219, 33–81.
- Feist-Burkhardt, S., Pross, J., 1999. Morphological analysis and description of Middle Jurassic dinoflagellate cyst marker species using confocal laser scanning microscopy, digital optical microscopy, and conventional light microscopy. *Bull. Centres Rech. Explor. Prod. Elf-Aquitaine* 22, 103–145.
- Feist-Burkhardt, S., Pross, J., 2010. Dinoflagellate cyst biostratigraphy of the Opalinuston Formation (Middle Jurassic) in the Aalenian type area in southwest Germany and north Switzerland. *Lethaia* 43, 10–31.
- Feist-Burkhardt, S., Wille, W., 1992. Jurassic palynology in southwest Germany — state of the art. *Cah. Micropaléontol. Nouv. Ser.* 7, 141–156.
- Fensome, R.A., 1979. Dinoflagellate cysts and acritarchs from the Middle and Upper Jurassic of Jameson Land, east Greenland. *Grøn. Geol. Unders. Bull.* 132, 1–98.
- Fensome, R.A., Taylor, F.J.R., Norris, G., Sarjeant, W.A.S., Wharton, D.I., Williams, G.L., 1993. A classification of fossil and living dinoflagellates. *Special Paper 7. Micropaleontology Press*, pp. 1–351.
- Fensome, R.A., MacRae, R.A., Moldovan, J.M., Taylor, F.J.R., Williams, G.L., 1996. The early Mesozoic radiation of dinoflagellates. *Paleobiology* 22, 329–338.
- Fenton, J.P.G., Fisher, M.J., 1978. Regional distribution of marine microplankton in the Bajocian and Bathonian of northwest Europe. *Palinol. Número Extraordin.* 1, 233–243.
- Fenton, J.P.G., Neves, R., Piel, K.M., 1980. Dinoflagellate cysts and acritarchs from Upper Bajocian to Middle Bathonian strata of central and southern England. *Palaeontology* 23, 151–170.
- Gedl, P., 2008. Organic-walled dinoflagellate cyst stratigraphy of dark Middle Jurassic marine deposits of the Pieniny Klippen Belt, West Carpathians. *Stud. Geol. Polon.* 131, 7–227.
- Gedl, P., 2012. Organic-walled dinoflagellate cysts from the Bathonian ore-bearing clays at Gnasyń, Kraków-Silesia Homocline, Poland — a palaeoenvironmental approach. *Acta Geol. Pol.* 62, 439–461.
- Gedl, P., 2013. Dinoflagellate cysts from the Szlachtowa Formation (Jurassic) and adjacent deposits (Jurassic-Cretaceous) of the Grajcarek Unit at Szczawnica-Zabianiszcz (Pieniny Klippen Belt, Carpathians, Poland). *Geol. Quart.* 57, 485–502.
- Gedl, P., Józsa, S., 2015. Early?–Middle Jurassic dinoflagellate cysts and foraminifera from the dark shale of the Pieniny Klippen belt between Jarabina and Litmanova (Slovakia): age and palaeoenvironment. *Ann. Soc. Geol. Pol.* 85, 91–122.
- Gedl, P., Kaim, A., Leonowicz, P., Boczarowski, A., Dudek, T., Kędzierski, M., Rees, J., Smoleń, J., Szczepaniak, P., Sztajner, P., Witkowska, M., Ziaja, J., 2012. Palaeoenvironmental reconstruction of Bathonian (Middle Jurassic) ore-bearing clays at Gnasyń, Kraków-Silesia Homocline, Poland. *Acta Geol. Pol.* 62, 463–484.
- Guinot, G., Cavin, L., 2015. “Fish” (Actinopterygii and Elasmobranchii) diversification patterns through deep time. *Biol. Rev.* 91, 950–981.
- Hallam, A., 1976. Stratigraphic distribution and ecology of European Jurassic bivalves. *Lethaia* 9, 245–259.
- Hallam, A., 2001. A review of the broad pattern of Jurassic sea-level changes and their possible causes in the light of current knowledge. *Palaeogeogr. Palaeoclimatol. Palaeoecol.* 167, 23–37.
- Hart, M.B., Hylton, M.D., Oxford, M.J., Price, G.D., Hudson, W., Smart, C.W., 2003. The search for the origin of the planktic foraminifera. *J. Geol. Soc. Lond.* 160, 341–343.
- Head, M., 1996. Modern dinoflagellate cysts and their biological affinities. In: Jansonius, J., McGregor, D.C. (Eds.), *Palynology: Principles and Applications* 3. American Association of Stratigraphic Palynologists, Dallas, Texas, pp. 1197–1248.
- Ibrahim, M., Kholeif, S., Al-Saad, H., 2003. Dinoflagellate cyst biostratigraphy and palaeoenvironment of the Lower–Middle Jurassic succession of Qatar, Arabian Gulf. *Rev. Esp. Micropaleontol.* 35, 171–194.
- Jacquin, T., Dardeau, G., Durlot, C., de Graciansky, P.-C., Hantzpergue, P., 1998. The North Sea cycle: an overview of 2nd-order transgressive/regressive facies cycles in western Europe. In: de Graciansky, P.-C., Hardenbol, J., Jacquin, T., Vail, P.R. (Eds.), *Mesozoic and Cenozoic Sequence Stratigraphy of European Basins. SEPM (Society for Sedimentary Geology) Special Publication Vol. 60*, pp. 445–466.
- Lignum, J., Jarvis, I., Pearce, M.A., 2008. A critical assessment of standard processing methods for the preparation of palynological samples. *Rev. Palaeobot. Palynol.* 149, 133–149.
- MacRae, R.A., Fensome, R.A., Williams, G.L., 1996. Fossil dinoflagellate diversity, origins, and extinctions and their significance. *Can. J. Bot.* 74, 1687–1694.
- Mantle, D.J., Riding, J.B., 2012. Palynology of the Middle Jurassic (Bajocian–Bathonian) *Wanaea verrucosa* dinoflagellate cyst zone of the North West Shelf of Australia. *Rev. Palaeobot. Palynol.* 180, 41–78.
- Marañón, E., 2015. Cell size as a key determinant of phytoplankton metabolism and community structure. *Annu. Rev. Mar. Sci.* 7, 241–264.
- Mertens, K.N., Verhoeven, K., Verleye, T., Louwey, S., Amorim, A., Ribeiro, S., Deaf, A.S., Harding, I.C., De Schepper, S., González, C., Kodrans-Nsiah, M., de Vernal, A., Henry, M., Radi, T., Dybbjaer, K., Poulsen, N.E., Feist-Burkhardt, S., Chitolie, J., Heilmann-Clausen, C., Londeix, L., Turon, J.-L., Marret, F., Matthiessen, J., McCarthy, F.M.G., Prasad, V., Pospelova, V., Hughes, J.E.K., Riding, J.B., Rochon, A., Sangiorgi, F., Welters, N., Sinclair, N., Thun, C., Soliman, A., Van Nieuwenhove, N., Vink, A., Young, M., 2009. Determining the absolute abundance of dinoflagellate cysts in recent marine sediments: the *Lycopodium* marker-grain method put to the test. *Rev. Palaeobot. Palynol.* 157, 238–252.
- Morgenroth, P., 1970. Dinoflagellate cysts from the Lias delta of Lühnde/Germany. *Neues Jahrb. Geol. Palaontol. Abh.* 136, 345–359.
- O'Dogherty, L., Sandoval, J., Bartolini, A., Bruchez, S., Bill, M., Guex, J., 2006. Carbon-isotope stratigraphy and ammonite faunal turnover for the Middle Jurassic in the Southern Iberian palaeomargin. *Palaeogeogr. Palaeoclimatol. Palaeoecol.* 239, 311–333.
- Pienkowski, G., Schudack, M.E., Bosak, P., Enay, R., Feldman-Olszewska, A., Golonka, J., Gutowski, J., Hergreen, G.F.W., Jordan, P., Krobicki, M., Lathuiliere, B., Leinfelder, R.R., Michalik, J., Moennig, E., Noe-Nygaard, N., Palfy, J., Pint, A., Rasser, M.W., Reisdorf, A.G., Schmid, D.U., Schweigert, G., Surlyk, F., Wetzel, A., Wong, T.E., 2008. Jurassic. In: McCann, T. (Ed.), *The Geology of Central Europe Volume 2: Mesozoic and Cenozoic*. The Geological Society of London, London, pp. 823–922.
- Poulsen, N.E., 1996. Dinoflagellate cysts from marine Jurassic deposits of Denmark and Poland. American Association of Stratigraphic Palynologists, Contributions Series Vol. 31. AASP Foundation, Dallas, Texas (909 pp.).
- Poulsen, N.E., 1998. Upper Bajocian to Callovian (Jurassic) dinoflagellate cysts from central Poland. *Acta Geol. Pol.* 48, 237–245.
- Poulsen, N.E., Riding, J.B., 2003. The Jurassic dinoflagellate cyst zonation of subboreal Northwest Europe. *Geol. Surv. Denmark Greenl. Bull.* 1, 115–144.
- Prauss, M., 1989. Dinozysten-Stratigraphie und Palynofazies im Oberen Lias und Dogger von NW-Deutschland. *Palaeontogr. Abt. B* 214, 1–124.
- Riding, J.B., 1983. The palynology of the Aalenian (Middle Jurassic) sediments of Jackdaw Quarry, Gloucestershire, England. *Mercian Geol.* 9, 111–120.
- Riding, J.B., 1984a. A palynological investigation of Toarcian to early Aalenian strata from the Blea Wyke area, Ravenscar, North Yorkshire. *Proc. Yorks. Geol. Soc.* 45, 109–122.
- Riding, J.B., 1984b. Observations on the Jurassic dinoflagellate cyst *Nannoceratopsis ambonis* Drugg, 1978. *J. Micropaleontol.* 3, 75–79.
- Riding, J.B., 2012. A compilation and review of the literature on Triassic, Jurassic, and earliest Cretaceous dinoflagellate cysts. American Association of Stratigraphic Palynologists Contributions Series Vol. 46. AASP Foundation, Dallas, Texas (119 pp.).
- Riding, J.B., 2013. The literature on Triassic, Jurassic and earliest Cretaceous dinoflagellate cysts: supplement 1. *Palynology* 37, 345–354.
- Riding, J.B., 2014. The literature on Triassic, Jurassic and earliest Cretaceous dinoflagellate cysts: supplement 2. *Palynology* 38, 334–347.
- Riding, J.B., Thomas, J.E., 1992. Dinoflagellate cysts of the Jurassic System. In: Powell, A.J. (Ed.), *A Stratigraphic Index of Dinoflagellate Cysts*. Chapman and Hall, London, pp. 7–97.
- Riding, J.B., Penn, I.E., Woollam, R., 1985. Dinoflagellate cysts from the type area of the Bathonian stage (Middle Jurassic; Southwest England). *Rev. Palaeobot. Palynol.* 45, 149–169.
- Riding, J.B., Walton, W., Shaw, D., 1991. Toarcian to Bathonian (Jurassic) palynology of the Inner Hebrides, Northwest Scotland. *Palynology* 15, 115–179.
- Riding, J.B., Mantle, D.J., Backhouse, J., 2010. A review of the chronostratigraphical ages of Middle Triassic to Late Jurassic dinoflagellate cyst biozones of the North West Shelf of Australia. *Rev. Palaeobot. Palynol.* 162, 543–575.
- Riout, M., Dugué, O., Duchene, R.J., Ponsot, C., Fily, G., Moron, J., Vail, P., 1991. Outcrop sequence stratigraphy of the Anglo-Paris Basin, Middle to Upper Jurassic (Normandy, Maine, Dorset). *Bull. Centres Rech. Explor. Prod. Elf-Aquitaine* 15, 101–194.
- Sarjeant, W.A.S., 1976. Dinoflagellate cysts and acritarchs from the Great Oolite Limestone (Jurassic: Bathonian) of Lincolnshire, England. *Geobios* 9, 5–46.
- Segit, T., Matyja, B.A., Wierzbowski, A., 2015. The Middle Jurassic succession in the central sector of the Pieniny Klippen Belt (Sprzycne Creek): implications for the timing of the Czorsztyn Ridge development. *Geol. Carpath.* 66, 285–302.
- Skupien, P., Pavluš, J., Falahatgar, M., Javidan, M., 2015. Middle Jurassic organic-walled dinoflagellate cysts and palynofacies from Telma-Dareh, south of Sari, northern Iran. *Rev. Palaeobot. Palynol.* 223, 128–137.
- Stukins, S., Jolley, D.W., McIlroy, D., Hartley, A.J., 2013. Middle Jurassic vegetation dynamics from allochthonous palynological assemblages: an example from a marginal marine depositional setting; Lajas Formation, Neuquén Basin, Argentina. *Palaeogeogr. Palaeoclimatol. Palaeoecol.* 392, 117–127.
- Suchéras-Marx, B., Mattioli, E., Giraud, F., Escarguel, G., 2015. Palaeoenvironmental and paleobiological origins of coccolithophorid genus *Watznaueria* emergence during the late Aalenian–early Bajocian. *Paleobiology* 41, 415–435.
- Wood, G., Gabriel, A., Lawson, J., 1996. Palynological techniques—processing and microscopy. In: Jansonius, J., McGregor, D.C. (Eds.), *Palynology: Principles and Applications* Vol. 1. American Association of Stratigraphic Palynologists Foundation, Dallas, Texas, pp. 29–50.
- Wood, S.E.L., Riding, J.B., Fensome, R.A., Williams, G.L., 2016. A review of the *Sentusidinium* complex of dinoflagellate cysts. *Rev. Palaeobot. Palynol.* 234, 61–93.
- Woollam, R., 1982. Early and Middle Jurassic dinocysts in the Winterborne Kingston borehole, Dorset. In: Rhys, G., Lott, G., Calver, M. (Eds.), *The Winterborne Kingston Borehole, Dorset, England 81/3*. Institute of Geological Sciences Report, pp. 89–90.
- Woollam, R., 1983. A review of the Jurassic dinocyst genera *Ctenidodinium* Deflandre 1938 and *Dichadogonyaulax* Sarjeant 1966. *Palynology* 7, 183–196.
- Woollam, R., Riding, J., 1983. Dinoflagellate cyst zonation of the English Jurassic. 83/2. Institute of Geological Sciences Report, pp. 1–42.
- Ziegler, P.A., 1990. second ed. Geological Atlas of Western and Central Europe vol. 1. Europe. Shell Internationale Petroleum Maatschappij B.V., The Hague (239 pp.).